Implementation of Measuring While Drilling Shafts in Florida (FLMWDS)

Final Report

FDOT Contract No. BDV31-977-91

Submitted to:
Project Manager: David Horhota, Ph.D., P.E.
Florida Department of Transportation

Submitted By:
UF Principal Investigator: Michael McVay, Ph.D.
UF Co-Principal Investigator: Michael Rodgers, Ph.D., P.E.
UF Graduate Researcher: Wyatt Kelch
UF Graduate Researcher: Kunyu Yang

June 30, 2020

University of Florida
Engineering School of Sustainable Infrastructure & Environment

Disclaimer

The opinions, findings, and conclusions expressed in this publication are those of the authors and not necessarily those of the State of Florida Department of Transportation.

SI (Modern Metric) Conversion Factors (from FHWA) Approximate Conversions to SI Units

SYMBOL	WHEN YOU KNOW	MULTIPLY BY	TO FIND	SYMBOL
LENGTH				
in	inches	25.4	millimeters	mm
ft	feet	0.305	meters	m
yd	yards	0.914	meters	m
mi	miles	1.61	kilometers	km
SYMBOL	WHEN YOU KNOW	MULTIPLY BY	TO FIND	SYMBOL
AREA				
in^2	square inches	645.2	square millimeters	mm^2
ft^2	square feet	0.093	square meters	m^2
yd^2	square yard	0.836	square meters	m^2
ac	acres	0.405	hectares	ha
mi^2	square miles	2.59	square kilometers	km^2
SYMBOL	WHEN YOU KNOW	MULTIPLY BY	TO FIND	SYMBOL
VOLUME				
fl oz	fluid ounces	29.57	milliliters	mL
gal	gallons	3.785	liters	L
ft^3	cubic feet	0.028	cubic meters	m^3
yd^3	cubic yards	0.765	cubic meters	m^3
NOTE: volumes greater than 1000 L shall be shown in m^3				
SYMBOL	WHEN YOU KNOW	MULTIPLY BY	TO FIND	SYMBOL
MASS				
oz	ounces	28.35	grams	g
lb	pounds	0.454	kilograms	kg
T	short tons (2000 lb)	0.907	megagrams (or "metric ton")	Mg (or "t")
SYMBOL	WHEN YOU KNOW	MULTIPLY BY	TO FIND	SYMBOL
TEMPERATURE (exact degrees)				
°F	Fahrenheit	5 (F-32)/9 or (F-32)/1.8	Celsius	°C
SYMBOL	WHEN YOU KNOW	MULTIPLY BY	TO FIND	SYMBOL
ILLUMINATION				
fc	foot-candles	10.76	lux	lx
fl	foot-Lamberts	3.426	candela/m^2	cd/m^2
SYMBOL	WHEN YOU KNOW	MULTIPLY BY	TO FIND	SYMBOL
FORCE and PRESSURE or STRESS				
lbf	pound force	4.45	newtons	N
lbf/in^2	pound force per square inch	6.89	kilopascals	kPa

Approximate Conversions to English Units

SYMBOL	WHEN YOU KNOW	MULTIPLY BY	TO FIND	SYMBOL
		LENGTH		
mm	millimeters	0.039	inches	in
m	meters	3.28	feet	ft
m	meters	1.09	yards	yd
km	kilometers	0.621	miles	mi
SYMBOL	WHEN YOU KNOW	MULTIPLY BY	TO FIND	SYMBOL
		AREA		
mm^2	square millimeters	0.0016	square inches	in^2
m^2	square meters	10.764	square feet	ft^2
m^2	square meters	1.195	square yards	yd^2
ha	hectares	2.47	acres	ac
km^2	square kilometers	0.386	square miles	mi^2
SYMBOL	WHEN YOU KNOW	MULTIPLY BY	TO FIND	SYMBOL
		VOLUME		
mL	milliliters	0.034	fluid ounces	fl oz
L	liters	0.264	gallons	gal
m^3	cubic meters	35.314	cubic feet	ft^3
m^3	cubic meters	1.307	cubic yards	yd^3
SYMBOL	WHEN YOU KNOW	MULTIPLY BY	TO FIND	SYMBOL
		MASS		
g	grams	0.035	ounces	oz
kg	kilograms	2.202	pounds	lb
Mg (or "t")	megagrams (or "metric ton")	1.103	short tons (2000 lb)	T
SYMBOL	WHEN YOU KNOW	MULTIPLY BY	TO FIND	SYMBOL
		TEMPERATURE (exact degrees)		
ºC	Celsius	1.8C+32	Fahrenheit	ºF
SYMBOL	WHEN YOU KNOW	MULTIPLY BY	TO FIND	SYMBOL
		ILLUMINATION		
lx	lux	0.0929	foot-candles	fc
cd/m^2	candela/m^2	0.2919	foot-Lamberts	fl
SYMBOL	WHEN YOU KNOW	MULTIPLY BY	TO FIND	SYMBOL
		FORCE and PRESSURE or STRESS		
N	newtons	0.225	pound force	lbf
kPa	kilopascals	0.145	pound force per square inch	lbf/in^2

Technical Report Documentation Page

1. Report No.	2. Government Accession No.	3. Recipient's Catalog No.	
4. Title and Subtitle Implementation of Measuring While Drilling Shafts in Florida (FLMWDS)		5. Report Date June 2020	
		6. Performing Organization University of Florida	
7. Author(s) Michael McVay and Michael Rodgers		8. Performing Organization Report No.	
9. Performing Organization Name and Address University of Florida –Engineering School of Sustainable Infrastructure and Environment 365 Weil Hall – P.O. Box 116580 Gainesville, FL 32511-6580		10. Work Unit No. (TRAIS)	
		11. Contract or Grant No. BDV31-977-91	
12. Sponsoring Agency Name and Address Florida Department of Transportation 605 Suwannee Street, MS 30 Tallahassee, FL 32399		13. Type of Report and Period Covered Final Report 01/2018 – 06/30/2020	
		14. Sponsoring Agency Code	
15. Supplementary Notes			

16. Abstract:

Measuring while drilling (MWD) is the application of monitoring and recording drilling data during the drilling process. Recent geotechnical MWD efforts have shown that specific energy obtained from MWD can be directly correlated to the unconfined compression strength (q_u) of rock. This is advantageous as foundations and structures supported by rock commonly use q_u in their design. For this research, MWD was conducted during the excavation of drilled shafts at two independent sites, Selmon Parkway in Tampa and County Road 250 in Dowling Park, Florida. At both sites, rock drilling buckets were used to excavate the shafts. This required a new correlation to be developed between specific energy and q_u for the unique drilling tools. This was accomplished using mobilized side shear data collected from load tests at Selmon Parkway, and the correlation was subsequently used to estimate rock strength at County Road 250. At both sites, data obtained from core samples and MWD were used to assess the site variability. It was concluded that conventional site investigation methods are limited to properly assess site variability, whereas the MWD approach significantly increases the number of strength assessments collected and can provide a correlation structure from a single sampled location, identify areal trends to quantify layering and zonal issues, and reduce the spatial uncertainty at each shaft location. These findings indicate MWD can be used to properly assess site variability and provide QA/QC during shaft construction; both of those will improve resistance factors used in design and lead to a reduction in cost per shaft.

17. Key Words Measuring While Drilling, Specific Energy, Drilled Shafts, Florida Limestone, Shaft Capacity, Geostatistics		18. Distribution Statement No restrictions.	
19. Security Classif. (of this report): Unclassified	20. Security Classif. (of this page): Unclassified	21. No. of Pages 119	22. Price

Acknowledgements

Executive Summary

Measuring while drilling (MWD) is now an emerging application within the field of geotechnical engineering in which the data collected can be used to improve the design of foundations and provide QA/QC during bored pile construction. MWD is the application of monitoring and recording drilling data during the drilling process. Computerized systems are used typically with sensors placed throughout the drill rig to continuously monitor a series of drilling parameters. The data can be viewed in real time and recorded for further analysis. The continuous sampling produces high resolution profiles of drilling parameters that can be used individually or in combinations (e.g., specific energy) to quantify changes in subsurface conditions.

Recent geotechnical MWD efforts (FDOT BDV31-977-20 and BDV31-820-006) have shown that specific energy can be directly correlated to the unconfined compression strength (q_u) of rock. This is advantageous in geotechnical engineering as foundations and structures supported by rock commonly use q_u in design. The high resolution sampling associated with MWD can generate highly detailed strength profiles within a rock mass and a significant increase in strength data for use in design and construction monitoring (Rodgers et al., 2018a, 2018b, 2018c, 2018d, and 2020).

For this research effort, MWD was conducted during the excavation of drilled shafts at two independent sites. The first site was Selmon Parkway in Tampa where MWD was conducted on three load-tested shafts, and the second site was County Road 250 (CR-250) in Dowling Park, where MWD was conducted on two load-tested shafts and two production shafts. During the research, rock drilling buckets were predominately used to excavate each shaft. In the previous study, BDV31-977-20, rock augers were used, and a direct correlation was developed between specific energy and q_u from laboratory testing. Unfortunately, the previously developed rock auger specific energy-q_u correlation could not be used at the new sites because of the inherent differences in mechanical efficiency associated with each drilling tool's geometry (i.e., rock auger vs. drilling bucket). Consequently, the researchers had to develop an alternative approach to estimate rock strength via MWD with rock drilling buckets.

From the data collected in the prior study (BDV31-977-20), it was found that specific energy is directly correlated to the mobilized side shear measured within individual segments of load tested shafts in which MWD was conducted. This provided a new approach to develop a unique relationship between specific energy and rock strength for different drilling tools used in practice. A new relationship was developed between specific energy and rock strength for rock drilling buckets using MWD data (specific energy) collected in 12 mobilized shaft segments at Selmon Parkway. The correlation was subsequently used to assess rock strength at CR-250 where a similar rock drilling bucket was employed.

Also completed during the research was the assessment of site variability using both MWD and core data collected at each site. Prior to the assessment of rock strength from specific energy obtained from MWD, there never was sufficient rock strength data collected in a single sampled location to develop a vertical variogram for a single shaft. However, due to the significant increase in rock strength assessments provided by MWD, it was found that a correlation structure within a single sampled location (i.e., a single shaft) could be developed. This is largely

beneficial as it allows various types of variability such as zonal anisotropy or layering, which is common in Florida's highly variable strata, to be identified. Through variogram analyses completed during this research, both types of site variability were identified.

Finally, the intent of this research was to further investigate the viability of the methods developed in the prior FDOT project, BDV31-977-20, in which MWD was used as a QA/QC tool for drilled shafts installed in Florida limestone. The findings from this effort further indicate that MWD can be used to assess shaft side shear and rock strength in situ during shaft construction, properly assess site variability, and provide QA/QC during the construction of untested production shafts. All of those will increase the reliability of the foundations, improve the resistance factors used in design, and lead to a reduction in cost per shaft. Therefore, it is recommended to continue the development of drilled shaft MWD within the state of Florida.

Table of Contents

List of Figures

xiii

List of Tables

1. Introduction and Background

1.1 *Introduction*

Interest in measuring while drilling, MWD, is growing worldwide as far more data can be obtained from continuously taking measurements during rock drilling. The International Organization for Standardization has already developed standards for MWD monitoring systems and procedures, published in ISO/IEC 22476-15:2016, *Geotechnical Investigation and Testing – Field Testing – Part 15: Measuring While Drilling*. However, this is a new area, and limited research has been performed on MWD techniques for measuring in situ rock strength, especially in Florida. The work completed in FDOT Contract BDV31-977-20 (McVay and Rodgers, 2016) on measuring rock strength during drilled shaft installation in Florida took the first steps in the delineation of subsurface variability and strength assessment through direct measurements during shaft construction. For every shaft that was drilled and monitored, UF researchers were able to provide a profile of rock strength with a degree of precision that could not be achieved through any current conventional methods. The monitoring approach directly addressed the spatial variability in both the horizontal and vertical directions that exist in Florida (e.g., strength coefficient of variability (CV) >1).

During BDV31-977-20, three separate drilled shaft sites were monitored with variations in the following categories: limestone formations encountered, drill rigs used to install the shafts, shaft diameters, drilling crews, and rock auger configurations. In total, 10 measured (Load test – conventional method) versus predicted (MWD – developed method) data points were obtained with an average error of 0.6% between the measured and predicted. The load tests included three of the most widely used methods: Bi-directional Osterberg, Top-down Static, and Statnamic. A bias analysis (measured vs. predicted) also indicated there was limited variability because the mean and median bias were 1.00 and the coefficient of variability (CV) was less than 0.07.

Using the same 10 data points collected in BDV31-977-20, it was recently discovered that the assessment of specific energy also shows excellent correlation with the mobilized unit side shear obtained from load testing (Figure 1-1). Figure 1-1 uses the data collected from all three monitored sites, each of which contained a different limestone formation. This is important because measuring rock strength through the assessment of specific energy in combination with load testing allows drilled shaft MWD to be used in any rock formation without using the "Florida-specific" compressive and tensile strength correlations developed in BDV31-977-20. To clarify, the drill rig monitoring efforts developed in BDV31-977-20 could potentially be expanded outside the state of Florida, increasing the value and importance of the previously completed research. Therefore, in this project, more drilled shaft monitoring was conducted to further validate the method.
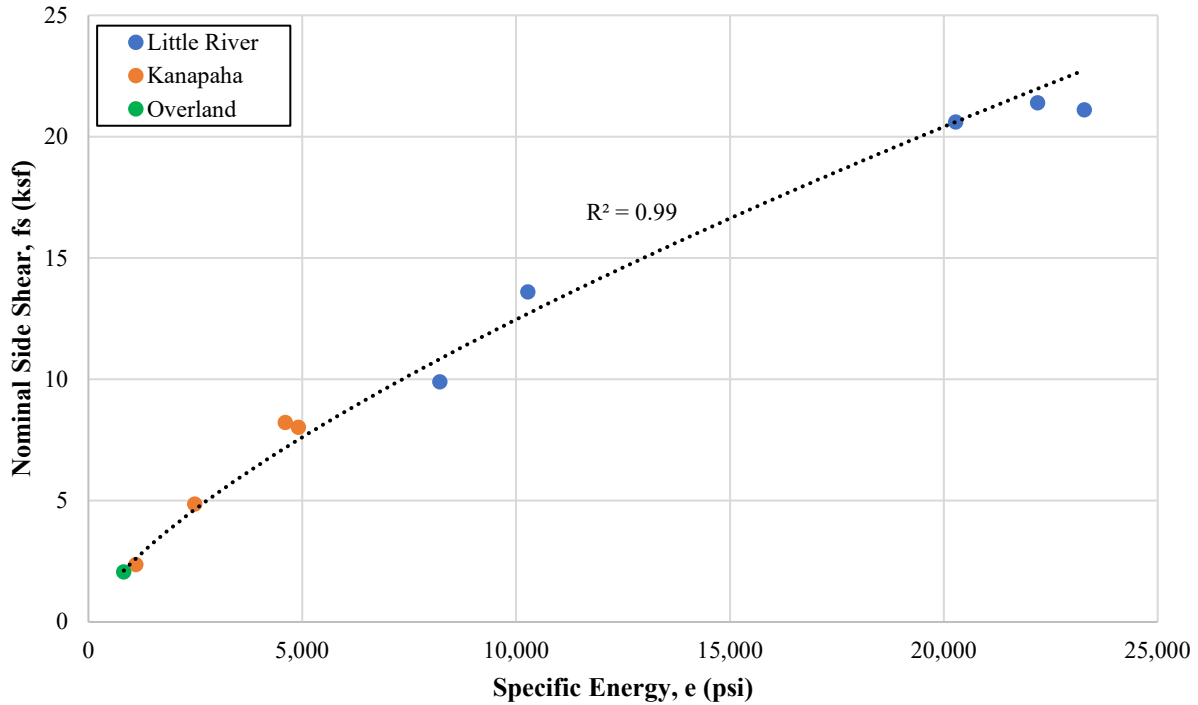
Figure 1-1. Mobilized unit side shear versus specific energy.

1.2 Background

In the previous study, BDV31-977-20, a new method was developed to estimate the rock strength of Florida limestone and intermediate-geomaterial (IGM: O'Neill et al. 1996) during drilled shaft installations while drilling using a rock auger. From the study, it was determined that the q_u of rock is directly correlated to specific energy (Teale 1965). The q_u and shaft side shear capacity (f_s) estimates from the MWD-developed specific energy correlation were found to be in good agreement with recovered core samples and load test results at three independent sites. In rock drilling, specific energy is defined as the energy required to remove/excavate a unit volume of rock. The specific energy equation Teale developed for non-percussive rotary drilling requires measuring five drilling parameters independently:

$$e = \frac{F}{A} + \frac{2\pi NT}{Au}$$

(Eq. 1-1)

Where:
- e = Specific Energy (psi);
- T = Torque (in-lbs);
- F = Crowd or downward axial force (lbf);
- u = Penetration rate (in/min);
- N = Rotational speed (RPMs); and
- A = Cross-sectional area of the excavation (in^2) defined by the bit diameter, d (in).

In order to conduct MWD on the drilled shaft rigs, a monitoring system was needed to measure each of the drilling parameters in real time. The monitoring system used during the study provided continuous measurements of each drilling parameter at a 1 kHz sampling rate that were automatically averaged for every two centimeters of penetration as the drill bit was advanced. This provided a depth profile of specific energy, and inherently q_u and f_s, with a degree of precision similar to that of a cone penetrometer test (CPT) for soils. The same type of monitoring system (Jean Lutz) used in the previous drilled shaft study was also used during this study.

The primary objectives of this research were to further validate the methods developed in BDV31-977-20, investigate any irregularities in strength prediction (different drilling tools, variable rock formations, etc.) and/or construction monitoring (rig malfunction), further investigate specific energy versus load testing, and continue to develop MWD as a QA/QC tool for drilled shaft construction similar to the practice of monitoring driven piles during construction. The secondary objective was to investigate monitoring mechanically driven drill rigs and to assess the variability of each site using data obtained from core samples and MWD. For the research, MWD was conducted at two separate locations, Selmon Parkway and County Road 250 (CR-250).

1.2.1 Selmon Parkway

At the start of the construction process at Selmon Parkway in Tampa, 4 drilled shafts were installed and subsequently load tested using a bi-directional Osterberg method, which provided an excellent opportunity to further investigate the methods developed in BDV31-977-20. MWD was conducted on three of the four test shafts installed at the site. The drilled shafts at Selmon Parkway provided a fourth MWD variation in limestone formations encountered, drill rigs used to install the shafts, shaft diameters, drilling crews, and drilling tool configurations.

1.2.2 County Road 250

MWD was also conducted at the CR-250 bridge site over the Suwannee River. This project added a fifth variation to all categories previously mentioned. At CR-250, two bi-directional load tests were completed on drilled shafts socketed into a limestone layer. In addition to monitoring the two load test shafts, MWD was also completed on two full-scale production shafts for comparison. A review of the soil/rock borings revealed that the limestone present at the site exhibits significant variability both vertically and horizontally. The highly variable nature at both sites also provided the opportunity to further investigate the Florida specific compressive and tensile strength correlations developed in BDV31-977-20, and the concept of index testing through core sample analyses.

2. Field Monitoring at Selmon Parkway

2.1 *Drilling Equipment*

Prior to the start of monitoring at Selmon Parkway, a new DIALOG (data acquisition module), junction box, and additional cabling were purchased. The purchased items are presented in Figure 2-1. The equipment was used to complete monitoring at Selmon Parkway and CR-250.
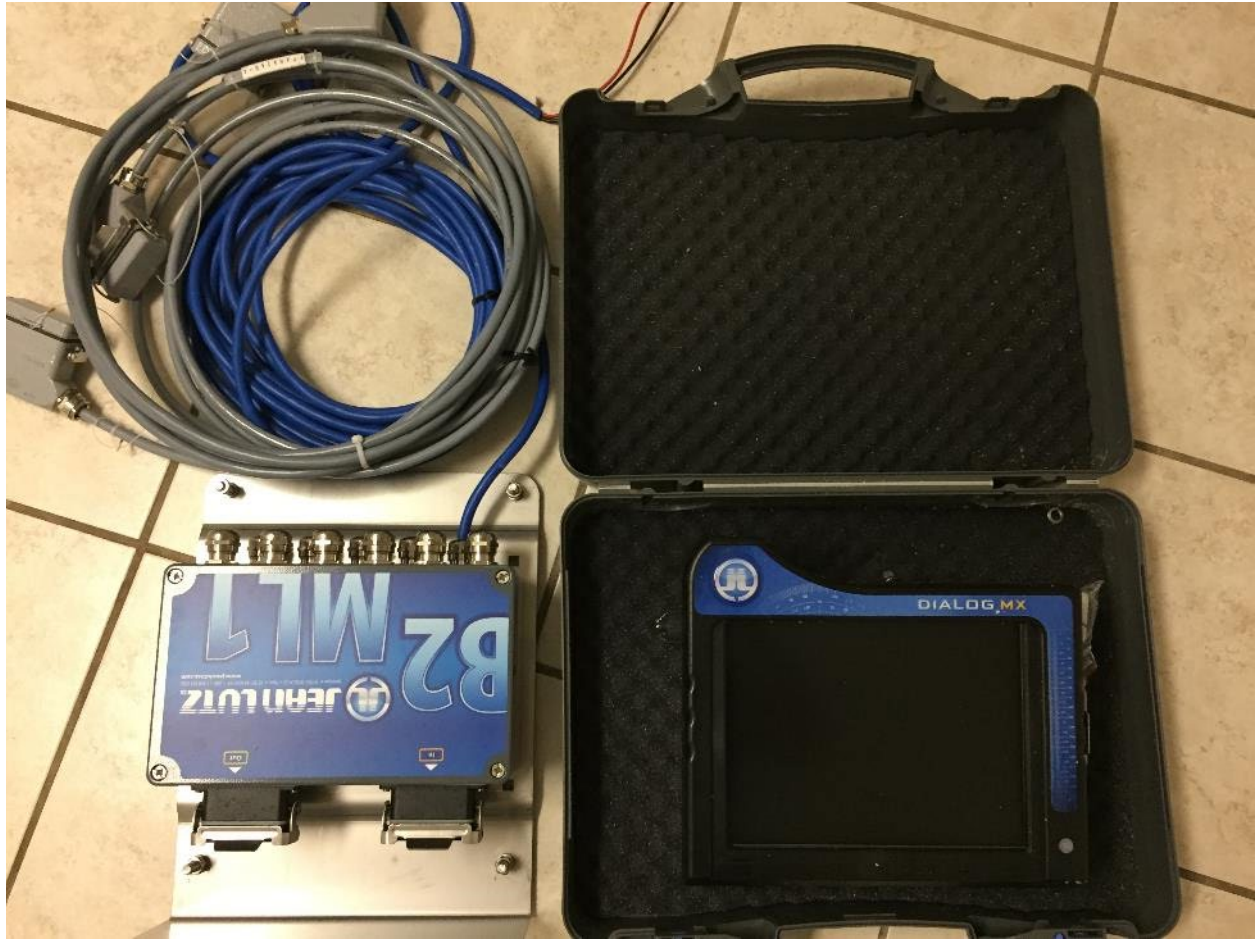
Figure 2-1. New monitoring equipment.

2.2 *Drill Rig Instrumentation and Calibration*

At Selmon Parkway, a Liebherr LB36 BAT-410 drill rig (Figure 2-2) was used to install the shafts. The rig was fully hydraulic with full instrumentation typically operated through Liebherr's Litronic drilling system which is comparable to Bauer's B-tronic system.

Figure 2-2. Liebehrr BAT 410 drill rig.

Since the drill rig was fully instrumented with sensors that are compatible with the Jean Lutz system, no additional sensors needed to be installed. Therefore, only the DIALOG and junction box needed to be integrated into the existing Litronic system. Due to limited space to mount the actual junction box, the internal components of the junction box were removed from the housing and mounted directly into the electrical unit of the drill rig (Figures 2-3 through 2-7). This included using two copy modules, one for torque and the other for crowd. Each module routed the respective signal to both the Jean Lutz and Litronic systems. The DIALOG was mounted in the cab of the drill rig in a position that did not interfere with the driller's line of site (Figure

2-8). This was completed using store bought mounting brackets that were easily integrated into the framework of the cab.

Figure 2-3. Liebehrr electrical unit.
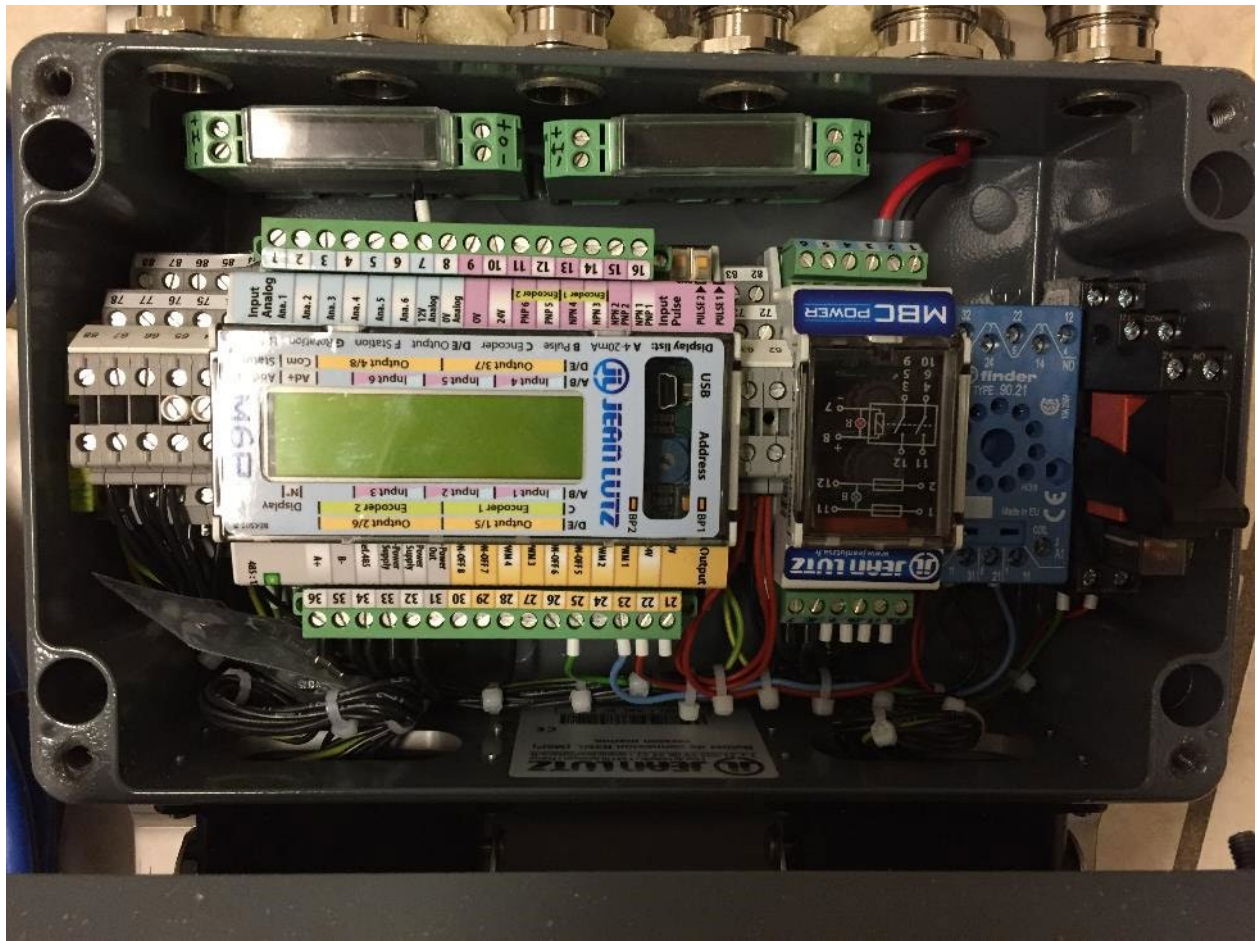
Figure 2-4. Internal components of the junction box.

Figure 2-5. Copy modules used to route torque and crowd readings to both systems.
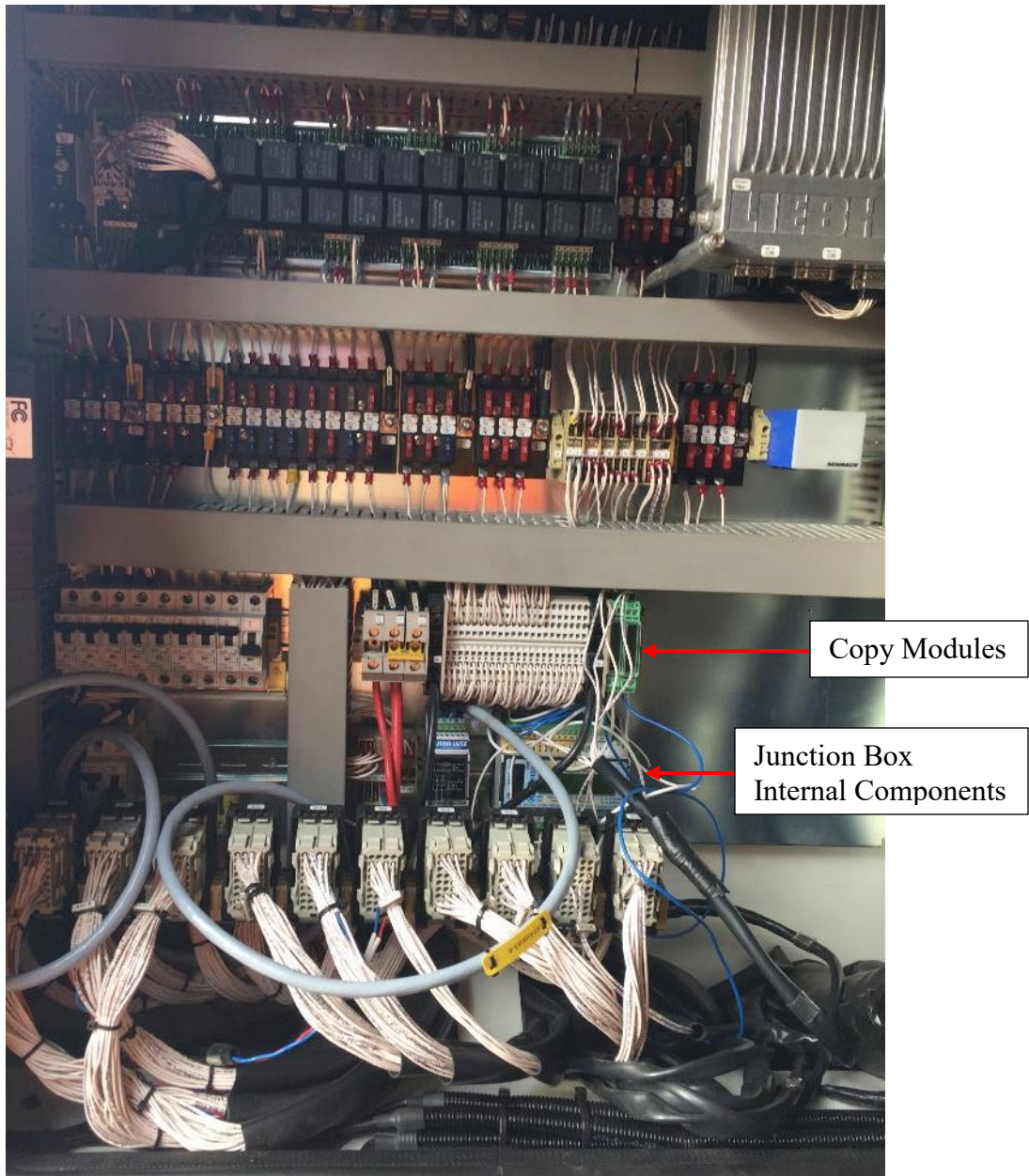
Figure 2-6. Jean Lutz junction box internal components mounted in the Liebehrr electrical unit.
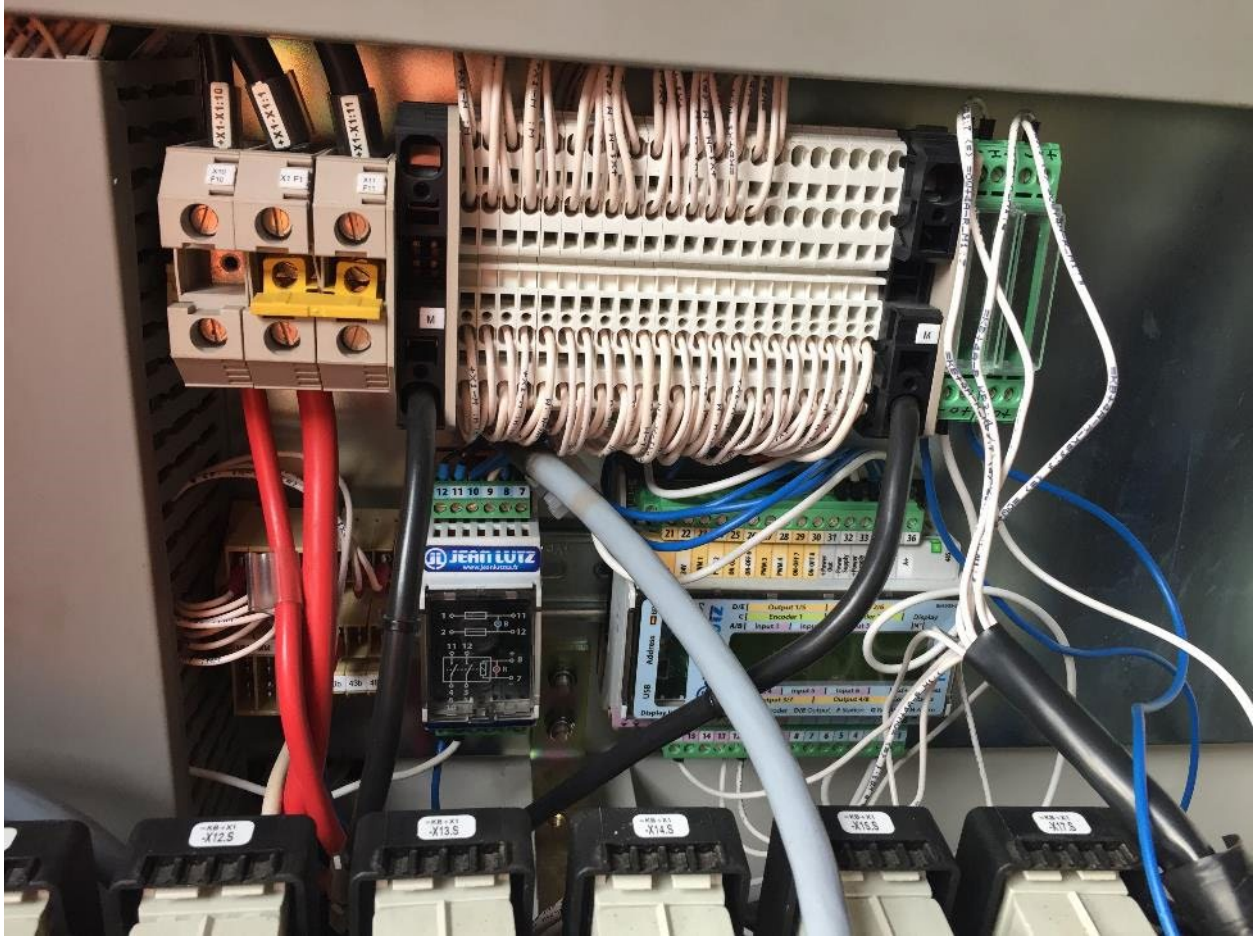
Figure 2-7. Jean Lutz junction box internal components mounted in the Liebehrr electrical unit.

Figure 2-8. DIALOG mounted in the cab in a position that does not interfere with the driller.

Once the installation was complete, calibration procedures commenced. This involved checking rotational speeds by counting the number of rotations over a minute several times and comparing with the DIALOG in-cab display. Penetration calibration involved comparing the DIALOG tracked movement with physical measurements and the Liebherr in-cab display. Torque pressure was checked by rotating without penetration and crowd pressure was checked by penetrating without rotation. This ensured the signals received were recorded by the appropriate port in the DIALOG (i.e., torque display reads torque pressure and crowd display reads crowd pressure).

2.3 *Drilled Shaft MWD at Selmon Parkway*

At Selmon Parkway, three test shafts were monitored. During the monitoring, two different drillers were used by the contractor. They will be referred to as Driller A and Driller B. Test Shaft 3 was drilled first by Driller A, who also drilled Test Shaft 1. Test Shaft 1 was the first shaft constructed on the site and was not monitored because it was installed before this research project began. Driller B drilled Test Shafts 2 and 4.

Presented below are images of the drilling at each location (Figures 2-9 through 2-12). Test Shafts 2 and 3 were installed in the median of a four-lane road. Monitoring (MWD) was conducted from adjacent parking lots to avoid disturbing the drilling process in any way. Test Shaft 4 was installed adjacent to an off-ramp. Monitoring was conducted from a safe distance within the lot adjacent to the off-ramp.

Figure 2-9. Drilling Test Shaft 3.

DIALOG in drill rig cab
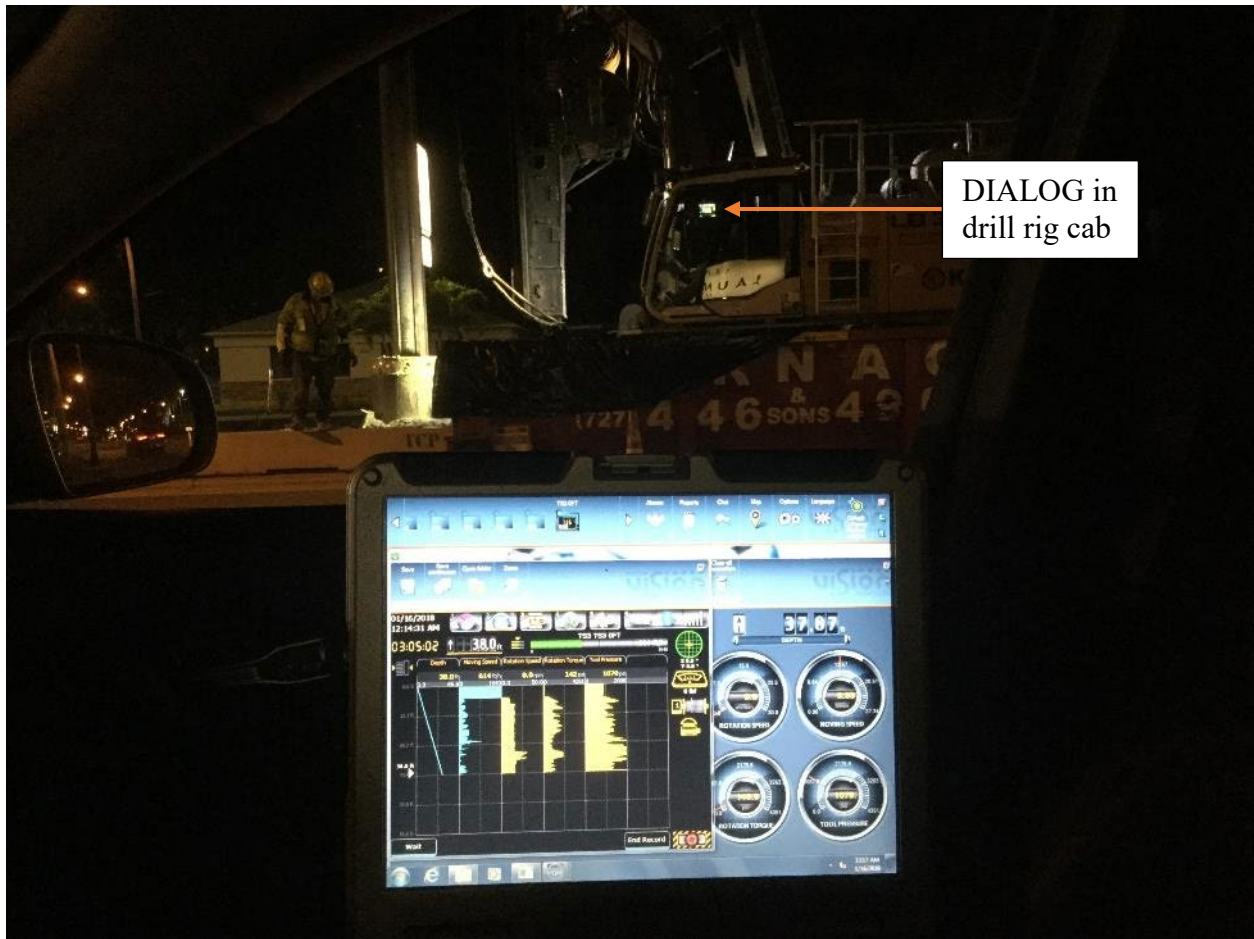
Figure 2-10. Monitoring from an adjacent parking lot inside researcher's vehicle.
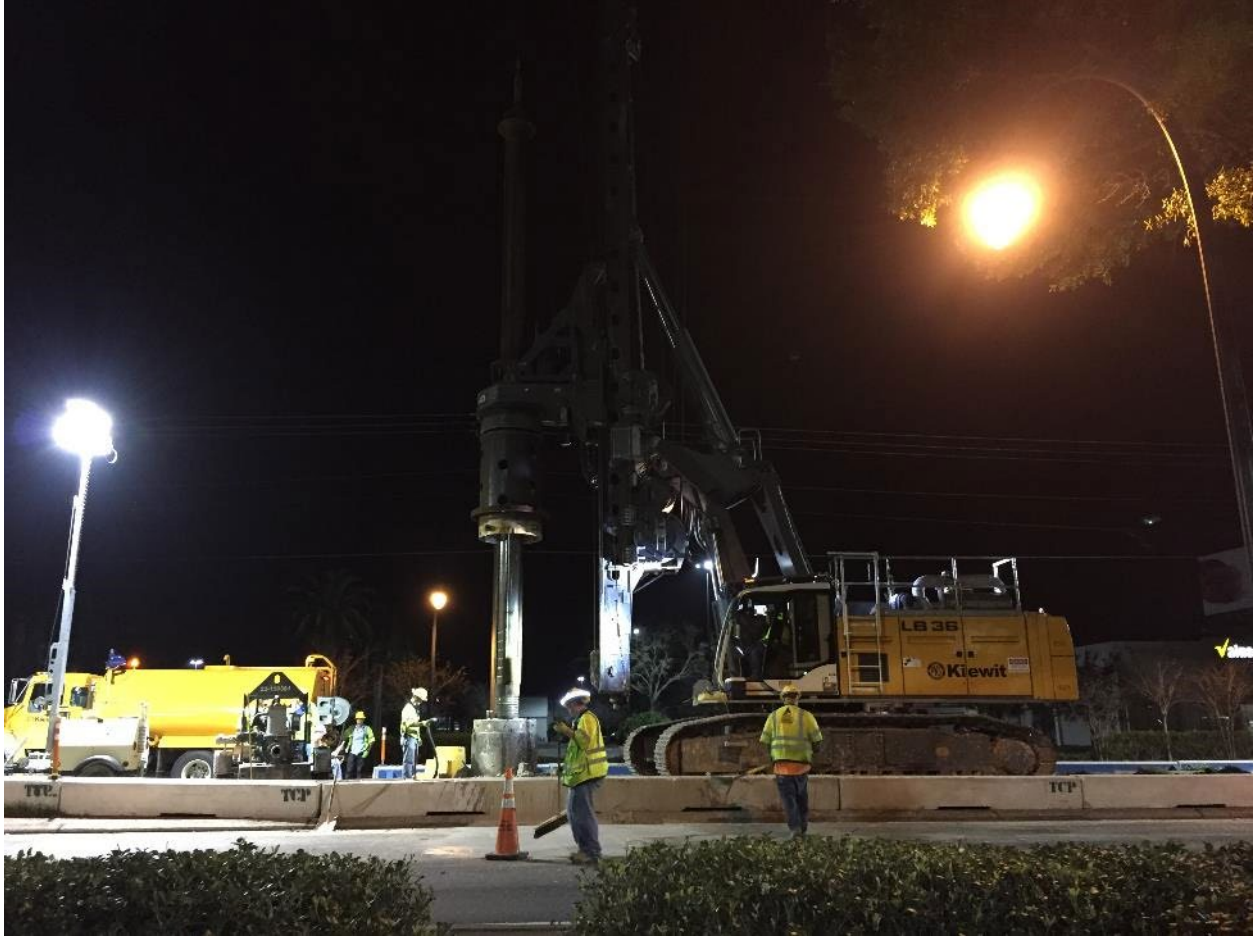
Figure 2-11. Drilling Test Shaft 2.

Figure 2-12. Drilling Test Shaft 4.

2.4 *Raw Data Profiles of Drilling Parameters*

As previously discussed, two drillers were used by the drilling contractor at the Selmon Parkway site. Driller A completed Test Shaft 3 and Driller B completed Test Shafts 2 and 4. The raw data drilling profiles are presented below in Figures 2-14 through 2-16. For each of the shafts installed, the same drilling tool (rock drilling bucket, Figure 2-13) was used for the entirety of each drilling until cleanout was conducted. The cleanout bucket was used only at the end of each drilling and because the researchers did not have time to re-zero the depth sensor, false penetration is displayed at the end of Test Shafts 3 and 4 (Figures 2-14 and 2-16). This is because the cleanout bucket is shorter in length than the drilling bucket and therefore gives an incorrect depth reading if the depth sensor is not re-zeroed after the tooling was switched.
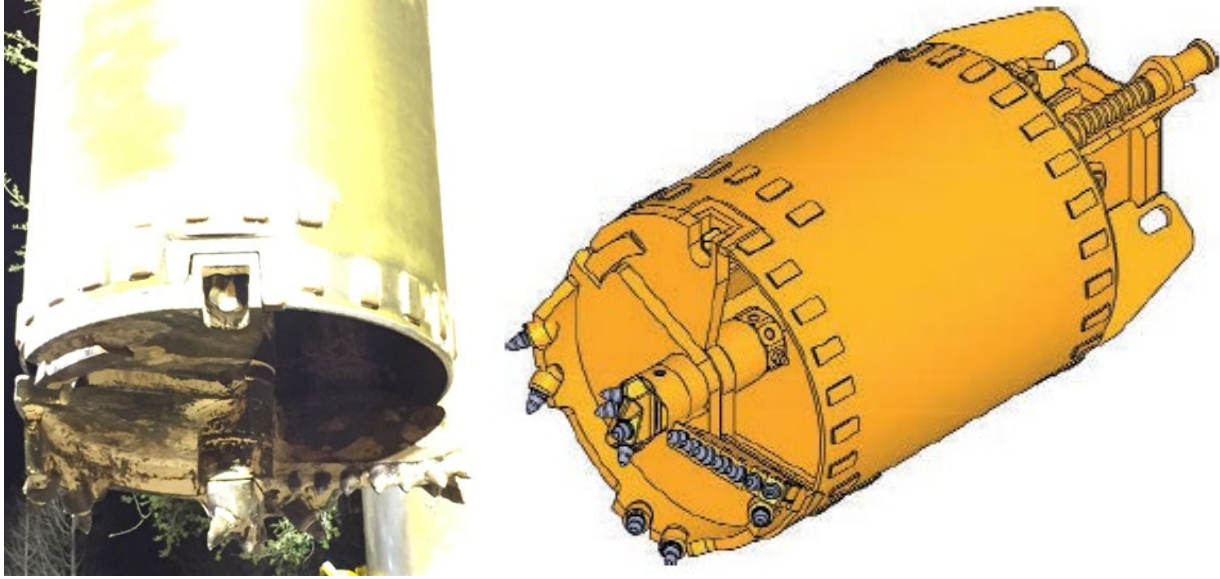
Figure 2-13. Bauer KBF-K rock drilling bucket.

Figure 2-14. Test Shaft 3 - raw data drilling profile.

Figure 2-15. Test Shaft 2 - raw data drilling profile.

Date : 2/20/2018
Begin : 9:41:57 PM
End : 2:49:05 AM

Rig : BAT410
Drill Depth : 0'0" – 108'8"

Test Shaft 4

DRDPR 2.10/DialogMX 945 EPF5.14.32

Penetration rate (in/min)	Rotation (rev/min)	Torque (psi)	Crowd (psi)
0 500 1000	0 17.5 35	0 1500 3000	0 1750 3500

www.jeanlutz.com
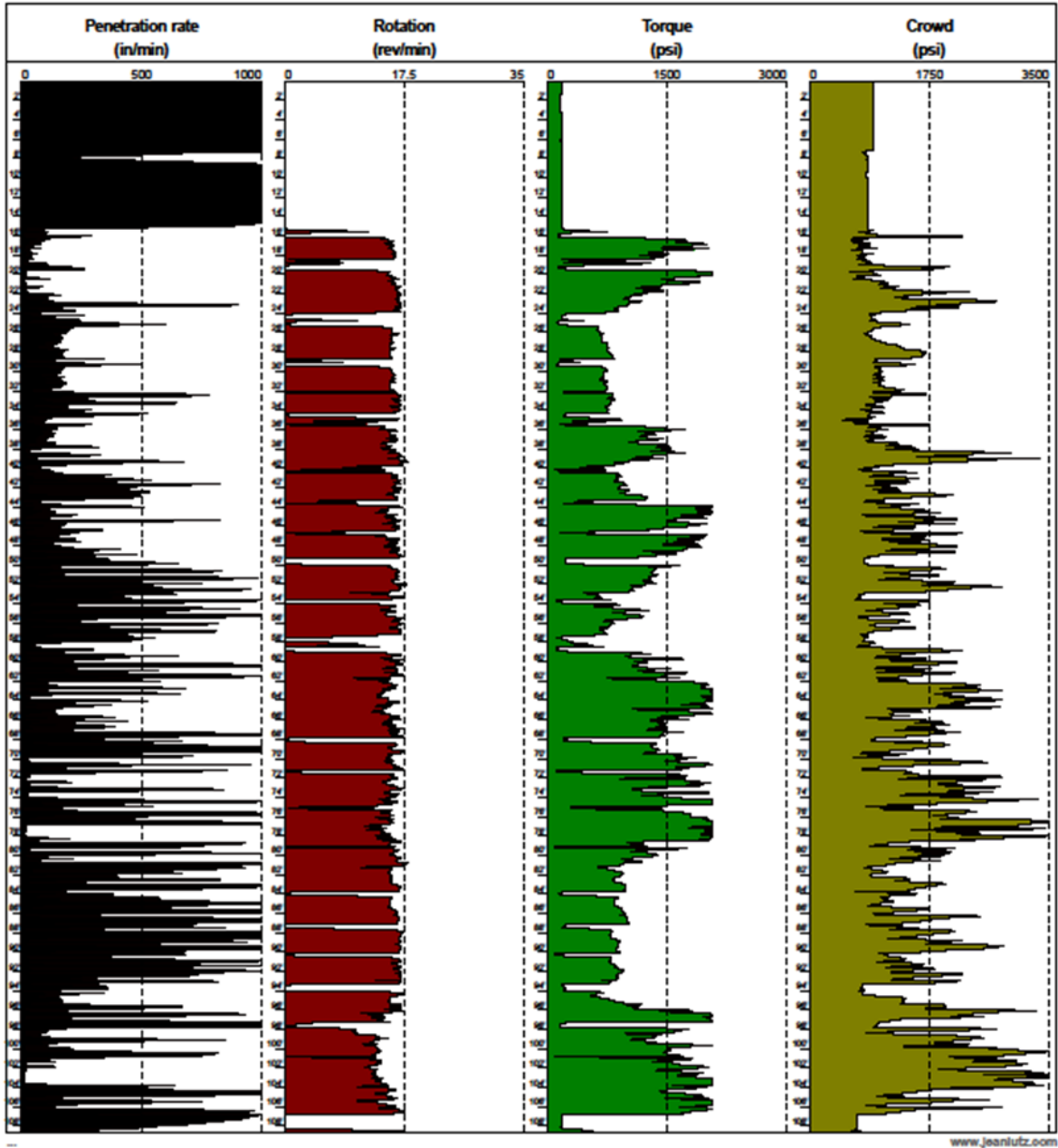
Figure 2-16. Test Shaft 4 - raw data drilling profile.

A review of Figure 2-14 suggests Driller A had a consistent drilling style. This produced limited loss of MWD data to use in comparison with the load test data. Comparing Figure 2-14 with Figures 2-15 and 2-16, it can be seen that Driller B's drilling style was far less consistent. There are several breaks in the drilling profiles that are likely a result of improper drilling which leads

19

to a loss of recovered MWD data. As stated, Driller A had the luxury of drilling a full length shaft (Test Shaft 1) at the site with the drill rig prior to being monitored during Test Shaft 3. Speaking with Driller B during the installation of Test Shaft 4, he stated that he was having difficulty seeing his rotary table, which may have led to some of his issues. He also informed the UF research team that Test Shaft 2 was his first time ever operating this particular drill rig. Driller B's second drilling (Test Shaft 4) does show improvement in his drilling method compared to his first drilled shaft (Test Shaft 2). This suggests a true benefit to installing a method shaft which is quantifiable through MWD.

UF researchers speculated that the loss of data from Driller B's shafts is from letting out too much cable from the main winch (attached to the Kelly bar) while reintroducing the drill bit down the hole, prior to advancing the drill bit with the rotary table to a lower depth than previously achieved. The DIALOG and the Litronic system track drill bit penetration by the rotation of the main winch. The drill rig controls the actual drill bit penetration via the rotary table which clamps down on the Kelly bar and pushes (crowd) the drill bit downward. There should not be slack in the main winch cable attached to the Kelly bar. When too much cable is let out and there is slack between the main winch and Kelly bar, the system records penetration that has not actually occurred and results in a loss of actual drilling data. In this scenario, the DIALOG would record high penetration, zero rotation, a baseline torque pressure, and a slightly higher than baseline pressure for crowd. The slightly higher crowd value is likely a result of the actual bit moving downward to the previous depth but not at the same rate in which the cable was being let out. This is similar to lowering the bit through a voided section as seen in the first five feet in Test Shaft 3 (Figure 2-14), where the surface casing was installed and drilled out prior to monitoring, and in the cleanout sections of Figures 2-15 and 2-16.

3. Data Reduction and Analysis – Selmon Parkway

3.1 *Converting Torque and Crowd for Specific Energy Assessment*

Prior to the assessment of specific energy from MWD, hydraulic torque and crowd must be converted to physical measures that are compatible with the specific energy equation. This requires gathering drill rig specifications from the operator's manual. From the Liebherr LB36-BAT410 manual, the following was identified:

Technical data

Rotary drive - torque	0 – 302,400 lbf-ft
Rotary drive - speed	0 – 37 rpm

Figure 3-1. Drill rig specifications for maximum torque.

↑ ꓕꓲꓲꓲꓲ Rope crowd system

Crowd force push/pull	89,925/89,925 lbf

Figure 3-2. Drill rig specifications for maximum crowd.

Hydraulic system

The main pumps are operated by a distributor gearbox. Axial piston displacement pumps work in open circuits supplying oil only when needed (flow control on demand).
The hydraulic pressure peaks are absorbed by the integrated automatic pressure compensation, which relieves the pump and saves fuel.

Pumps for working tools	2x 92.4 gal/min
Separate pump for kinematics	47.6 gal/min
Hydraulic oil tank	211 gal
Max. working pressure	5076 PSI

Figure 3-3. Drill rig specifications for maximum operating pressure.

To summarize:

- Maximum Torque (T_{max})= 302,400 ft-lbf = 3,628,800 in-lbf

- Maximum Crowd (F_{max}) = 89,925 lbf
- Maximum Operating Pressure (P_{max}) = 5,076 psi
- Hydraulic Flow Rate (Q) = 184.8 GPM = 42,688.8 in³/min

3.1.1 Converting Torque

From the specifications gathered, the maximum motor displacement (δ_{max}) can be determined:

$$\delta_{max} = \frac{2\times\pi\times T_{max}}{P_{max}} = \frac{2\times\pi\times3,628,800\ in-lbf}{5076\ psi} = 4,492\ {in^3}/{rev} \tag{Eq. 3-1}$$

Next, the minimum rotational speed (N_{min}) that coincides with T_{max} can be determined:

$$N_{min} = \frac{Q}{\delta_{max}} = \frac{42,688.8\ in^3/min}{4,492\ in^3/rev} = 9.5\ RPM \tag{Eq. 3-2}$$

The value of N_{min} indicates that in a rotational speed range of 0 to 9.5 RPM, the maximum torque of 3,628,800 in-lbf can be achieved. This rotational speed range is commonly referred to as "Rock Drilling Mode" on modern drill rigs. At rotational speeds above 9.5 RPM, the maximum torque available begins to decrease and can be determined by Equation 3-3:

$$T = \frac{PQ}{2\times\pi\times N} \tag{Eq. 3-3}$$

From the information gathered, a torque versus rotational speed chart can be developed.
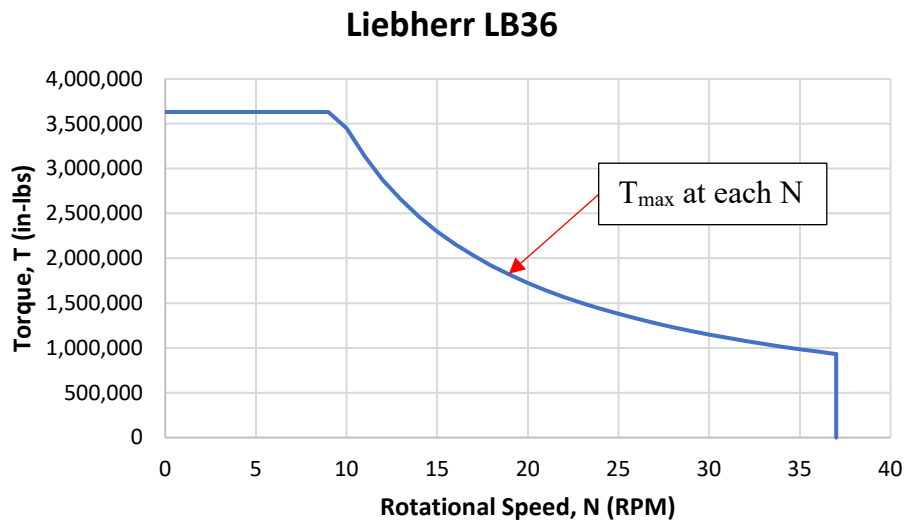
Figure 3-4. Liebherr LB36 BAT-410 T-N chart.

The blue line in Figure 3-4 indicates the maximum torque that can be achieved at any rotational speed for the given drill rig. The torque requirement is a function of the penetration rate and the

strength of the rock encountered. To optimize the drilling process, the rotational speed can be adjusted to maintain an efficient penetration rate based on the material encountered and the torque requirement. For example, during rock drilling more torque is required to break apart the strong cohesive bonds of the rock and lower RPMs are ideal, whereas, drilling through soil (discontinuous mass) or IGM (weaker bonding) less torque is required and higher RPMs are ideal to achieve higher penetration rates. These concepts also suggest that an optimum penetration rate for each rotational speed is achieved when the available torque is at a maximum. However, this approach is likely not ideal in terms rig efficiency as it could lead to quicker rig wear and downtime for repair. Therefore, a balance must be maintained between rig efficiency and drilling efficiency.

3.1.2 Converting Crowd

To convert crowd, a conversion coefficient (K_F, force/pressure) must be developed. The following rig specific parameters were gathered for crowd including the crowd baseline pressure (the pressure required to circulate the hydraulic fluid through the system) was determined from the drill rig after it was warmed up, Figure 3-5:

- Maximum Crowd (F_{max}) = 89,925 lbs
- Maximum Operating Pressure (P_{max}) = 5,076 psi
- Crowd Baseline Pressure (BP_{Crowd}) = 595 psi

Solve for K_F using the identified and measured input parameters:

$$K_F = \frac{F_{max}}{P_{max} - BP_{Crowd}} = \frac{89,925\ lbf}{5,076\ psi - 595\ psi} = 20.1\ \frac{lbf}{psi} \tag{Eq. 3-4}$$

The developed conversion coefficients will then be used to transform the "real time" measured crowd hydraulic pressures to physical measures (lbf) as presented in Equation 3-5.

$$F\ (lbf) = K_F \left(\frac{lbf}{psi}\right) \times [F_{Pressure}(psi) - BP_{Crowd}(psi)] \tag{Eq. 3-5}$$

where,

$F_{pressure}$ = the crowd operating pressure applied during drilling.

After conversion takes place, measurements of torque and crowd become compatible with Teale's specific energy equation (Eq. 1-1).
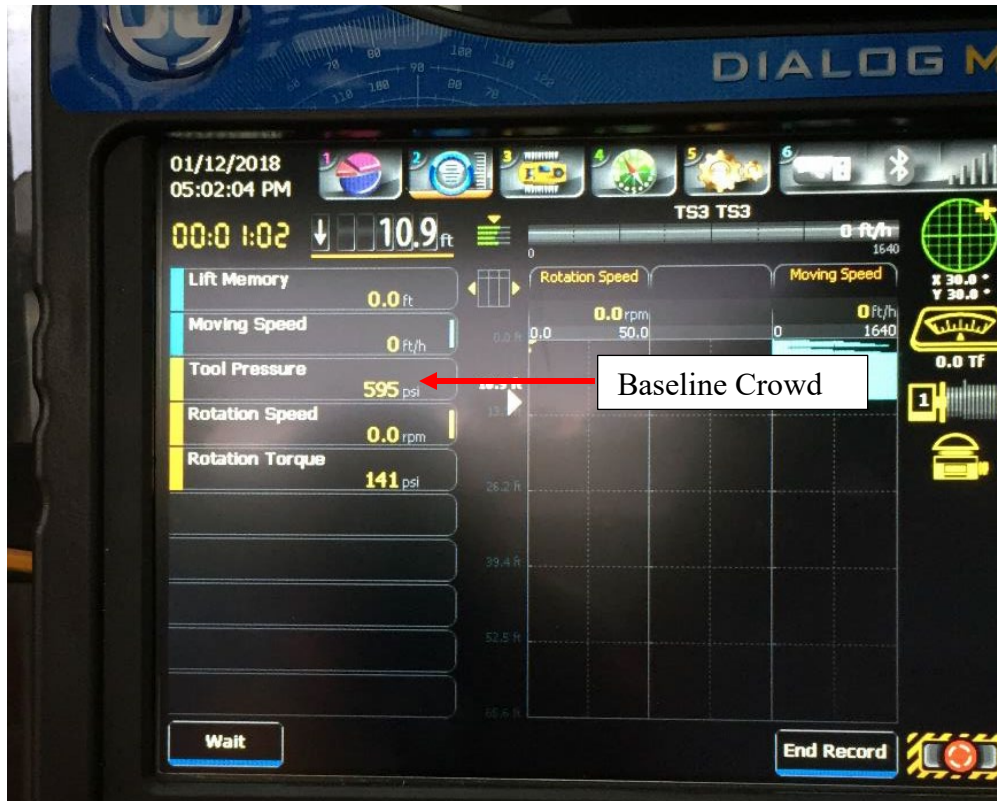
Figure 3-5. Identifying baseline pressure for crowd after warming up the hydraulics.

3.2 Initial Correlation

From the monitored data collected at Selmon Parkway, the researchers determined there were 12 potential data points (i.e., 12 mobilized shaft segments with MWD data) that could be used to develop correlation between specific energy (e) and side shear (f_s) based on the load test and MWD data. Of the 12 data points, 10 were initially considered valid based on mobilization of the section and limited loss of MWD data within each respective section. Using the 10 valid data points, a preliminary correlation was developed between MWD specific energy and the nominal side shear obtained from the load test results (Figure 3-6). The remaining 2 data points were further investigated and will be discussed throughout the following sections as well as corrections made to the reported load test values for Test Shaft 2 (TS 2).
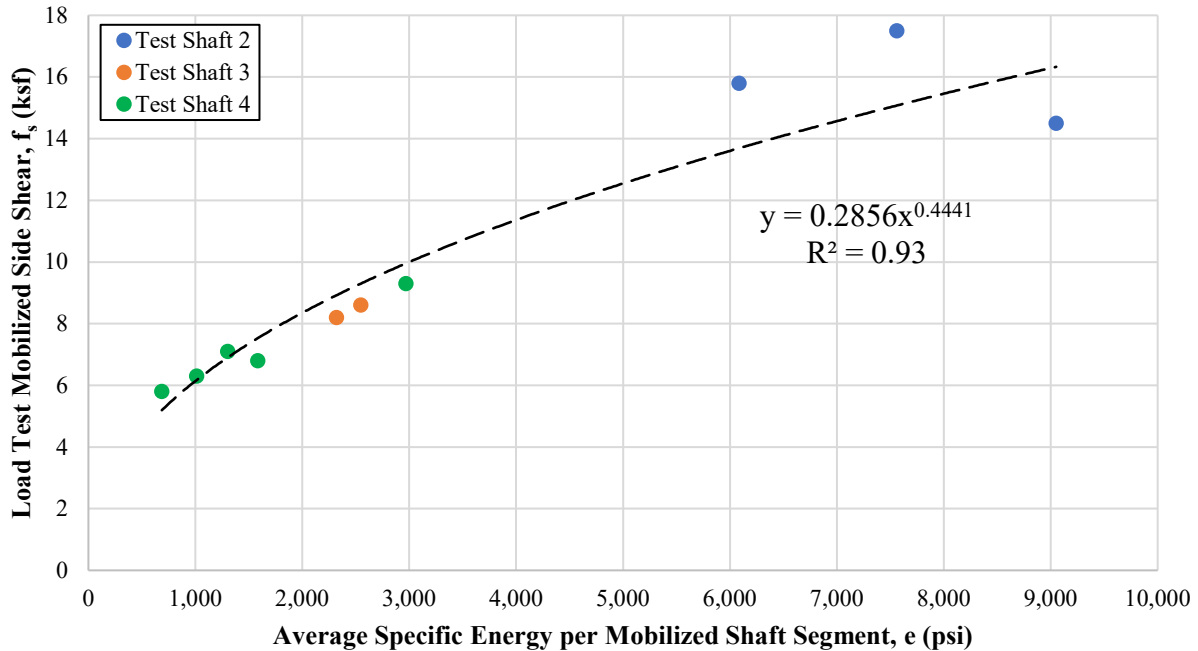
Figure 3-6. Preliminary side shear versus specific energy curve.

3.3   *Load Test Mechanics*

In order to properly convey the logic in determining valid data points, the mechanics and operation of the load tests must first be discussed. For each of the three load tested shafts, Osterberg cells (O-cells) were placed in two locations of the shafts. For each shaft, there was an upper and lower O-cell. During the load tests, the shafts were loaded in three separate stages which are depicted in Figure 3-7. The loading operations were as follows:

A) Stage 1. The upper O-cell is locked, and the lower O-cell is loaded. The intent of Stage 1 is to use the soil/rock resistance in the portion of the shaft above the lower O-cell to mobilize the section below the lower O-cell. A soft toe device was placed at the base of the shaft in an attempt to remove the influence of end bearing thereby providing isolated side shear within the lower section of the shaft during Stage 1 loading.

B) Stage 2. The lower O-cell is vented (open), and the upper O-cell is loaded. The intent of Stage 2 is to use the soil/rock resistance in the portion of the shaft above the upper O-cell to mobilize the section between the upper and lower O-cells. The lower O-cell is vented in attempt to remove any end bearing which ideally provides isolated side shear within the segment between the O-cells.

C) Stage 3. The lower O-cell is locked, and the upper O-cell is loaded. The intent of Stage 3 is to use the soil/rock resistance in the portion of the shaft below the upper O-cell to mobilize the section above the upper O-cell. This creates an isolated side shear condition in which the buoyant weight of the upper shaft segment must be considered in order to properly calculate the side shear resistance.

25
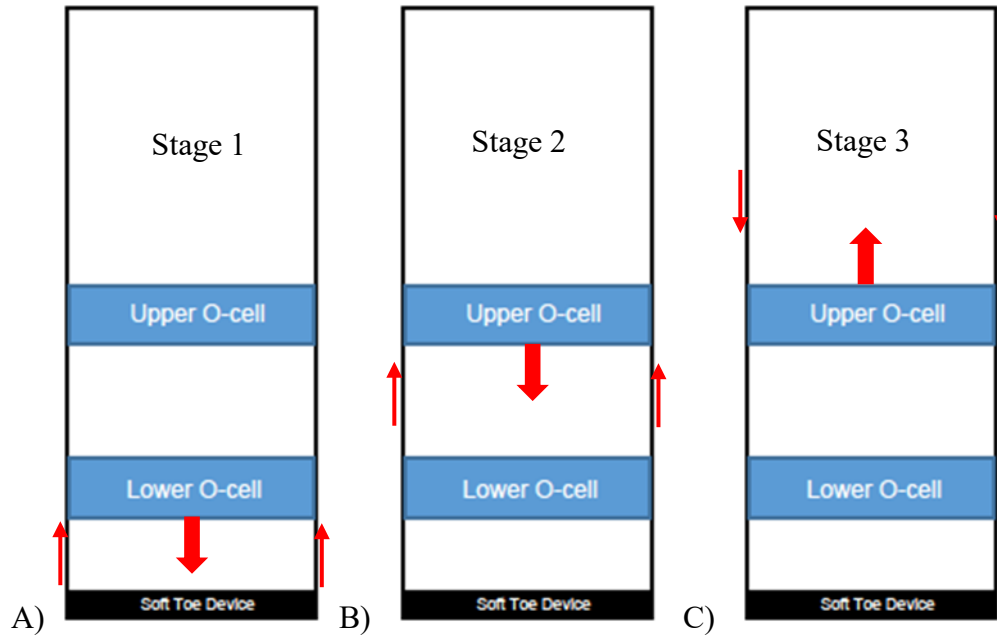
Figure 3-7. Load Test Stages

3.4 *Test Shaft 2 Segment 18 and Toe Segment*

Segment 18 was located below the lower O-cell in Test Shaft 2 and was mobilized during Stage 1 loading. The final displacement was 1.130 inches with a final unit side shear value of approximately 17 ksf based on the T-Z curve (Figure 3-8). However, due to the irregular shape of the T-Z curve, the engineers that analyzed the load test could not draw a final conclusion on the proper side shear value to report. The load test report stated, "Some engineering judgment will be required to determine the appropriate design unit side shear value for this portion of shaft". Although the final displacement is somewhat larger than expected (typically 0.4 to 0.6 inches) for limestone mobilization, this degree of displacement was not uncommon for shaft mobilization at the site. The side shear measurement at the final displacement is also in agreement with the three segments above the mobilized section, where side shear values ranged from 13.7 to 17.1 ksf. The boring in the footprint of the shaft (Figure 3-9) also indicated similar strength rock was present in all four of the aforementioned segments. However, the associated displacements for the three segments above Segment 18 were all approximately 0.33 inches. Based on the final MWD specific energy-side shear correlation, MWD provided an estimated side shear value of 16.4 ksf which is in agreement with the range from the three segments above Segment 18 and the boring. When Segment 18 and the Toe Segment are combined, MWD indicated an average side shear value of 14.8 ksf which is in good agreement with the average from the three segments above Segment 18. The average for the three segments above Segment 18 was 15.1 ksf from MWD and 15.5 ksf from the load test. These observations indicate that MWD could be used to make an informed engineering decision as to which side shear values should be considered in design. For the final correlation developed, Segment 18 and the Toe Segment were combined. A side shear value of 14.8 ksf was used in the final specific energy correlation.

Lower Section Unit Side Shear (τz)
Selmon West Extension
LT-2 – Stage 1 - Loading Lower Cell Level
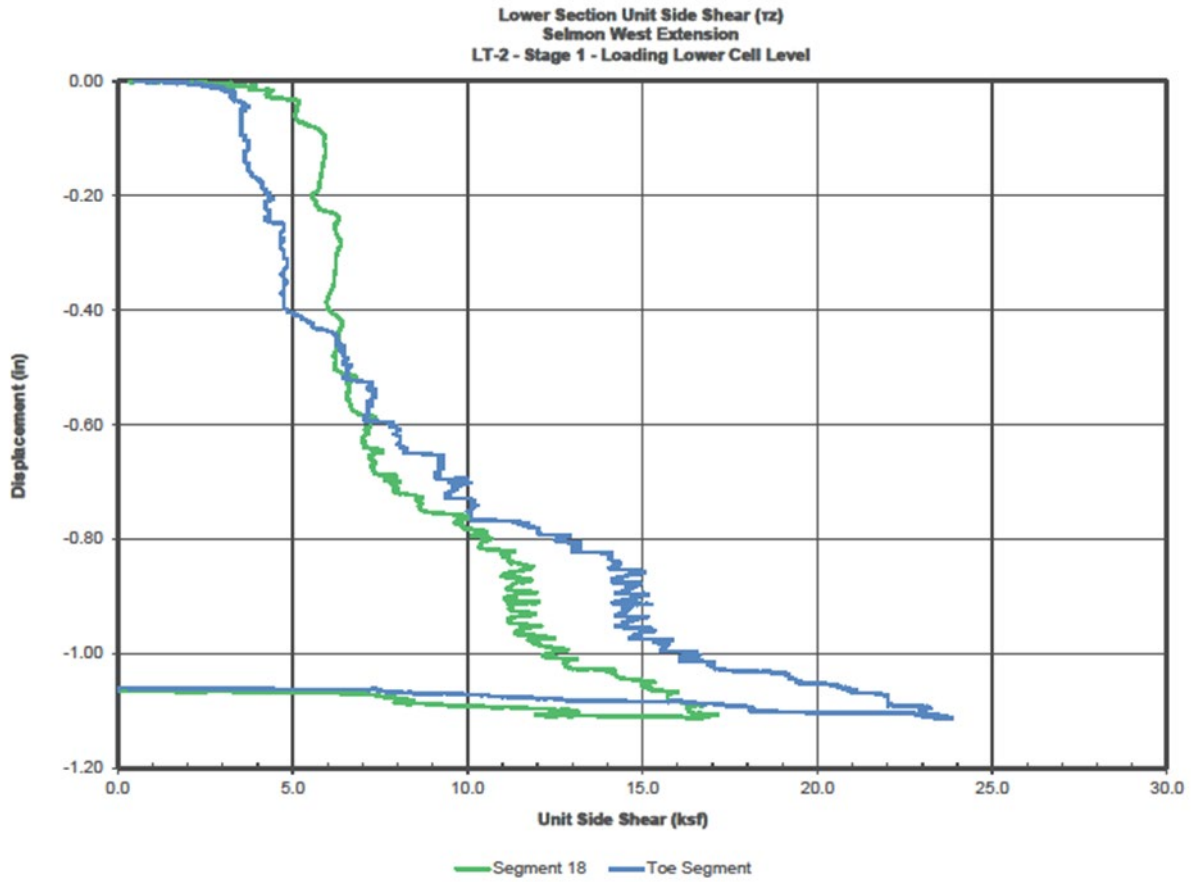
Figure 3-8. T-Z curve from Test Shaft 2, Segment 18 and Toe Segment.

LT-2 Ø42" x 116' Test Shaft - AsBuilt
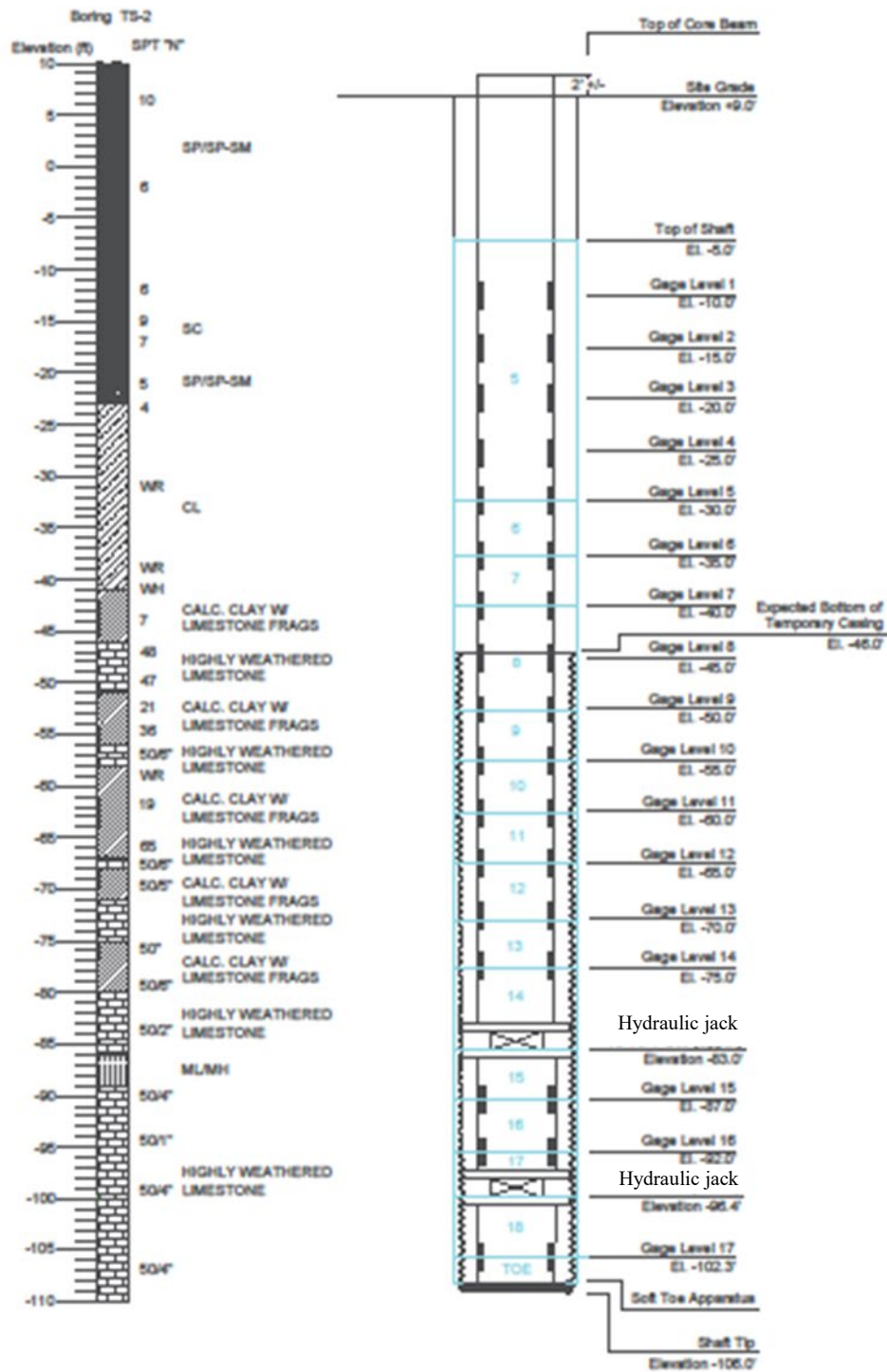
Figure 3-9. Test Shaft 2 boring profile and instrumentation locations.

3.5   *Test Shaft 3 Segment 13*

Segments 12 and 13 were located between the upper and lower O-cells in Test Shaft 3. Per the load test report, Segment 12 was mobilized in Stage 2 and Segment 13 was mobilized in Stage 3. Load transfer to the lower O-cell was observed in Stage 2 which is what terminated the stage and indicates the isolated shear resistance was likely mobilized in both Segments 12 and 13. The final displacement in Stage 2 was 1.71" and the peak resistance in Segment 12 first occurred at approximately 1.25" of displacement. However, the reported side shear value for Segment 13 was from Stage 3 loading at 5.9" of displacement (Figure 3-10). It is the researchers' opinion that 5.9" of displacement is excessive and the side shear value for Segment 13 should have been reported from Stage 2 at approximately 1.25" which corresponds to a skin friction value in the range of 6.5 to 7 ksf. Side shear estimated from MWD was 6.7 ksf. A side shear value of 6.7 ksf was used in the final specific energy correlation.
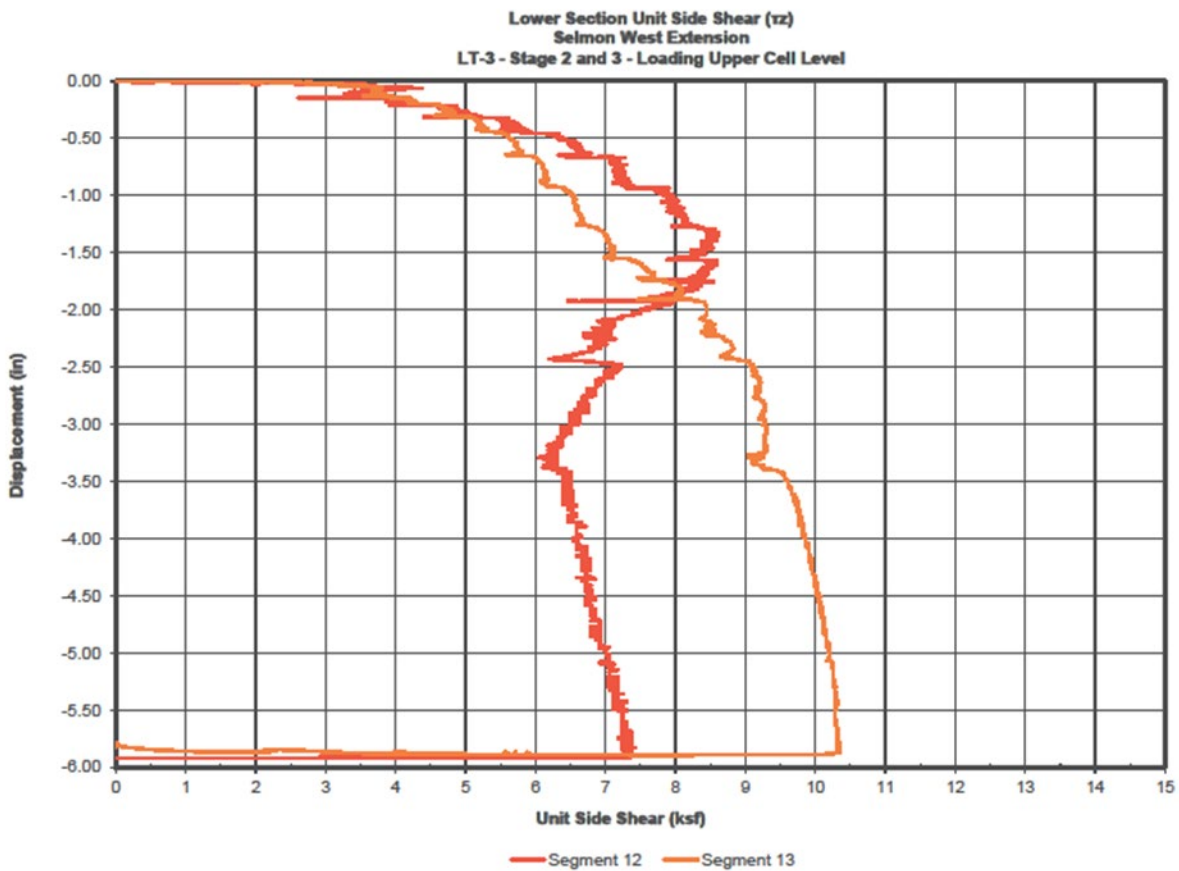
Figure 3-10. T-Z curve from Test Shaft 3, Segments 12 and 13.

3.6   *Test Shaft 2 Load Test Corrections*

Segments 15, 16, and 17 were located between the upper and lower O-cells in Test Shaft 2. The load distributions were corrected by the researchers due to miscalculations observed in the load test report. In general, the average side shear from MWD (15.1 ksf) was in good agreement with

the average load test side shear (15.5 ksf) within the portion of the shaft, where isolated shear was observed throughout Stage 2 loading (i.e., no load transfer was observed in the lower O-cell). However, observations of Figure 3-6 (preliminary correlation) show higher variability in this portion of the specific energy-side shear relationship. Upon inspection of the load distribution for Stage 2 loading, it was observed that the loads used to determine the final side shear values were inaccurate. The correct peak loads that occurred at the final displacement of 0.33" were then identified and used to recalculate the respective side shear values. A caliper profile provided in the load test report was used to estimate the appropriate shaft diameters for each segment. Figure 3-11 provides the load distribution and Table 3-1 provides the corrected side shear values. These values were used to build the final correlation between MWD specific energy and load tested side shear.
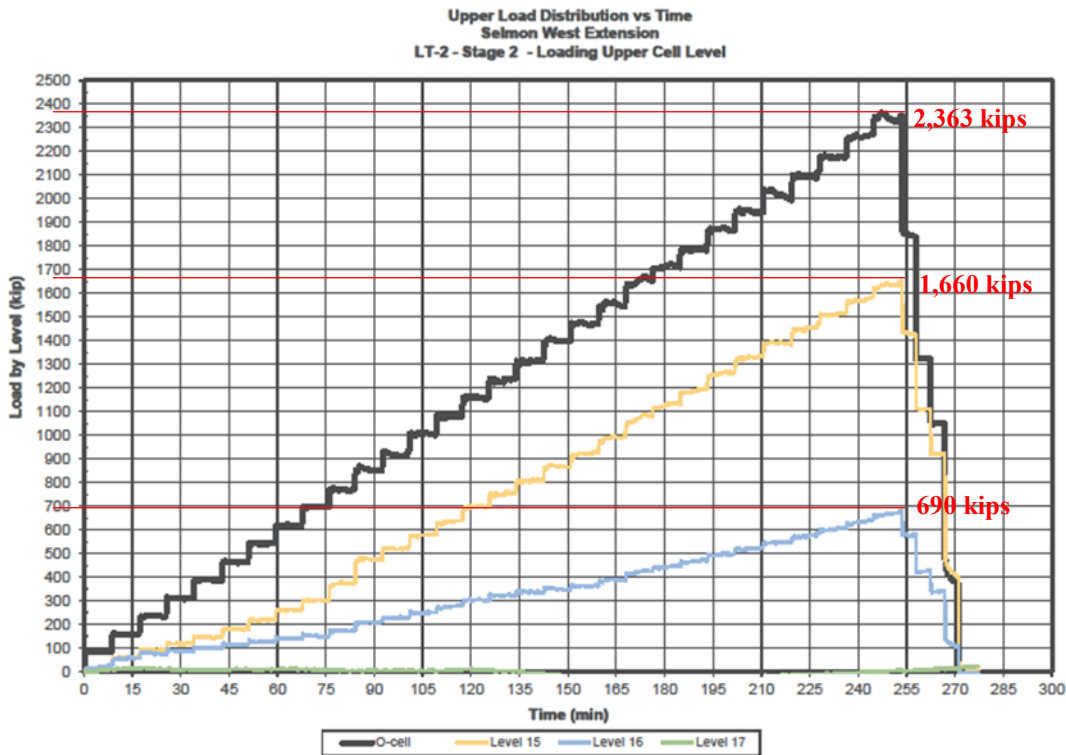
Figure 3-11. Test Shaft 2 load distribution with corrections.

30

Table 3-1. Test Shaft 2 side shear corrections.

	Test Shaft 2 - Load Distribution Side Shear Calculations					
Segment	EL_{TOP} (ft)	EL_{BOT} (ft)	D (in)	P_1 (kips)	P_2 (kips)	f_s (ksf)
15	-83.0	-87.0	43.8	2,363	1,660	15.3
16	-87.0	-92.0	43.4	1,660	690	17.1
17	-92.0	-96.4	43.6	690	0	13.7

3.7   *Building Correlation and Comparative Analysis*

From all three test shafts, 12 data points were used to develop the final correlation between MWD specific energy and load test side shear. This included four segments from Test Shaft 2, three segments from Test Shaft 3, and five segments from Test Shaft 4. The side shear values ranged from 5.8 ksf to 17.1 ksf; and the specific energy values ranged from 686 psi to 9,051 psi (99 ksf to 1,303 ksf). When similar units are compared (ksf), the specific energy range is two orders of magnitude greater than the side shear range, which provides good sensitivity for real-time MWD side shear estimations. Figure 3-12 provides the final correlation, and Table 3-2 provides the summary of statistics with the MWD results compared to the load test results. Table 3-2 specific energy calculations start with calculating the specific energy for each individual data point as shown in Equation 1-1. Once the specific energy has been calculated for each individual data point, an average specific energy value is then calculated for a specified elevation range that corresponds to each load test shaft segment. These average values for each shaft segment, comprising each respective individual data point, are presented in Table 3-2 to develop a correlation between specific energy and side shear.
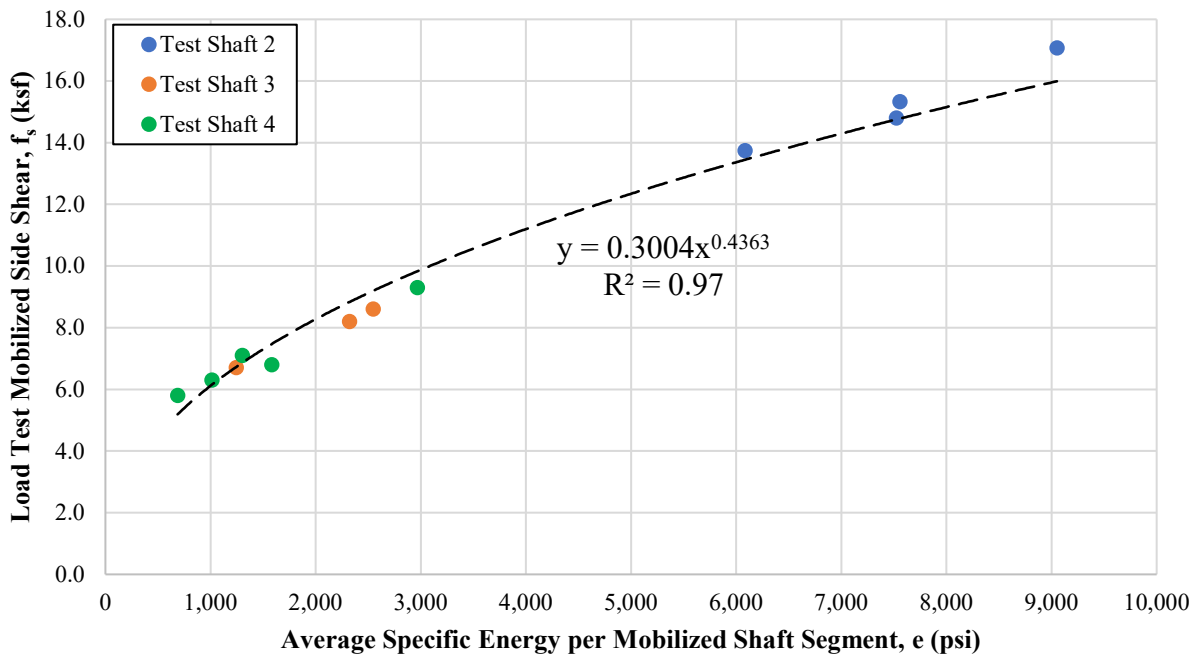
Figure 3-12. Specific energy-side shear correlation at Selmon Parkway using a rock bucket.

Note: The sensitivity of the individual data point specific energy calculations are dependent upon the significant figures used in the calculation.

As observed in Figure 3-12, excellent correlation ($R^2 = 0.97$) was found between specific energy and unit side shear at the Selmon Parkway site using a unique drilling tool (Bauer rock drilling bucket). Based on the developed correlation, MWD side shear estimates were calculated and compared to the load test results reported in each respective segment (Table 3-2). From Table 3-2, the average error between the load test results and the MWD estimates was negligible. These results indicate that MWD could have been used during production shaft drilling (assuming the same drilling tool was used) to ensure the required shaft capacities were achieved at each shaft location; thereby providing reliability that the as-built foundations can sustain the intended loading with tolerable shaft displacement and settlement of the superstructure.

Table 3-2. Summary of statistics and side shear comparison between load test results and MWD.

Specific Energy-Side Shear Correlation Summary of Statistics								
Test Shaft	Segment	EL_{Top} (ft)	EL_{Bot} (ft)	e (psi)	e (ksf)	LT f_s (ksf)	MWD f_s (ksf)	% Error
2	15	-83	-87	7,559	1,089	15.3	14.8	-3.4%
	16	-87	-92	9,051	1,303	17.1	16.0	-6.3%
	17	-92	-96.4	6,086	876	13.7	13.5	-1.7%
	18/Toe	-96.4	-106	7,525	1,084	14.8	14.8	0.0%
3	12	-61	-68.1	2,548	367	8.6	9.2	7.0%
	13	-68.1	-73	1,243	179	6.7	6.7	0.0%
	Toe	-73	-81.3	2,321	334	8.2	8.8	7.3%
4	5	-25	-30	686	99	5.8	5.2	-10.3%
	10	-50	-58	1,013	146	6.3	6.2	-1.6%
	11	-58	-63	1,302	188	7.1	6.9	-2.8%
	12	-63	-67	1,582	228	6.8	7.5	10.3%
	16.2	-88	-93.5	2,969	427	9.3	9.8	5.4%
							Average Error =	0.3%

3.8 *Rock Strength Assessment*

Per the scope of work, rock strength assessment for unconfined compression strength (q_u) was needed to compare with core strengths recovered from the site and tested in the laboratory. In the prior drilled shaft project (BDV31-977-20), direct correlation was developed between specific energy and q_u in a small-scale drilling environment using rock augers. Displayed in Figure 3-13, the mechanical efficiency of a rock drilling bucket differs from that of a rock auger. Consequently, the previously developed rock auger specific energy-unconfined compression strength correlation could not be used with the rock drilling bucket to estimate q_u. Therefore, the researchers had to develop an alternative approach to estimate q_u via MWD while drilling with the rock drilling bucket.
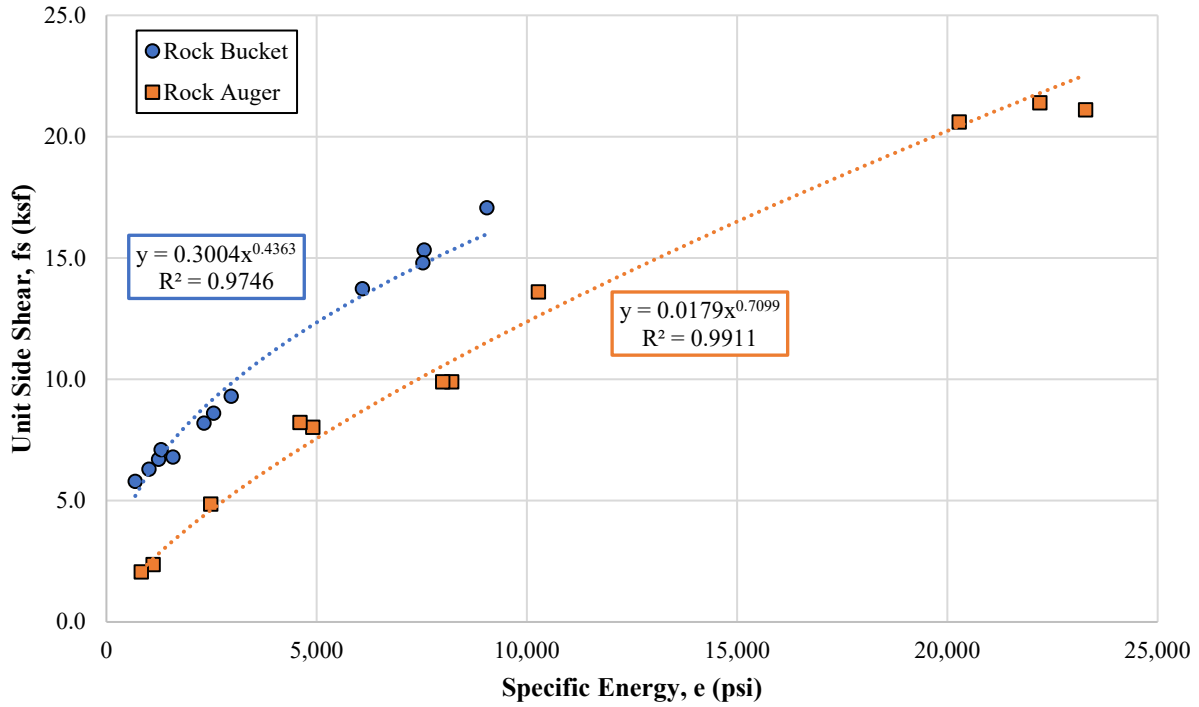
Figure 3-13. Comparison of mechanical efficiency between a rock bucket and a rock auger.

In the prior study (BDV31-977-20) and reported in Rodgers et al. (2018d), excellent side shear estimates were made using the FDOT's Soils and Foundation Handbook (SFH, FDOT 2015) recommended side shear equation (McVay et al., 1992) with q_u measured via MWD. In order to use McVay et al. for real time side shear assessment via MWD, the estimation of tensile strength (q_t, direct tension) was also needed. This led to the development of a new equation (Florida Geomaterials Equation) that defined the general relationship between q_u and q_t which can be found in Rodgers et al. (2018d). Based on the developed relationship, predictions of q_u were made using q_{st} (splitting tension) data collected at the same 23 sites spread across Florida. It was found that the predictions were in excellent agreement with the measured q_u values which is presented in Figures 3-14 and 3-15 (full details including the relationship between direct tension and splitting tension can be found in Rodgers et al. 2018d).
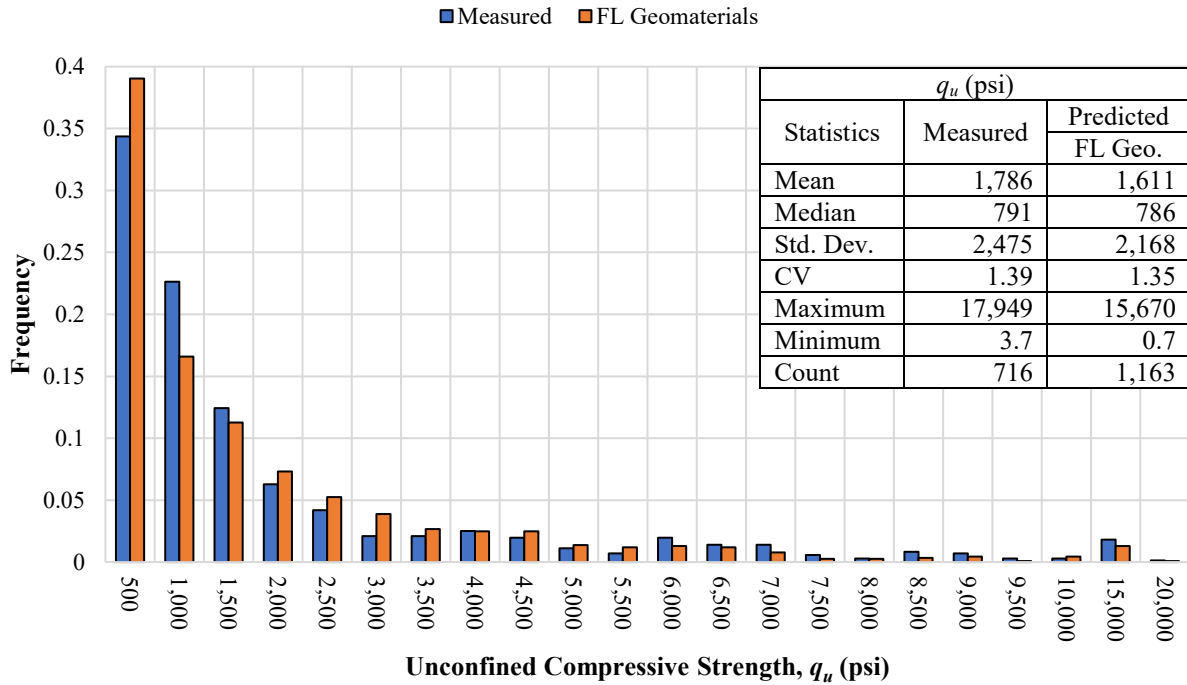
Figure 3-14. Frequency distribution comparing predicted q_u values with measured q_u values.
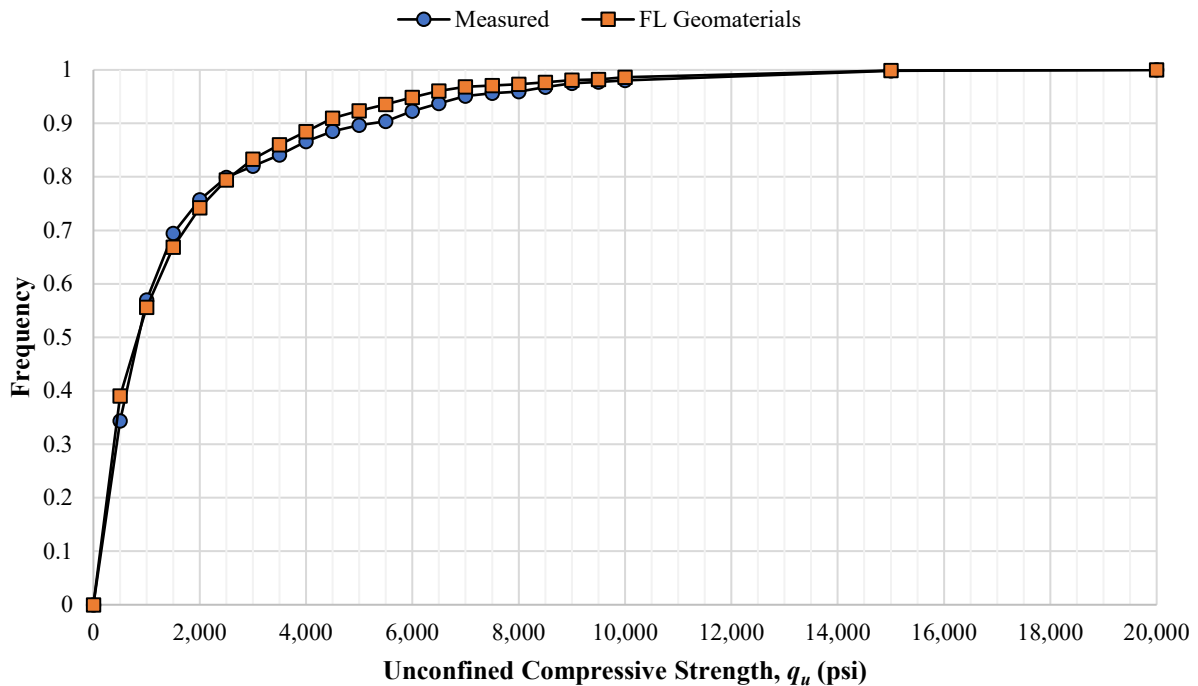
Figure 3-15. Cumulative Frequency distribution comparing predicted and measured q_u values.

These observations in combination with the excellent side shear predictions (compared to mobilized load test sections) indicated the developed relationship between q_u and q_t provides a

good estimate of tensile strength based on measured unconfined compression strength. This also provides a means to estimate q_u using load tested and MWD side shear values. First, the Florida Geomaterials equation (Eq. 3-6) must be integrated into the SFH recommended side shear equation (Eq. 3-7) to get the final equation (Eq. 3-8) provided in Rodgers et al. (2018d) in which f_s can be directly calculated using q_u and the SFH equation without the need for q_t (direct tension). Then, the equation must be rearranged to solve for q_u based on measured f_s. The following provides the equation development.

Substituting the Florida Geomaterials equation,

$$q_t = 0.436 \times q_u^{0.825}$$ (Eq. 3-6)

into the skin friction equation developed by McVay et al.,

$$f_s = \frac{1}{2} \times q_u^{0.5} \times q_t^{0.5}$$ (Eq. 3-7)

f_s can be solved directly using only q_u,

$$f_s = 0.3302 \times q_u^{0.9125}$$ (Eq. 3-8)

rearrange Equation 3-9 to solve for q_u based on measured f_s,

$$q_u = \left(\frac{f_s}{0.3302}\right)^{\left(1/0.9125\right)}$$ (Eq. 3-9)

Equation 3-9 was used to estimate q_u based on f_s measured from the load test results and MWD for rock strength assessment which produced a new relationship between specific energy and q_u for the rock drilling bucket (Figure 3-16).
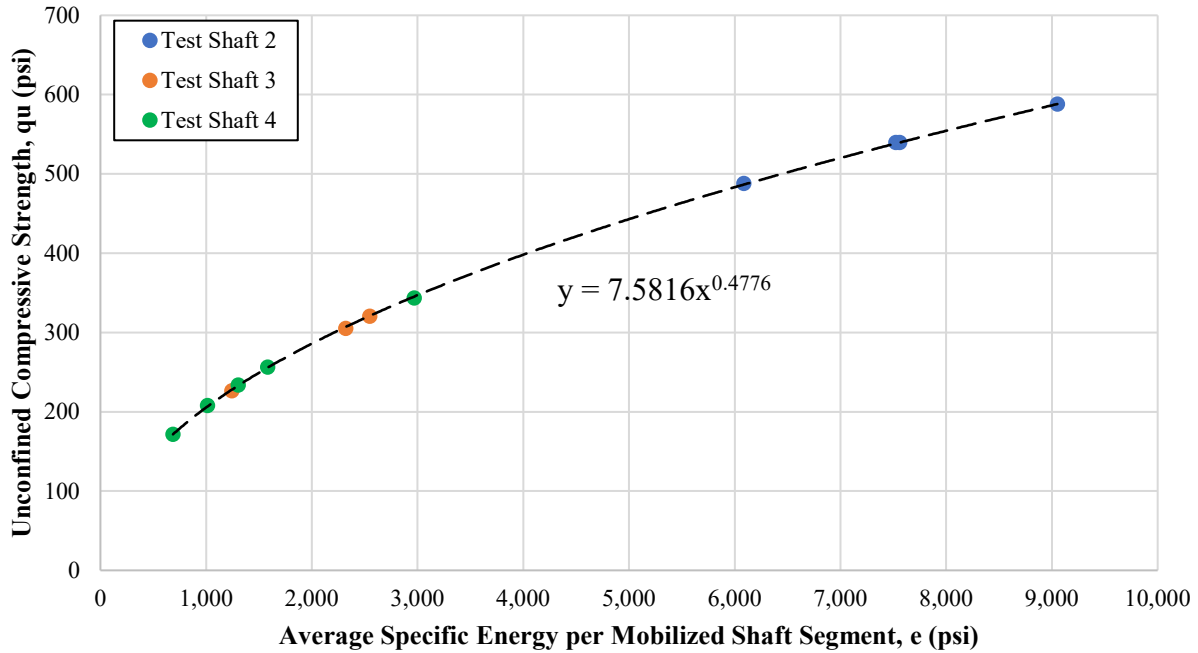
Figure 3-16. q_u vs. e correlation using a rock drilling bucket.

3.8.1 Preliminary Rock Strength Assessment

Using the relationship between specific energy and q_u in Figure 3-16, q_u was estimated for each individual MWD data point. The averages for each segment were then compared to the respective load test estimated q_u which is found in Table 3-3.

Note: Segment 18/Toe from Test Shaft 2 and Segment 13 from Test Shaft 3 were not used during this initial analysis because engineering judgment was used to estimate the appropriate side shear value for each respective segment (i.e., removing bias).

Table 3-3. Compressive Strength Comparison (Load Test vs. MWD) – All MWD data points.

Test Shaft	Segment	e (psi)	LT q_u (ksf)	MWD q_u (ksf)	% Error
	15	7,559	561	261	-54%
2	16	9,051	631	282	-55%
	17	6,086	497	239	-52%
3	12	2,548	298	277	-7%
	Toe	2,321	283	250	-12%
	5	686	193	145	-25%
	10	1,013	212	158	-25%
4	11	1,302	241	185	-23%
	12	1,582	230	197	-14%
	16.2	2,969	324	270	-17%
				Average Error =	-28%

36

As seen, MWD provided a conservative estimate for q_u compared to the load test data. The conservative nature of the MWD q_u predictions are far more pronounced in Test Shaft 2 where a high degree of layering was encountered. This can be observed to some degree in the boring presented in Figure 3-9. However, the drilling data from Test Shaft 2 provides a better representation of the significant layering encountered at the shaft location. Presented in Table 3-4 are the drilling parameters and strength estimates for a linear foot of drilling from Test Shaft 2.

Table 3-4. Test Shaft 2 MWD measurements.

			Test Shaft 2				
Elevation	Penetration Rate	Rotational Speed	Torque	Crowd	Specific Energy	Side Shear	U.C.S.
El.	u	N	T	F	e	fs	qu
(ft)	(in/min)	(rpm)	(in-lbs)	(lbf)	(psi)	(ksf)	(psi)
-88.05	105.8	14.2	919,162	27,265	586	4.8	151
-88.11	1	13.9	836,185	37,929	50,818	34	1,250
-88.18	532.3	10.8	628,147	32,916	83	2.1	60
-88.24	532.3	10.8	628,147	32,916	83	2.1	60
-88.31	421.1	10.1	748,737	30,182	104	2.3	67
-88.38	19.3	14	643,221	28,547	2,151	8.5	280
-88.44	1.9	14	748,881	37,982	25,011	24.9	894
-88.51	387.6	12.6	571,300	36,570	112	2.4	69
-88.57	183.8	11.2	755,474	33,788	236	3.3	98
-88.64	2.2	14.1	701,132	36,741	20,954	23.1	822
-88.7	441.1	10.1	1,119,894	41,639	148	2.7	79
-88.77	111	14	790,863	36,639	484	4.5	138
-88.83	0.4	13.8	857,710	37,104	150,451	54.5	2,090
-88.9	83.5	13.7	728,158	32,773	574	4.8	150
-88.97	476.1	10.5	891,056	31,023	113	2.4	69
-89.03	85.3	12.7	824,311	26,307	582	4.8	151
-89.1	1.6	13.8	870,136	41,107	34,372	28.6	1,039

Observed in Table 3-4, MWD (specific energy) provides great insight to the true degree of variability in the shaft location where strong layers of limestone are interlaced with weak layers of calcareous clay with limestone fragments, soil, and voids. Initially the cyclic layering was thought to be a result of the drilling operations with a rock drilling bucket. However, upon inspection of drilling data collected in Test Shafts 3 and 4, it can be seen that similar drilling techniques were being applied that are typical of rock augers, core barrels, and tri-cone roller bits based on MWD observations. Presented first is a linear foot of drilling from Test Shaft 3 in which the boring in the footprint indicated limited layering (Table 3-5). As seen in Table 3-5, the drilling operation is far more consistent which is representative of the material encountered. Test Shaft 3 was drilled by a different rig operator than Test Shaft 2, however, the same drilling consistency displayed in Test Shaft 3 was observed by the Test Shaft 2 rig operator while drilling the lower portion of Test Shaft 4 (Table 3-6). The boring in the footprint of Test Shaft 4 also indicated more consistency in the lower portion of the shaft, similar to Test Shaft 3. In the upper and middle portion of Test Shaft 4, some layering was observed but to a lesser extent than Test Shaft 2 (Table 3-7). In these portions of the shaft, larger layers of weathered limestone were interlaced with smaller weak layers of calcareous clay with limestone fragments and soil.

Table 3-5. Test Shaft 3 MWD measurements.

			Test Shaft 3				
Elevation	Penetration Rate	Rotational Speed	Torque	Crowd	Specific Energy	Side Shear	U.C.S.
El.	u	N	T	F	e	fs	qu
(ft)	(in/min)	(rpm)	(in-lbs)	(lbf)	(psi)	(ksf)	(psi)
-67.03	4.0	12	454,340	7,806	6,451	13.8	470
-67.09	5.4	12	435,174	7,103	4,521	11.8	398
-67.16	2.9	12	358,328	5,366	7,044	14.3	490
-67.22	1.1	12	311,678	4,772	16,211	20.6	728
-67.29	15.0	12	416,678	7,300	1,508	7.3	236
-67.35	5.4	12	407,526	6,658	4,255	11.5	386
-67.42	13.9	12	415,655	7,724	1,672	7.7	248
-67.49	3.4	12	392,278	6,246	6,476	13.8	471
-67.55	15.6	12	379,667	7,214	1,364	7.0	225
-67.62	10.7	12	473,414	7,655	2,475	9.1	299
-67.68	12.2	12	416,689	7,128	1,925	8.1	265
-67.75	11.0	12	454,984	7,898	2,319	8.8	290
-67.81	6.0	12	380,857	6,211	3,593	10.7	357
-67.88	3.3	12	334,825	5,283	5,813	13.2	448
-67.94	8.8	12	337,004	6,233	2,164	8.6	280
-68.01	9.7	12	467,676	8,395	2,675	9.4	310
-68.08	16.3	12	548,869	11,067	1,843	8.0	260

Table 3-6. Test Shaft 4 MWD measurements for the lower section.

			Test Shaft 4 - Lower Shaft Section				
Elevation	Penetration Rate	Rotational Speed	Torque	Crowd	Specific Energy	Side Shear	U.C.S.
El.	u	N	T	F	e	fs	qu
(ft)	(in/min)	(rpm)	(in-lbs)	(lbf)	(psi)	(ksf)	(psi)
-91.33	14.2	14	860,816	21,793	3,843	11.0	368
-91.4	13.4	13	904,071	21,076	4,185	11.4	383
-91.47	13.9	14	673,055	25,876	3,054	10.0	330
-91.53	13.2	13	734,884	43,194	3,283	10.3	342
-91.6	5.8	13	671,552	20,681	7,144	14.4	494
-91.66	13.2	13	857,621	51,334	3,953	11.1	373
-91.73	13.5	13	987,471	50,935	4,363	11.6	391
-91.79	13.6	13	1,079,124	52,257	4,743	12.1	407
-91.86	11.2	13	968,528	45,426	5,291	12.7	428
-91.92	12.9	13	891,346	54,310	4,216	11.5	385
-91.99	3.2	13	772,005	29,907	14,810	19.8	697
-92.06	9.9	13	828,539	53,393	5,206	12.6	425
-92.12	3.6	13	828,969	47,804	14,414	19.6	688
-92.19	4.1	13	909,688	47,307	13,605	19.1	670
-92.25	7.2	14	980,706	50,680	8,866	15.9	547
-92.32	11.8	13	1,071,778	43,478	5,504	12.9	436
-92.38	9.6	13	1,084,643	36,323	6,747	14.1	481

Table 3-7. Test Shaft 4 MWD measurements for the middle section.

			Test Shaft 4 - Middle Shaft Section				
Elevation	Penetration Rate	Rotational Speed	Torque	Crowd	Specific Energy	Side Shear	U.C.S.
El.	u	N	T	F	e	fs	*qu*
(ft)	(in/min)	(rpm)	(in-lbs)	(lbf)	(psi)	(ksf)	(psi)
-61.94	23.2	16	782,417	16,506	2,431	9.0	296
-62	34.0	16	831,046	33,295	1,765	7.8	255
-62.07	34.2	16	803,638	22,014	1,787	7.9	256
-62.13	34.8	17	570,685	20,099	1,266	6.8	218
-62.2	31.9	15	590,057	41,650	1,303	6.9	221
-62.27	44.3	17	685,164	38,236	1,221	6.7	214
-62.33	773.9	18	417,986	29,625	66	1.9	54
-62.4	773.9	18	417,986	29,625	66	1.9	54
-62.46	863.7	16	445,204	26,487	57	1.8	50
-62.53	863.7	16	445,204	26,487	57	1.8	50
-62.59	527.3	15	537,135	23,391	87	2.1	61
-62.66	24.1	16	564,042	23,382	1,735	7.8	253
-62.73	24.2	15	803,296	39,034	2,365	8.9	293
-62.79	25.6	15	856,339	35,892	2,299	8.8	289
-62.86	28.6	16	849,915	27,408	2,239	8.7	285
-62.92	26.1	16	803,804	19,779	2,207	8.6	283
-62.99	24.1	16	761,121	13,023	2,387	8.9	294

Based on these observations, it was determined that elimination criteria would be required to identify and remove the layers of calcareous clay for the rock core data comparison.

Note: The calcareous clay and soil layers were not removed from the specific energy-side shear correlation because these layers effect both strength estimates, load test and MWD. To clarify, the calcareous clay and soil layers would produce lower drilling resistance, as observed in Tables 3-3 and 3-6, and lower shaft capacity measured by the load test. Therefore, including the layers in the MWD-load test correlation is necessary to properly develop the shaft capacity relationship with specific energy as similar layering would likely be encountered throughout the site in which MWD must take into account for production shaft monitoring.

3.8.2   Developing MWD Elimination Criteria for Core Comparisons

In order to provide a more accurate rock strength assessment for core comparison, elimination criteria were developed to remove data points that were likely voids, calcareous clay, or soil layers interlaced within the layers of rock. The first part of the elimination criteria involved removing any data point that had an identical specific energy value recorded above or below the data point in question. This criterion was developed based on observations in BDV31-977-20 where it was observed that even a 1 psi change in rock strength resulted in a noticeable change in specific energy ($\approx$ 100 psi). As previously discussed, MWD specific energy provides good sensitivity for rock strength assessment. These repeated values were likely a result of applying 20 to 50 kips of crowd during rock drilling and then a quick release in drilling resistance when the rock layers transitioned into a soft soil layer. In this scenario, the penetration rate would

drastically increase, and the specific energy would drastically decrease which is what was observed in Table 3-4.

Incorporating the first criterion improved the MWD q_u averages compared to the load test q_u averages. However, the estimates were still too conservative as some of the calcareous clay and soil layer data points did record a very small change in specific energy. Based on these observations, a second elimination criterion was developed. This involved creating a penetration rate (u) control that would eliminate any compressive strength value from consideration if the respective penetration rate exceeded the u-control input (defining the operational limit). Through an iterative process it was determined that 470 in/min was the penetration limit that would produce minimal average error compared to the load tested estimated q_u values. To clarify, any data point in which the penetration rate exceeded 470 in/min was eliminated from consideration for the core comparison. To ensure the data points in which the penetration rate exceeded 470 in/min were not a result of overcrowding the bit, a comparison was made between the crowd recorded when u > 470 in/min and when u < 470 in/min in the investigated layers (Table 3-8). As seen in Table 3-8, the crowd statistics for Test Shaft 2 indicate very little difference in the applied crowd (mean, median, CV, and the range) which indicates the high rates of penetration were due to weak layers in Test Shaft 2. Test Shaft 3, which was drilled by a different driller in rock layering that was more consistent, shows the same degree of variability in applied crowd, further validating the layering of Test Shaft 2. Test Shaft 4, which was drilled by the same rig operator as Test Shaft 2, shows higher crowd was used when u < 470 in/min which is indicative of higher strength geomaterial. Also of importance, more crowd variability was observed in Test Shaft 4 where layering in the upper and middle portions of the shaft were similar to Test Shaft 2 and the lower portion of the shaft was similar to the consistency of Test Shaft 3. Interestingly, the rig operator for Test Shafts 2 and 4 applied the same range of crowd in both shafts which was nearly double that of the rig operator for Test Shaft 3, signifying a difference in drilling styles. Based on these observations, the u-control criterion was determined to be valid and new compressive strength estimates were derived and provided in Table 3-9.

Table 3-8. Crowd comparison when penetration rate was above or below 400 in/min.

| | Crowd, F (lbf) | | | | | |
| Stats | Test Shaft 2 | | Test Shaft 3 | | Test Shaft 4 | |
	u < 470	u > 470	u < 470	u > 470	u < 470	u > 470
Average	24,285	24,713	12,210	12,048	24,686	20,963
Std. Dev.	12,460	11,660	5,405	6,216	14,456	13,601
CV	0.51	0.47	0.44	0.52	0.59	0.65
Median	24,113	23,745	11,160	9,500	23,595	19,652
Maximum	51,466	51,726	27,202	24,853	55,633	55,010
Minimum	191	404	1,858	3,325	252	209
Count	304	360	264	33	262	128

Table 3-9. Compressive Strength Comparison (Load Test vs. MWD) – MWD criteria applied.

Compressive Strength Comparison (Load Test vs. MWD)				
Test Shaft	Segment	LT q_u (psi)	MWD q_u (psi)	% Error
2	15	561	538	-4.1%
	16	631	539	-14.6%
	17	497	440	-11.7%
3	12	298	305	2.3%
	Toe	283	290	2.6%
4	5	193	168	-13.2%
	10	212	226	6.5%
	11	241	259	7.2%
	12	230	283	22.8%
	16.2	324	324	-0.2%
			Avg. % Difference =	-0.2%

To further validate the q_u estimates provided in Table 3-9, the rock auger data collected during BDV31-977-20 was analyzed in a similar manner without any elimination criteria applied. To clarify, correlation was developed between specific energy and side shear obtained from the load tests when a rock auger was employed in the prior project which is presented in Figure 3-17.

Note: Two additional segments from Little River were added to the correlation in Figure 3-17 compared to the correlation presented in Figure 1-1.
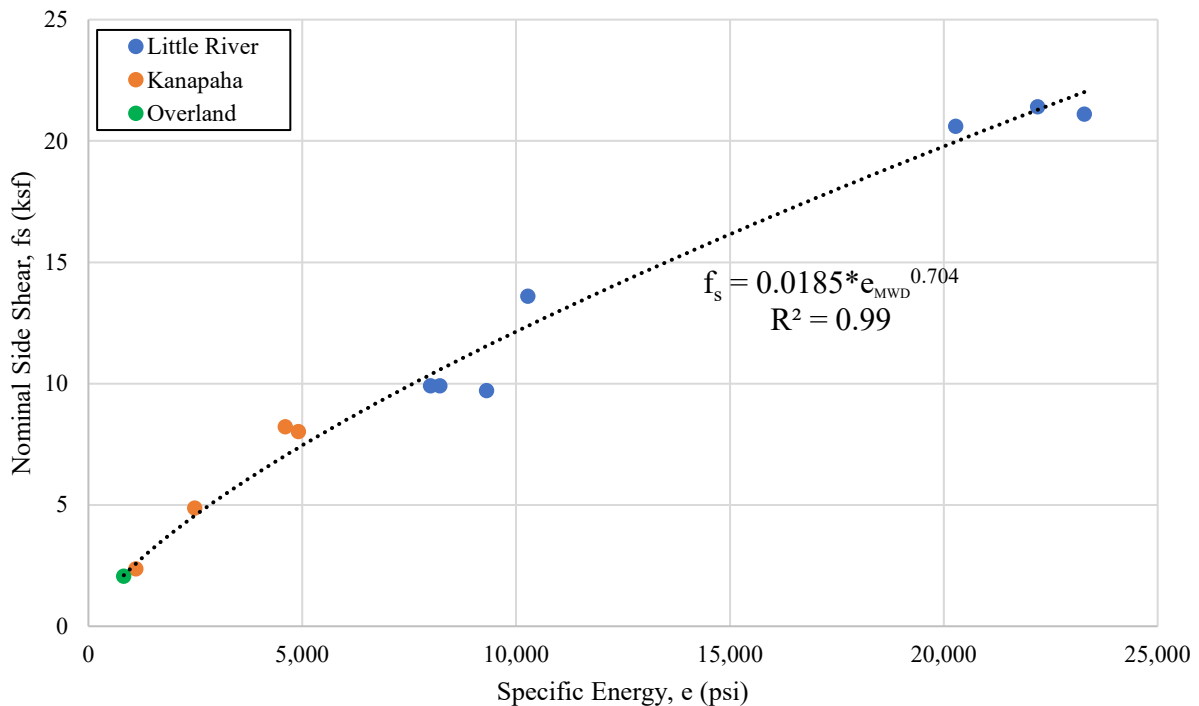
Figure 3-17. Specific energy side shear correlation using a rock auger.

The correlation developed was then used to compare the side shear from MWD and the load test data (Table 3-10), similar to Table 3-2. As seen in Table 3-10, the average error for side shear between the load test data and MWD is -0.3% and nearly identical to the average error in Table 3-2 when a rock drilling bucket was used. The side shear values presented in Table 3-10 were derived from the average specific energy recorded over each monitored shaft segment, which is the same procedure used in the Table 3-2 comparison. However, when compressive strength is calculated for each individual data point and then the average is taken for a shaft segment, MWD provides a conservative average q_u estimate compared to the load test q_u estimate. This can be seen in Table 3-11 where the MWD and load test q_u values are compared. In Table 3-11, it can be seen that the error between the q_u estimates is significantly less than Test Shaft 2 in Table 3-3 and similar to the range of error found throughout Table 3-9, further validating the elimination criteria.

Table 3-10. Rock Auger Side Shear Comparison (MWD vs. Load Test) – MWD layer averages.

Rock Auger Side Shear Comparison (MWD vs. Load Test)				
Section Details		Side Shear, f_s (ksf)		
Location	Segment	Load Test	MWD	% Error
Little River	SG8 to SG7	9.9	10.5	6.1%
	SG7 to SG6	21.1	22.0	4.3%
	SG6 to O-cell	20.6	19.9	-3.4%
	O-cell to SG5	21.4	21.2	-0.9%
	SG5 to SG4	13.6	12.3	-9.6%
	SG4 to SG3	9.9	10.3	4.0%
	SG3 to SG2	9.7	11.5	18.6%
Kanapaha	TS SG1 to SG2	8.0	7.3	-8.8%
	TS SG2 to SG3	8.2	7.0	-14.6%
	TS SG4 to Base	4.9	4.5	-8.2%
	ES SG1 to SG2	2.4	2.6	8.3%
Overland	Segment 2	2.1	2.1	0.0%
			Average Error =	-0.3%

Table 3-11. Rock Auger q_u Comparison (MWD vs. Load Test) – All MWD data points.

Section Details		Compressive Strength, q_u (ksf)		
Location	Segment	Load Test	MWD	% Diff.
	SG8 to SG7	347	328	-5.6%
	SG7 to SG6	796	666	-16.3%
	SG6 to O-cell	775	680	-12.4%
Little River	O-cell to SG5	809	647	-19.9%
	SG5 to SG4	492	407	-17.4%
	SG4 to SG3	347	412	18.5%
	SG3 to SG2	340	331	-2.5%
	TS SG1 to SG2	276	242	-12.1%
Kanapaha	TS SG2 to SG3	283	230	-18.7%
	TS SG4 to Base	159	142	-10.8%
	ES SG1 to SG2	72	71	-1.2%
Overland	Segment 2	62	61	-2.5%
			Average Error =	-8.4%

Rock Auger q_u Comparison (MWD vs. Load Test)

As discussed, the MWD approach is more conservative than the load test approach for estimating q_u. However, the MWD approach compared well with the Little River core data where a good amount of core samples were recovered. Also, the MWD approach can provide more insight to the true variability where load test data is limited. As seen in Table 3-12, the average q_u values are fairly similar as well as the CV values. It should be noted that the CV value in Table 3-12 for the core data includes data from several sampled locations, whereas the MWD data was obtained from one sampled location. Therefore, the core data CV includes the horizontal variability of the site, whereas the MWD data only includes the vertical variability.

Table 3-12. Little River q_u Comparison – All Little River MWD data points.

Little River q_u Comparison		
Stats	q_u (psi)	
	Core Data	MWD
Average	530	473
Std. Dev.	949	698
CV	1.79	1.47
Count	152	568

3.8.3 Rock Bucket q_u Equation Development

Based on the prior discussion, a new rock drilling bucket q_u equation was needed. This required deriving the cumulative rock socket length within each mobilized shaft segment and adjusting the measured side shear values based on the length of rock per length of the shaft segment. For

example, if the theoretical shaft illustrated in Figure 3-18 was mobilized under 502.7 kips of load (P), a load test would report the average f_s = 8 ksf.

$$f_{s-rock} = \frac{P}{\pi \times D \times L_{segment}} = \frac{502.7\ kips}{\pi \times 4\ ft \times 5\ ft} = 8\ ksf \qquad\qquad \text{(Eq. 3-10)}$$
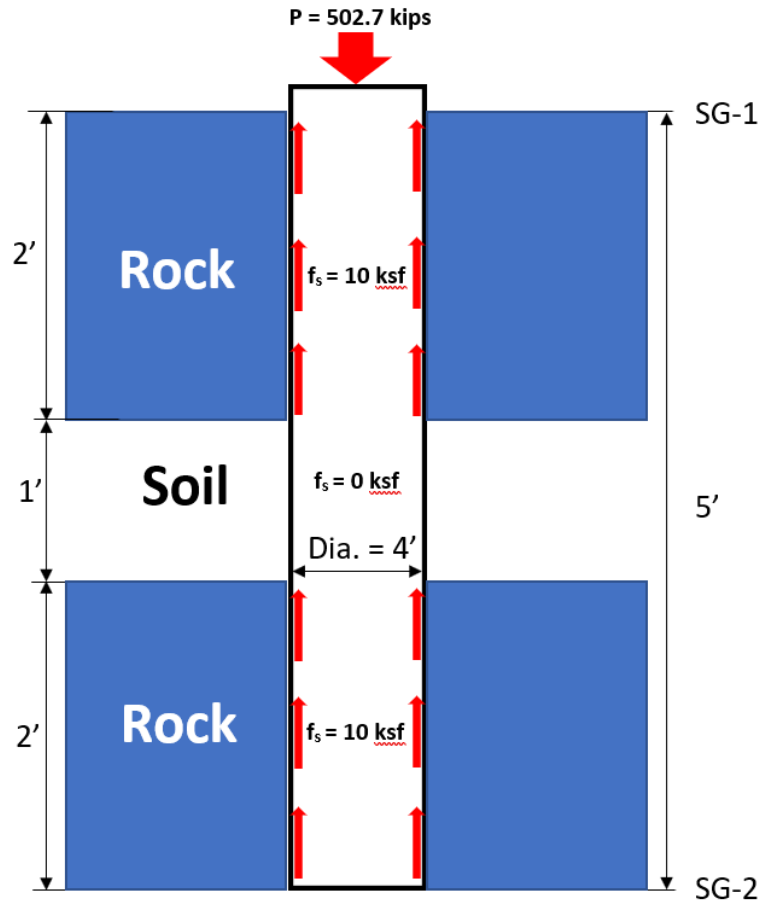
Figure 3-18. Side shear adjustment theoretical shaft diagram.

However, the shaft segment between strain gage levels SG1 and SG2 contains one foot of soil in which the average f_s would be negligible and MWD would record limited specific energy reducing the average over the segment length. Therefore, to get a better estimate of the true side shear (rock strength) of the rock layers, the total load of 502.7 kips must be distributed over the length of rock (4 feet) and not the segment length of five feet.

$$f_{s-rock} = \frac{P}{\pi \times D \times L_{rock}} = \frac{502.7\ kips}{\pi \times 4\ ft \times 4\ ft} = 10\ ksf \qquad\qquad \text{(Eq. 3-11)}$$

Measuring while drilling the shafts provided a means to estimate the length of soil and voided layers via the u-control iterations. Consequently, the length of rock was able to be estimated and the side shear values readjusted based on the length of rock within each segment. When the voided/soil sections of each segment were removed due to the elimination criteria (u control) the average specific energy also increased as many of the low specific energy values (soil) were

removed from the average. When the u-control method of assessment is applied to assess only rock strength, the adjusted specific energy and load tested side shear and q_u estimates are derived (Table 3-13) which produces a new relationship between specific energy and unconfined compressive strength for rock drilling buckets (Figure 3-19 and Equation 3-12).

Table 3-13. Adjusted specific energy, load test side shear and load test q_u.

Test Shaft	Segment	e (psi)	LT f_s (ksf)	LT q_u (psi)
2	15	16,687	34.1	1,345
	16	18,015	33.6	1,326
	17	12,068	27.5	1,063
	18/Toe	13,240	26.2	1,010
3	12	2,694	9.2	320
	13	1,423	8.0	274
	Toe	2,620	9.3	326
4	5	821	7.7	264
	10	1,570	10.3	363
	11	1,887	10.7	376
	12	2,329	11.7	416
	16.2	3,461	10.9	364
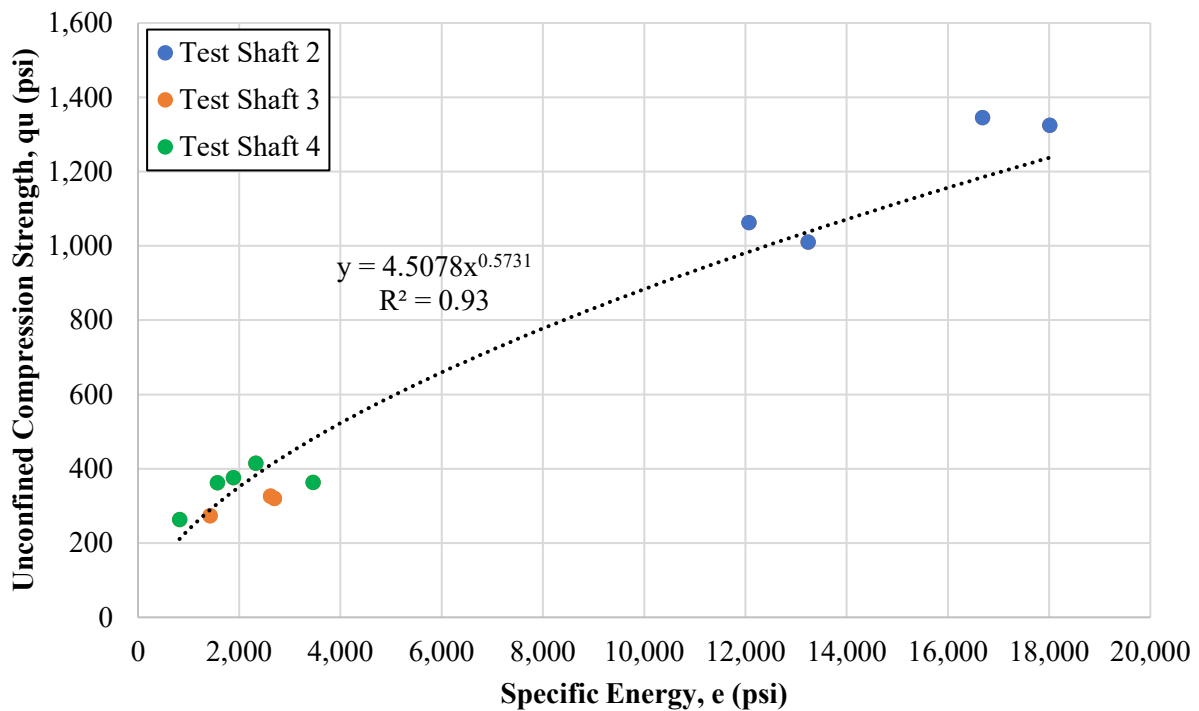
Figure 3-19. Final q_u vs. e relationship for rock drilling buckets.

$$q_u(psi) = 4.5078 \times e^{0.5731} \qquad \text{(Eq. 3-12)}$$

4. Core Data and Site Variability Analysis at Selmon Parkway

Due to the large number of MWD assessments of rock strength in a shaft, it is now possible to develop a correlation structure within an individual shaft. The latter is very important in identifying various types of variability such as zonal anisotropy or layering for highly variable sites often encountered in Florida.

4.1 *Laboratory Rock Core Strength Data*

Presented in Figures 4-1 and 4-2 are frequency and cumulative frequency distribution plots of all laboratory q_u data (260 samples) collected at the Selmon Parkway site. Examination of the distributions revealed there was a significant range (i.e., variability) of rock strengths. Also, as expected there are far more, lower strength values than higher ones. The frequency distribution has a log-normal shape, but also displays bimodal characteristics. Discussion of individual boring data in the footprint of each test shaft (e.g., frequency, correlation, etc.) will be presented with the MWD results.
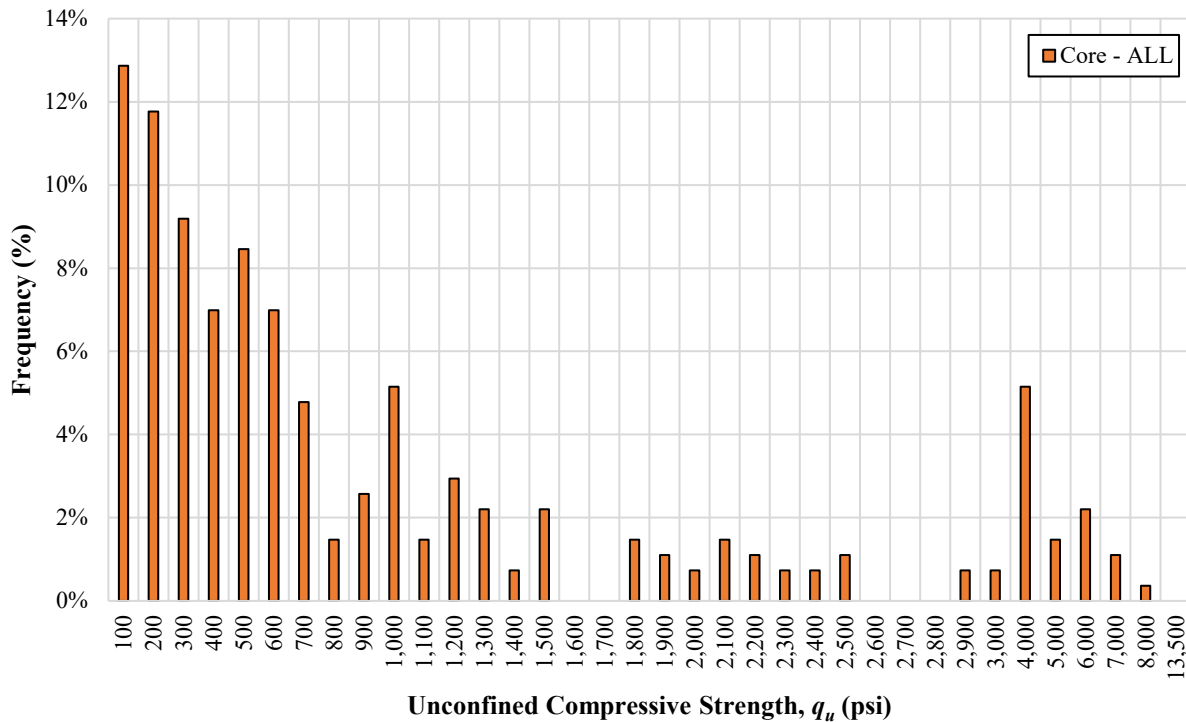
Figure 4-1. Frequency Distribution of q_u data, Selmon Extension.
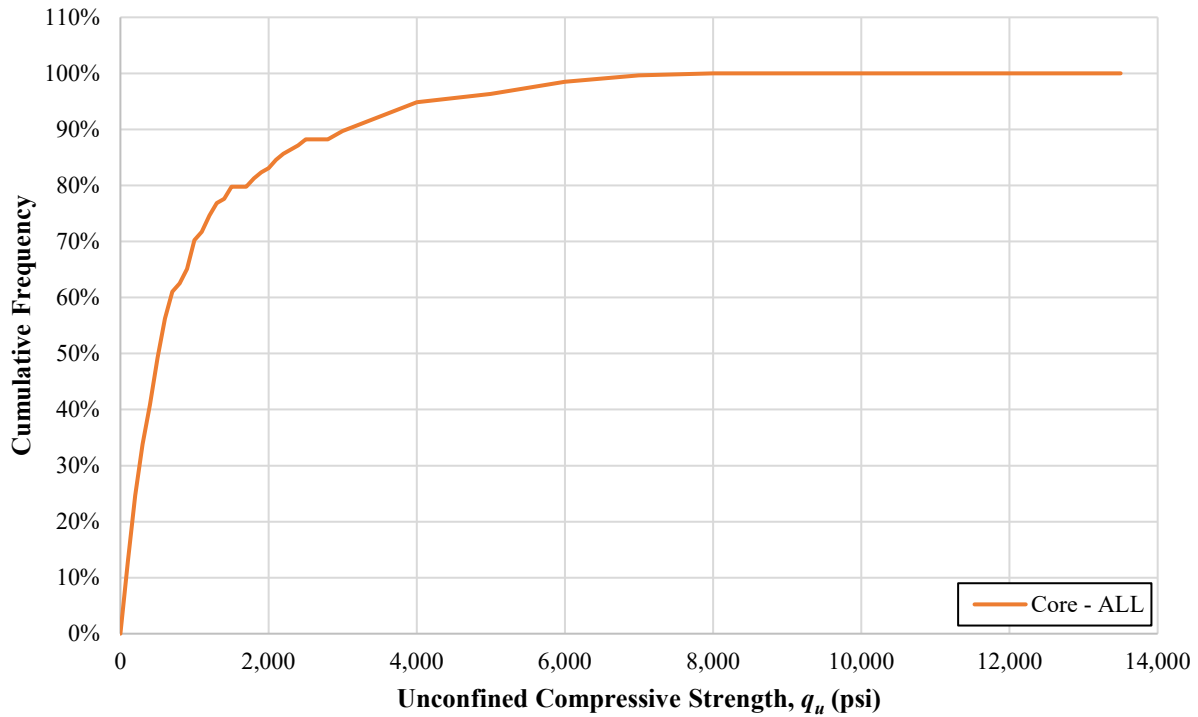
Figure 4-2. Cumulative Frequency Distribution of q_u data, Selmon Extension.

4.2 Comparison of MWD q_u vs. Laboratory q_u Data

To begin the MWD-core data comparisons, all core data collected within proximity (100 feet) of each of the three test shafts, within the elevation ranges where rock was found, were analyzed. This resulted in the following statistics:

Table 4-1. Summary of statistics for Selmon core data collected within 100' of the Test Shafts.

Stats	q_u (psi)
Mean	995
Median	610
Std. Dev.	1,014
CV	1.02
Max	3,905
Min	50
Count	18

Due to the limited number of core samples collected within proximity of the Test Shafts, the distance considered for the analyses was expanded to include more core samples. This required a limit to be placed on the q_u data such that the initial statistics would not be impacted by higher strength outlying values (i.e., influence the summary of statistics and variogram analyses for each shaft). As is the practice of the FDOT (SFH, FDOT 2015), any value outside of 1-standard deviation ($1\sigma = 1,014$ psi) from the original mean ($q_u = 995$ psi) would be eliminated as the core

47

sample distance considered was increased. At each of Test Shaft locations, including cores recovered from borings up to a distance of 2,500 feet (≈ ½ mile) from the test shaft was required to generate enough core data to evaluate the statistics, develop frequency and cumulative frequency distribution plots, and perform variogram analyses to compare with MWD.

4.2.1 Test Shaft 2 Strength Comparison

Using the recorded specific energy and the q_u vs. specific energy relationship (Equation 3-12), the q_u vs. elevation for Test Shaft 2 was found (Figure 4-3). Also shown in the figure is the core data within 2,500 feet of the test shaft. Table 4-2 provides the summary of statistics and Figures 4-4 and 4-5 provide the frequency and cumulative frequency distributions for MWD and the core data.

Evident from Figure 4-3 there is quite a lot of strength variability in both the MWD data and the laboratory tested core data. However, both the frequency distributions and cumulative frequency distributions (Figures 4-4 and 4-5) are expected to result in similar statistics for the MWD q_u and core q_u data. This is verified in Table 4-2, where MWD had a mean $q_u = 447$ psi, a median of 172 psi, and a CV of 1.13, whereas the core data had a mean $q_u = 446$ psi, a median of 310 psi, and a CV of 0.90. This comparison supports the use of Equation 3-12.

Figure 4-3. Test Shaft 2 MWD q_u vs. core q_u – 2,500 ft proximity.

Table 4-2. Test Shaft 2 summary of statistics.

Stats	q_u (psi)	
	MWD	Core
Mean	447	446
Median	172	310
Std. Dev.	505	399
CV	1.13	0.90
Max	1,971	1,920
Min	39	40
Count	289	66
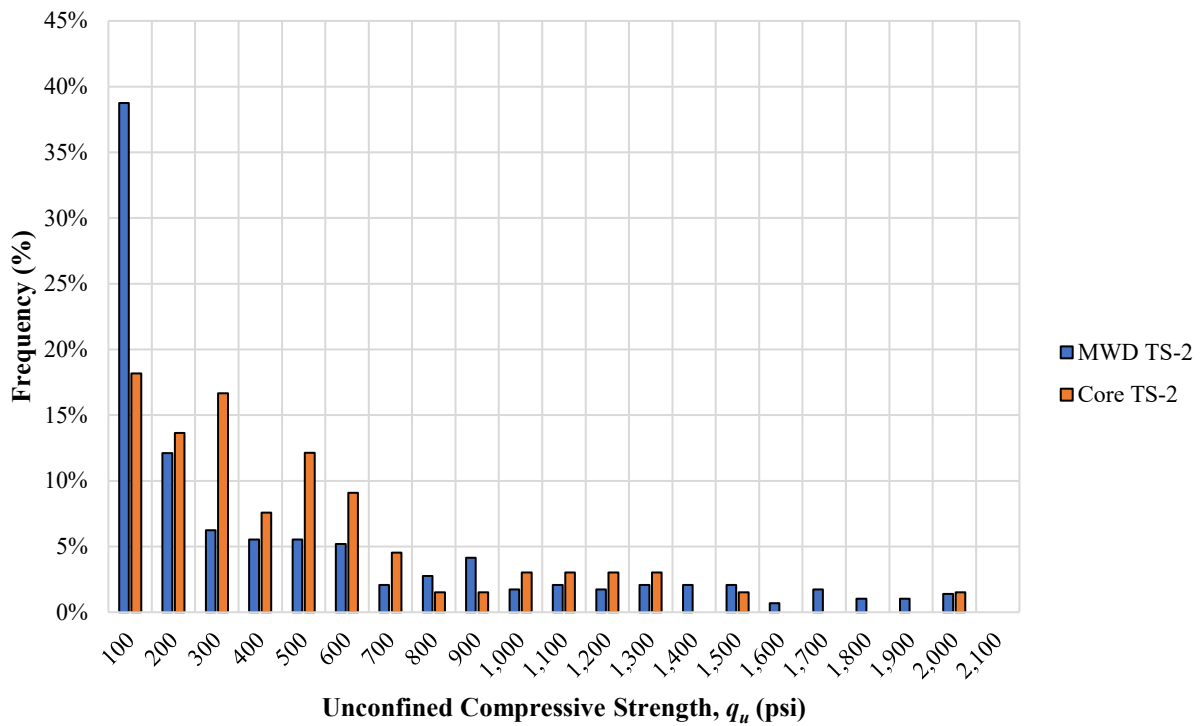
Figure 4-4. Frequency Distribution MWD q_u Test Shaft 2 and Core q_u (2,500 ft).

Figure 4-5. Cumulative Frequency Distribution MWD Test Shaft 2 q_u and Core q_u (2,500 ft).

4.2.2 Test Shaft 3 Strength Comparison

In the case of Test Shaft 3, only five core samples were collected within 100 ft of shaft. Expanding the distance considered to 2,500 feet produced a total of 29 core data values. However, no core data was available within the elevation range of -20 feet to -48 feet, whereas, MWD and load testing both indicated rock was present within this elevation range. The q_u strength profiles for Test Shaft 3, MWD and core data, are presented in Figure 4-6. The summary of statistics for Test Shaft 3 are provided in Table 4-3, and the frequency distributions and cumulative frequency distributions are provided in Figures 4-7 and 4-8. Although the core data was limited, the statistics and distributions of q_u strengths (MWD q_u and core q_u) are quite similar. From Table 4-3, MWD had a mean q_u = 419 psi, a median of 297 psi, and a CV of 0.83, whereas the core data had a mean q_u = 469 psi, a median of 375 psi, and a CV of 0.96.
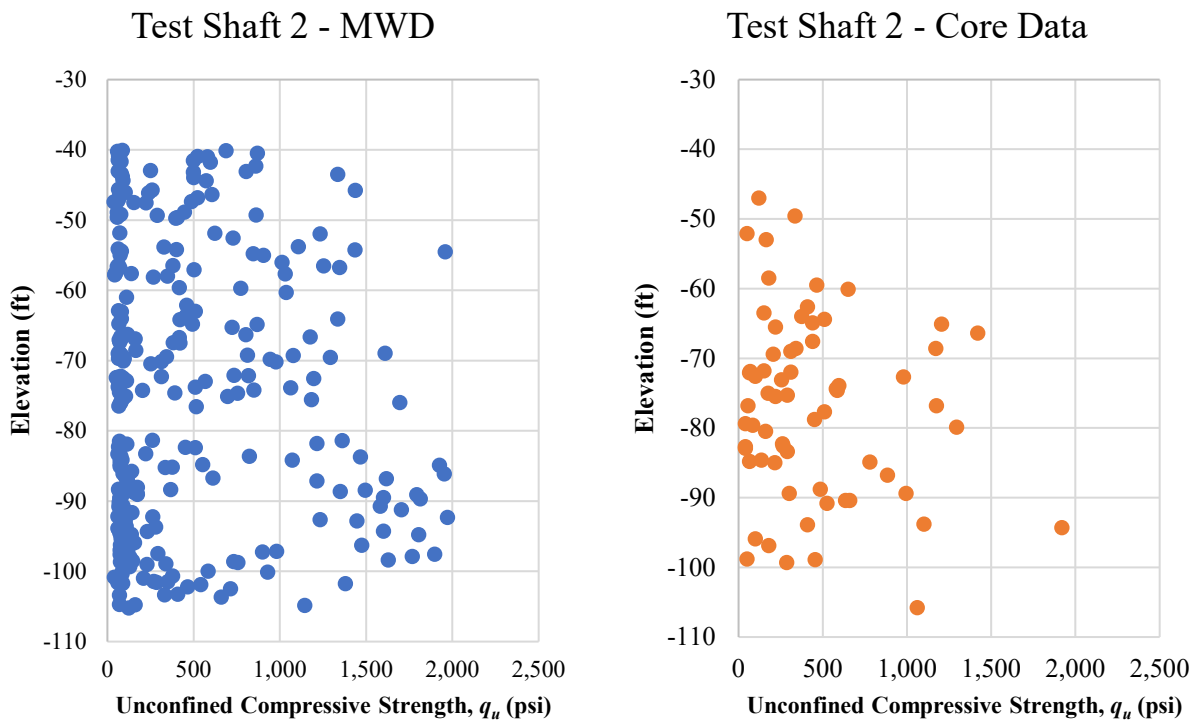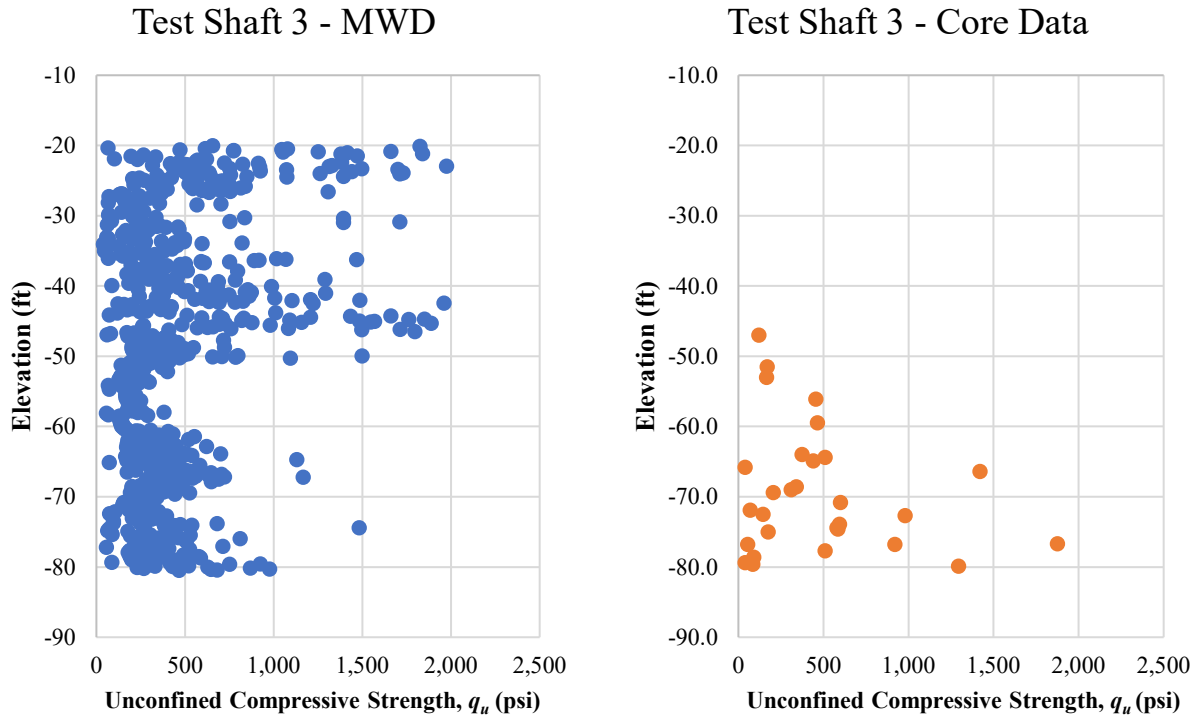
Figure 4-6. Test Shaft 3 MWD q_u vs. core q_u – 2,500 ft proximity.

Table 4-3. Test Shaft 3 summary of statistics.

| Stats	q_u (psi)	
	MWD	Core
Mean	419	469
Median	297	375
Std. Dev.	346	451
CV	0.83	0.96
Max	1,974	1,875
Min	40	40
Count	798	29
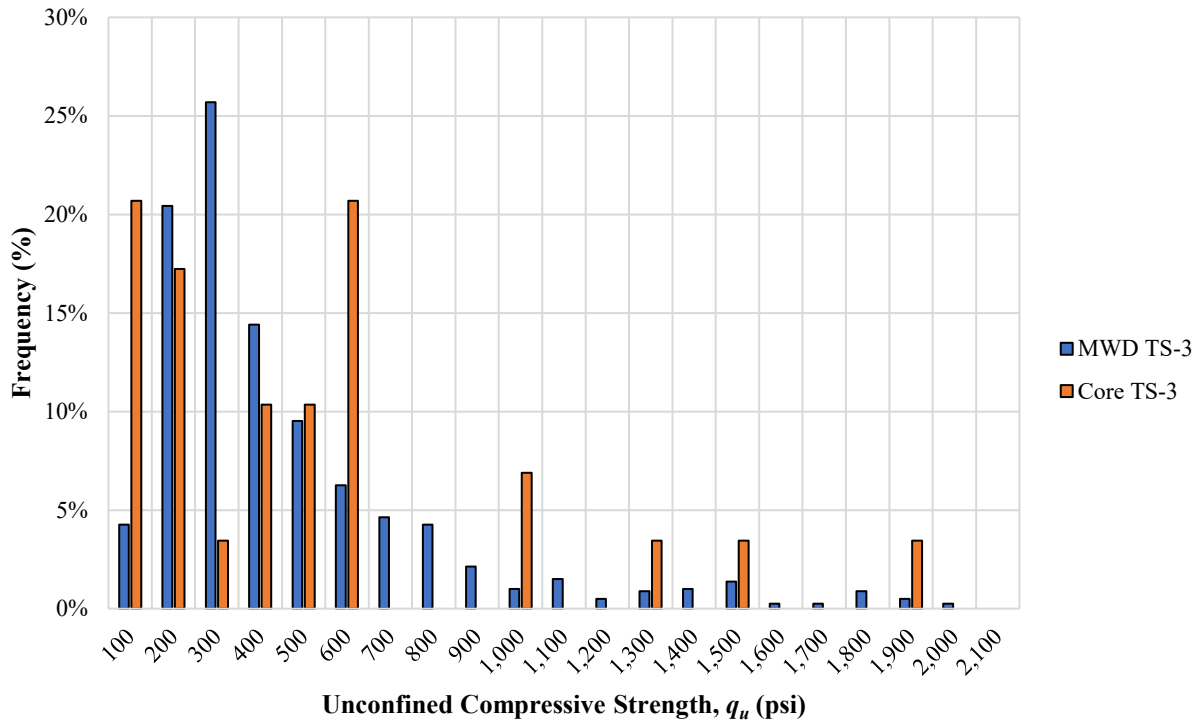
Figure 4-7. Frequency Distribution MWD q_u Test Shaft 3 and Core q_u (2,500 ft).
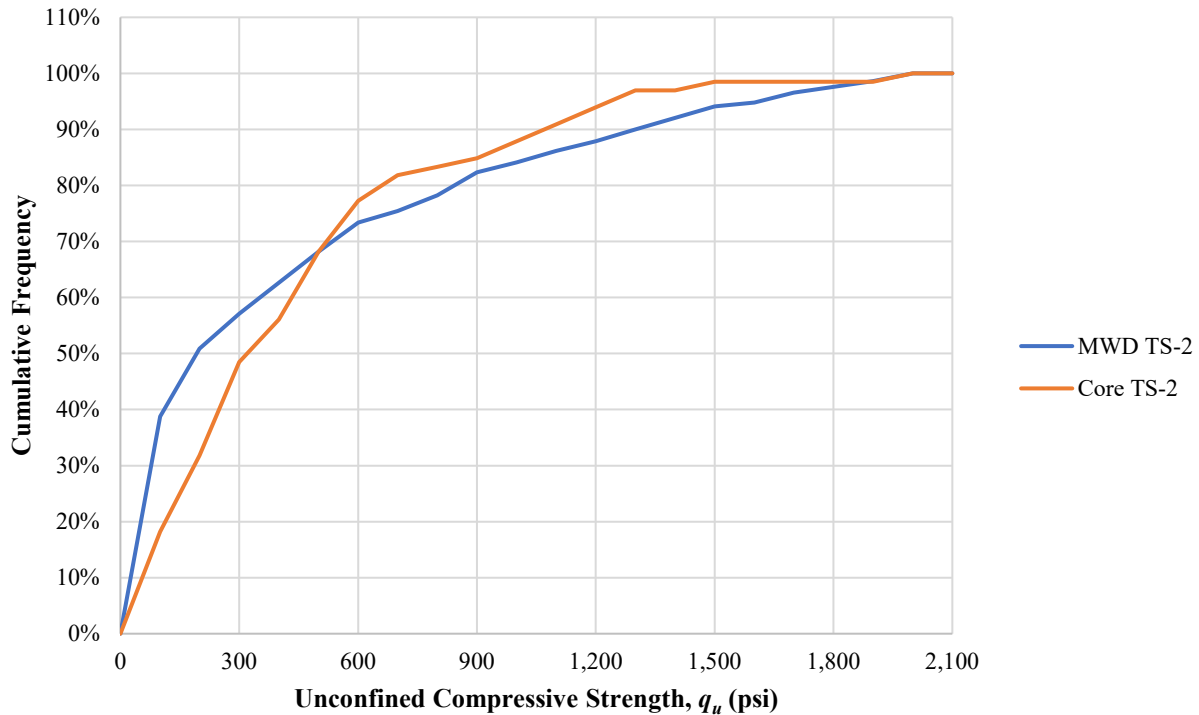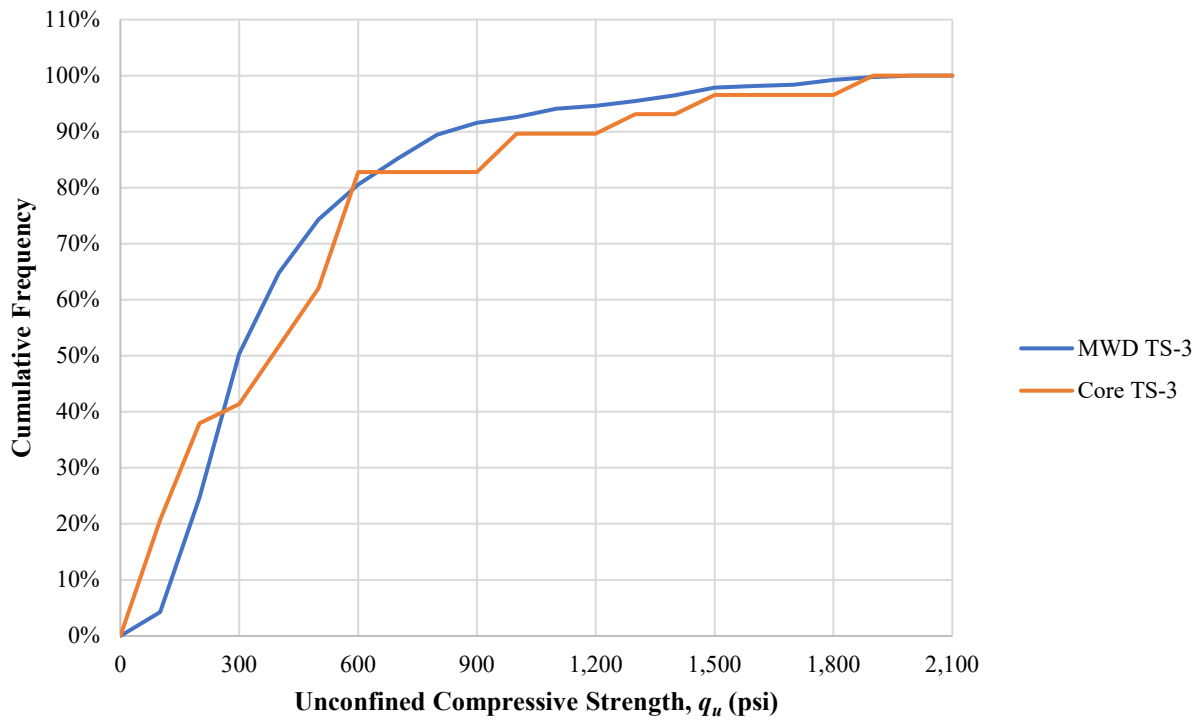

Figure 4-8. Cumulative Frequency Distribution MWD Test Shaft 3 q_u and Core q_u (2,500 ft).

4.2.3 Test Shaft 4 Strength Comparison

Similar to Test Shaft 3, only five core samples were collected within 100 feet of Test Shaft 4 in the elevation range in which rock was identified by MWD and load testing. After the distance considered was expanded to 2,500 feet, 33 core data values were available to complete the analyses (Figure 4-9). At Test Shaft 4, no rock was present between elevations -70 and -85 feet (silt was present). However, the core borings outside the 100-foot proximity of the shaft did show rock, and it was assumed that their characteristics are similar for the elevation range of -50 to -95 feet. The summary of statistics for Test Shaft 4 are provided in Table 4-4, and the frequency distributions and cumulative frequency distributions are provided in Figures 4-10 and 4-11. Even with the limited amount of core data available, the statistics and distributions of strength (MWD q_u and core q_u) are quite similar. From Table 4-4, MWD had a mean $q_u = 338$ psi, a median of 323 psi, and a CV of 0.61, whereas the core data had a mean $q_u = 390$ psi, a median of 290 psi, and a CV of 0.89. Also observed, the maximum strength from MWD and the core data did not exceed the q_u limitation ($q_u = 2,009$ psi), indicating a weaker zone within the vicinity of Test Shaft 4.
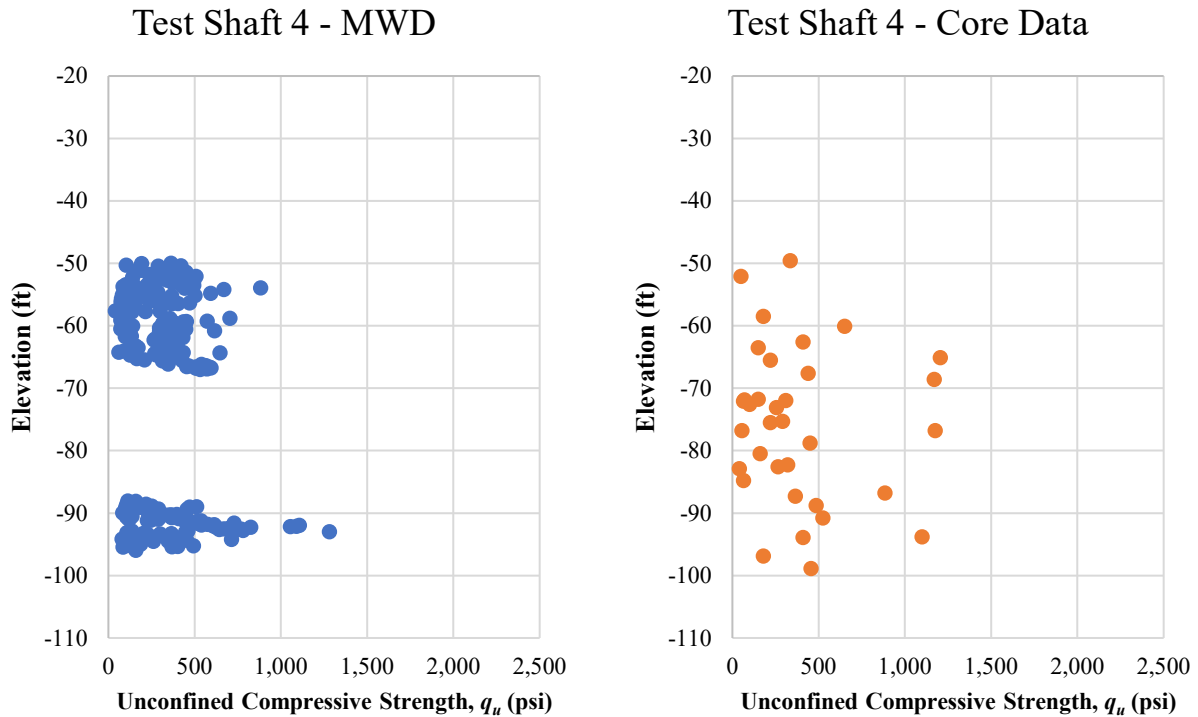
Figure 4-9. Test Shaft 4, MWD q_u vs. core q_u – 2,500 ft proximity.

Table 4-4. Test Shaft 4 summary of statistics.

| Stats	q_u (psi)	
	MWD	Core
Mean	338	390
Median	323	290
Std. Dev.	207	347
CV	0.61	0.89
Max	1,282	1,205
Min	40	40
Count	240	33
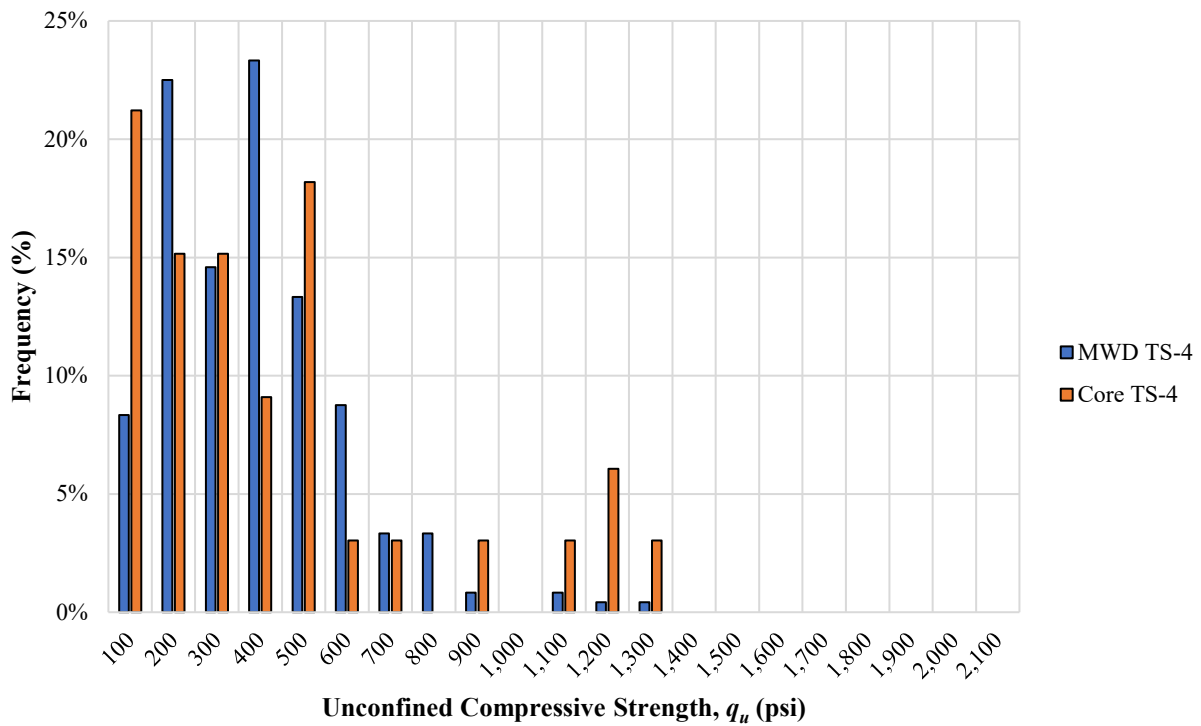
Figure 4-10. Frequency Distribution MWD q_u Test Shaft 4 and Core q_u (2,500 ft).
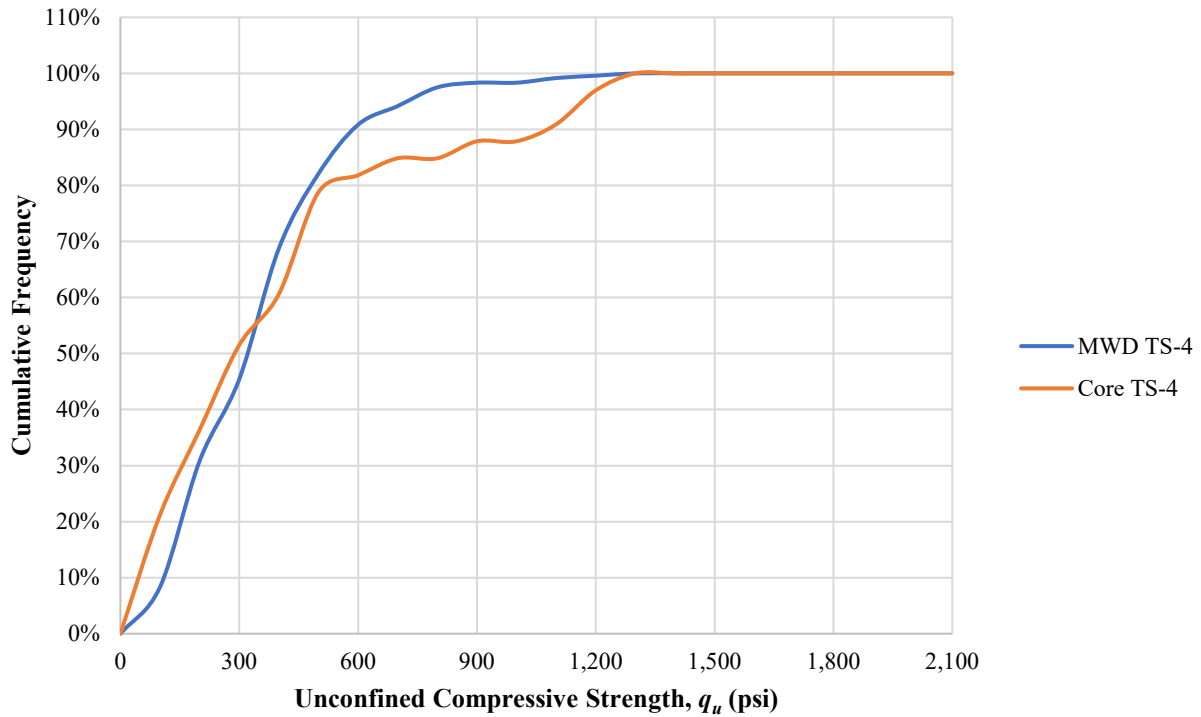
Figure 4-11. Cumulative Frequency Distribution MWD Test Shaft 4 q_u and Core q_u (2,500 ft).

4.3   Variogram Analyses

4.3.1   Introduction to Variograms

Comparing the statistics of the data (MWD q_u vs. Laboratory q_u) for individual test shafts is important when estimating the capacity of individual shafts, but it does not necessarily address the capacities of production shafts that are located further away. An evaluation of that behavior is obtained by looking at the variograms of the data, Figure 4-12.
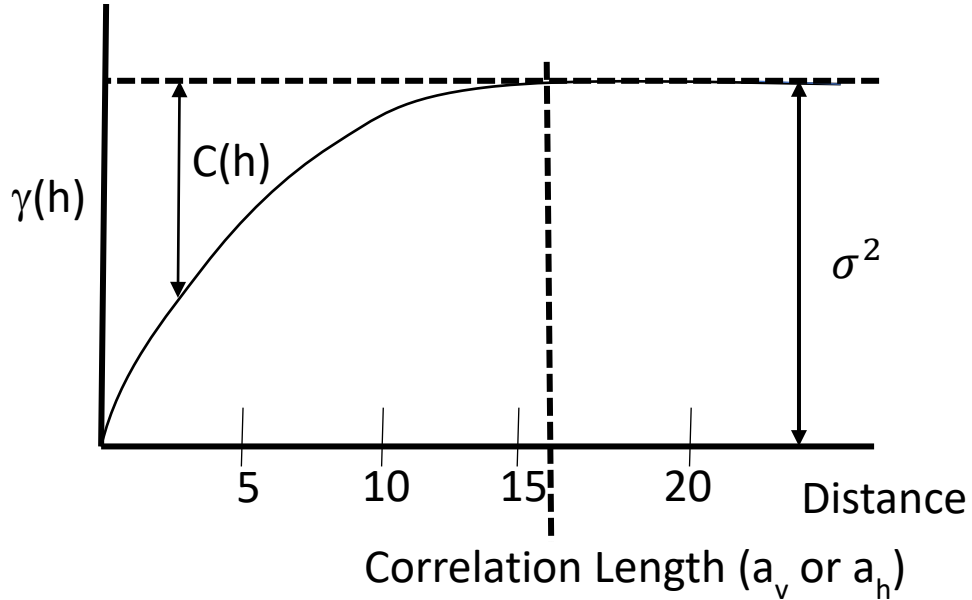
Figure 4-12. Variogram, Covariance, and Sill (σ^2) as function of distance between points, h.

From Figure 4-12, γ(h) is the variogram function,

$$\gamma(h) = \frac{1}{2N}\sum_{i=1}^{n}(V(t)_i - V(t+h)_i)^2 \qquad \text{(Eq. 4-1)}$$

and C(h) is the covariance function, defined by,

$$C(h) = \sigma^2 - \gamma(h) \qquad \text{(Eq. 4-2)}$$

Where h is the distance separating any 2 points; V (t) and V (t+h) are the values of the 2 points of interest. The sill (σ^2) is the variance (i.e., standard deviation squared) of the data set. Where γ(h) is less than the sill, the data is correlated (i.e., C(h) is greater than zero). From Figure 4-12, the data is correlated up to a distance of "a" from one another. If Equation 4-2 were to be divided by the sill (variance), the Y-axis would be γ(h) / σ^2 and is called the normalized variogram which has a value that ranges from 0 and 1 (Figure 4-13). The normalized covariance function (C(h) / σ^2) would also vary between 0 and 1 and the correlation between the points is called ρ and is defined as C(h) / σ^2.
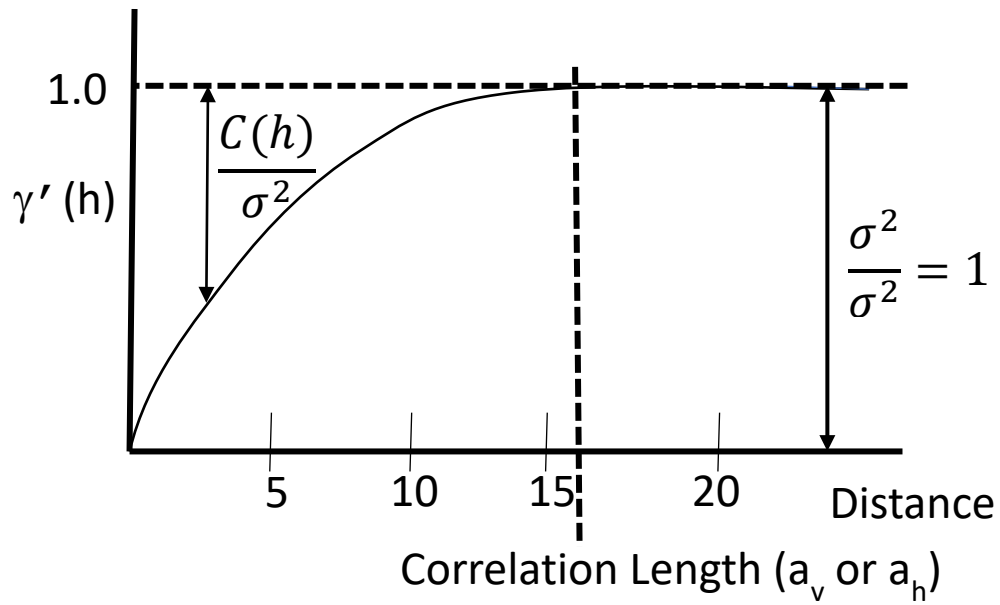
Figure 4-13. Normalized variogram.

4.3.2 MWD Variogram Analyses

Prior to MWD monitoring of test shafts to assess strength from specific energy, collecting sufficient data points within individual borings to develop a valid vertical variogram for a single shaft or boring was nearly impossible. However, with MWD data recorded every two centimeters, this is now possible (200 to 800 data points for each shaft). Figures 4-14 and 4-15 present individual and normalized variograms of each test shaft's MWD q_u data for the site.
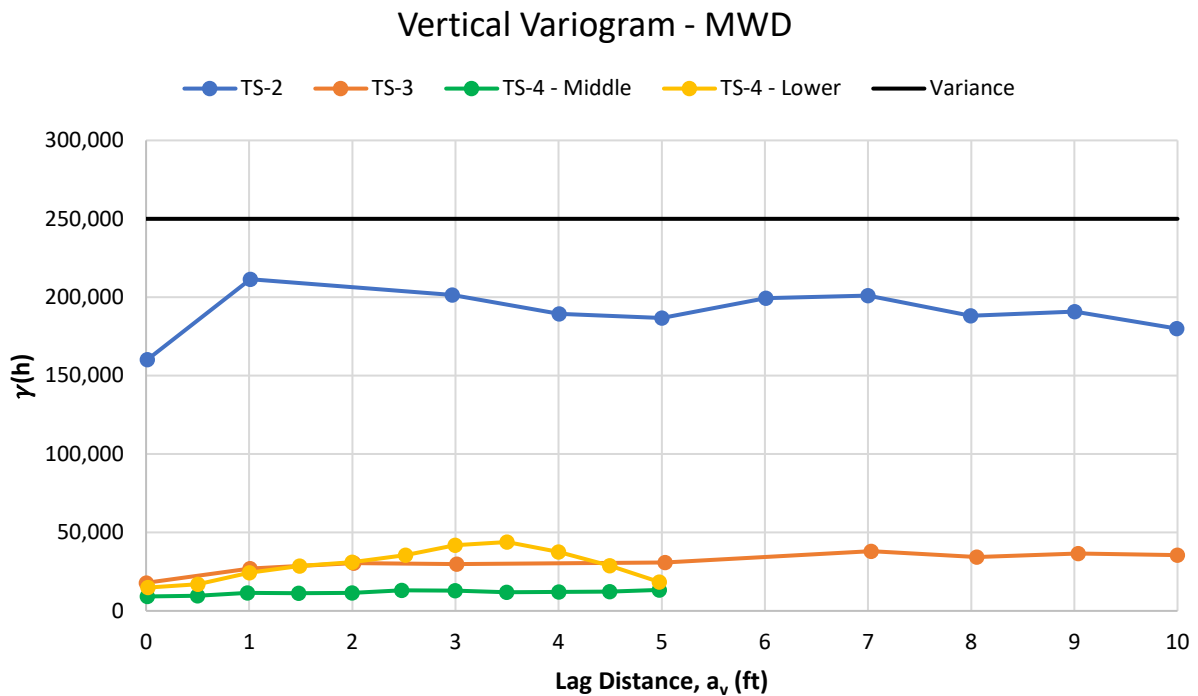
Figure 4-14. Variograms for Test Shafts 2, 3 and 4 from MWD q_u data.
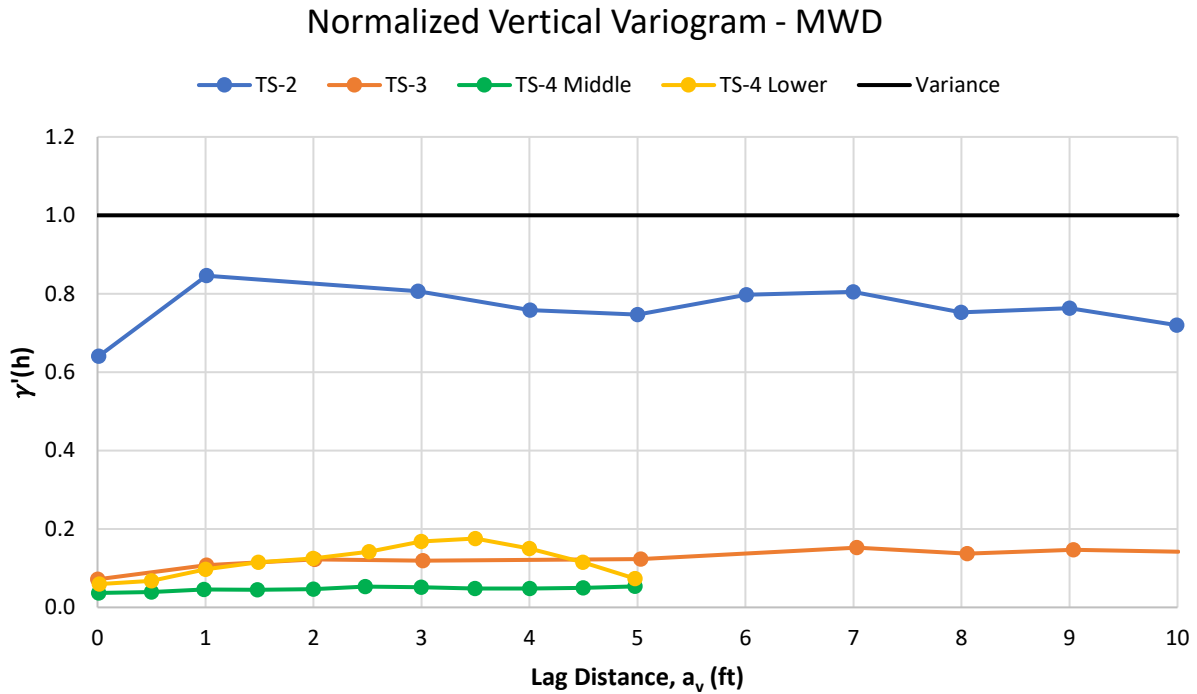
Figure 4-15. Normalized Variograms for Test Shafts 2,3, and 4 from MWD q_u data.

Evident from Figure 4-15, the correlation for Test Shaft 2 compared to Test Shafts 3 and 4 is quite different. Specifically, correlation for Test Shaft 2 varies from 0.35 (1 – 0.65: Figure 4-15) at small distances (a_v < 1 ft) and is approximately 0.20 (1 – 0.80) for larger point spacing, 5 to 7 ft. However, for Test Shafts 3 and 4, the strength correlation is approximately 0.85 (1 – 0.15) for large distances (0 < h < 10 ft). This is verified by observing the large range of q_u values about the mean as a function of depth for Test Shaft 2 (Figure 4-3) vs. Test Shaft 4 (Figure 4-9). In geostatistics, this is known as an "areal trend". Gringarten and Deutsch (2001) identify areal trends as having an influence on the vertical variogram—that is, the vertical variogram will not encounter the full variability of petrophysical property (γ(h) / σ^2 not equal to 1). There will be positive correlation (variogram below variance or sill) for large distances in the vertical direction. This type of behavior is called "zonal anisotropy" and is shown in Figure 4-16.
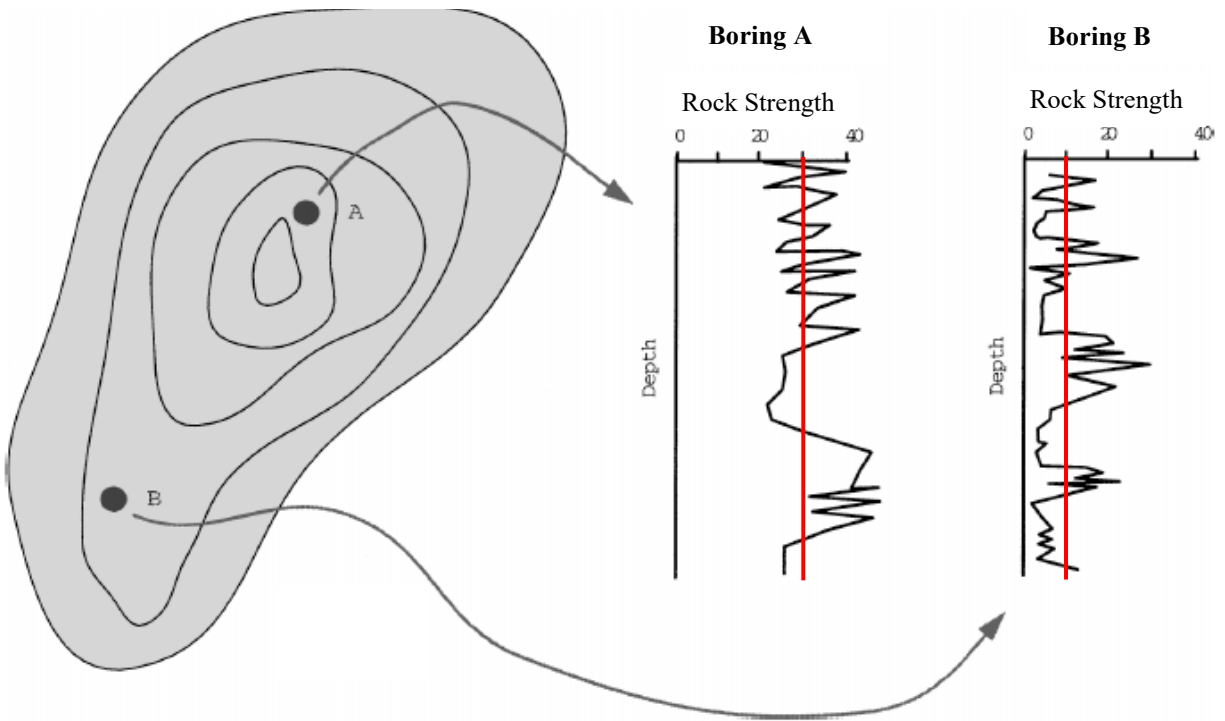
Figure 4-16. Area Trends with Zonal Anisotropy.

In Figure 4-16, Boring B shows a mean of approximately 10 and a range of 20, whereas, Boring A shows a mean of approximately 30 and range of 20. If Borings A and B are combined (i.e., all data), it will show a mean of approximately 20 and a range of 40 (i.e., much higher variance (range) in the case of all data vs. each boring). Areal trends (zonal anisotropy) are significantly important in drilled shaft design and construction. Generally, geotechnical engineers collect strength data throughout a site and then estimate the shaft capacities based on the mean or median from all the data combined instead of looking at individual boring data. This is because in most cases there is insufficient (Table 4-1) data collected within one boring. Moreover, many sites are designed with less than 100 data values for the whole site; not the 1,250 data values obtained by monitoring three test shafts with MWD reported herein. The areal trend or zonal anisotropy shown from the MWD q_u data also explains the 200% to 300% difference in the measured unit skin friction from the load test reported for Test Shaft 2 vs. Test Shafts 3 or 4.

Of interest is also the comparison of the normalized variogram using the core strength q_u data, Figure 4-17 with the MWD q_u (Figure 4-15). Evident, the same areal trends observed between Test Shaft 2 vs. 3 and 4 are in the core q_u results (Figure 4-17). The slight differences in the initial portion of Test Shaft 2 (0 to 3 ft) is attributed the large area (1/2 mile radius) that the core data was collected from. As a result of the larger area, the initial section of the normalized variogram for Test Shaft 2 is seeing (i.e., using data from) the lower zonal trend (e.g., TS-3 and TS-4) which has closely spaced data.
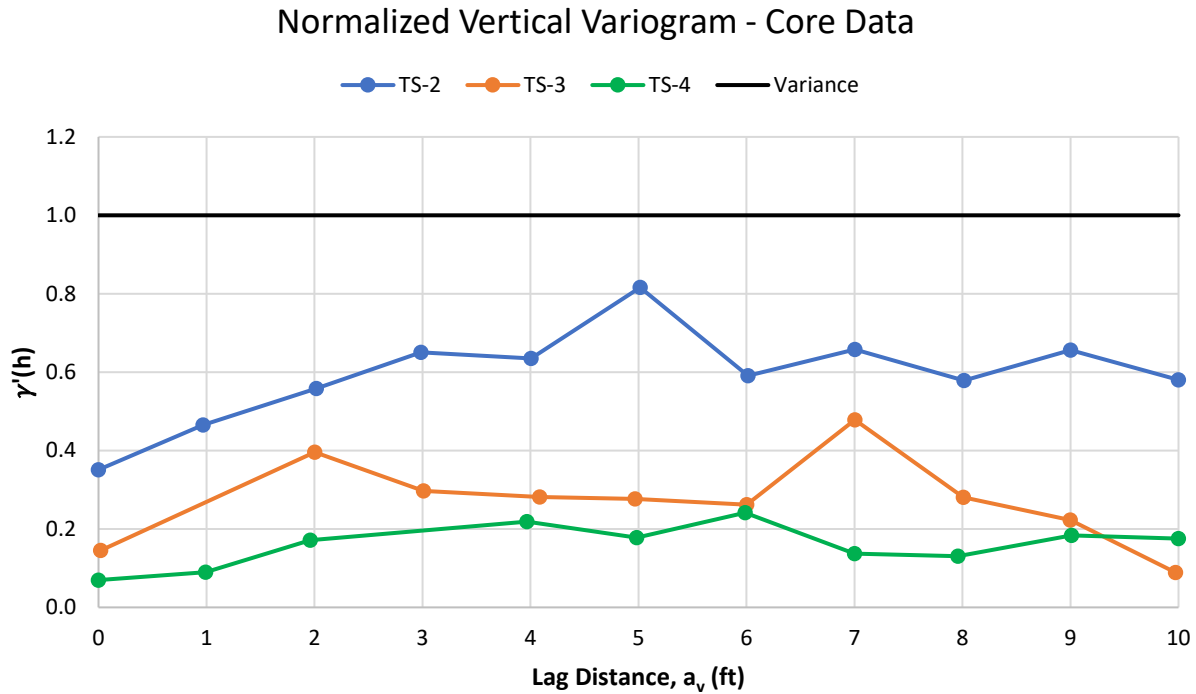
Figure 4-17. Normalized Variograms for Test Shafts 2,3, and 4 from core q_u data.

Also of interest, is if other sites exhibit the Areal trend phenomenon that was discovered at the Selmon Site. Shown in Figure 4-18 are side shear (f_s) estimates from the core data obtained within a 35 foot zone at 17th Street Bridge in Fort Lauderdale. Presented on the left is a plan view layout of the borings (each 40 ft into rock) and their proximity. Next to each boring in parenthesis are the mean f_s for the whole boring and its standard deviation. For instance, for boring located at x = 9 ft and y=24 ft, the mean f_s over the whole boring is 11.8 tsf and its standard deviation was 5.3 tsf. Evident from an examination of each boring's summary of statistics, there is a clear areal trend (means vary from 11 to 20 tsf with standard deviations ranging from 5 to 9 tsf) between the borings. If all the data is combined (right side Figure 4-18), the mean and range of all the data (Mean = 17.0 tsf; Standard Deviation = 9.0 tsf) is quite different from the boring located at x = 9 ft and y = 24 ft. It should be noted that all of data shown in Figure 4-18 were obtained for a research project. At the time of construction, the plan borings only presented one boring within the pier location with limited laboratory test results. A solution to limited core borings would be to employ MWD during the exploratory drilling process. This would lead to a significant increase in design data and would allow areal trends to be identified.
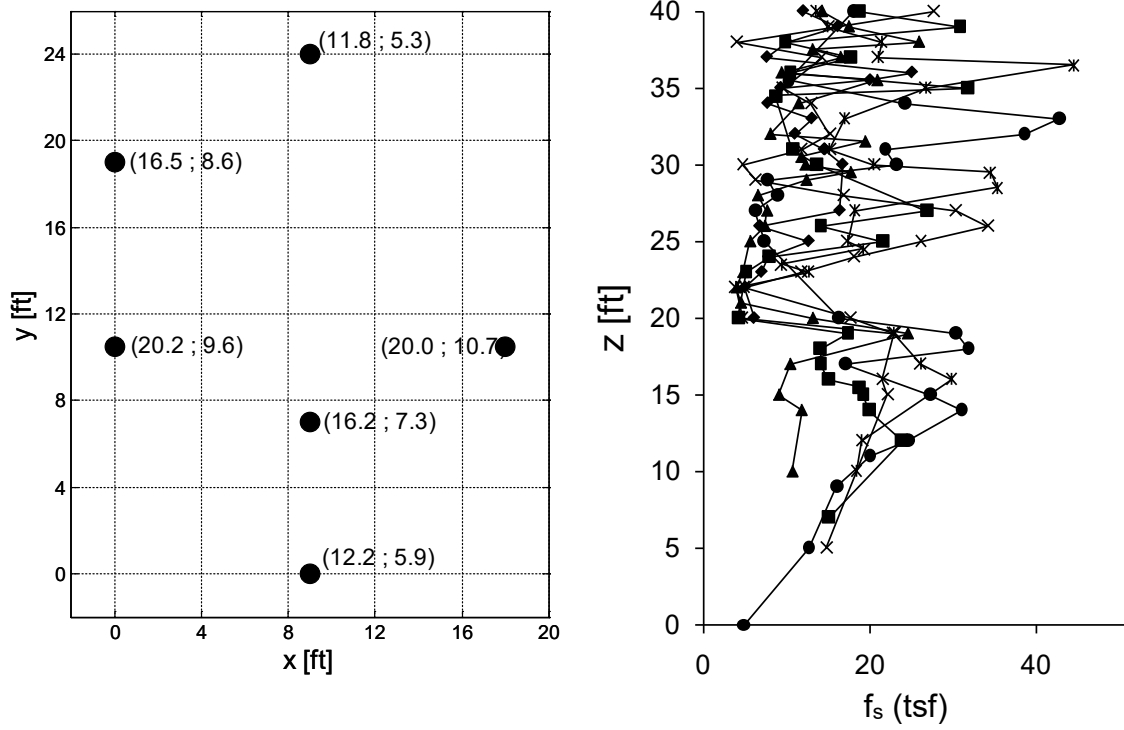
Figure 4-18. f_s data from six borings at 17th Street Bridge in Fort Lauderdale.

5. Laboratory vs. MWD Rock Strength by Depth, Layer, and Shaft at CR250

The second site using MWD was at County Road 250 in Dowling Park, Florida. At the CR-250 site, a similar Bauer rock drilling bucket was used to complete the majority of drilling for each shaft. A core barrel and cross-cutter were used in the strongest rock layers, which occurred at the base of a few shafts. Figure 5-1 depicts the rock buckets from both monitored sites in which the only difference is the additional cutting teeth and slightly different tooth configuration on the rock bucket from CR-250. At the CR-250 site, two test shafts and two production shafts were monitored that spanned nearly the entire bridge length. This provided sufficient MWD data across the full site to compare with core data collected and load test results.
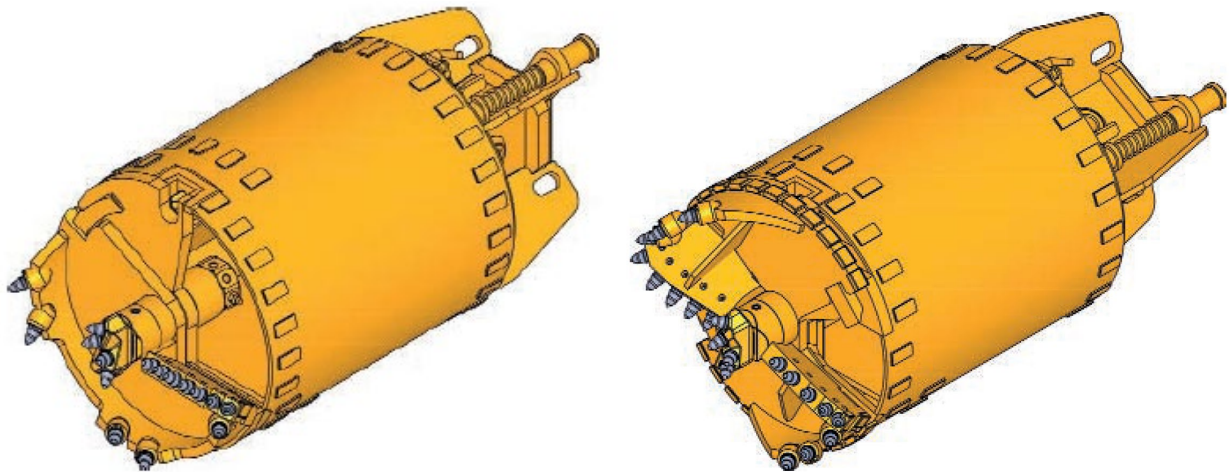
Figure 5-1. Rock drilling buckets used at Selmon Parkway (left) and CR-250 (right).

5.1 *CR-250 MWD Instrumentation*

The drill rig used at CR-250 was a Bauer BG39 Premium Line. The drill rig had all of the necessary instrumentation in place. Therefore, the Jean Lutz junction box was placed in the electrical unit/box and hardwired into the existing sensors (Figure 5-2).
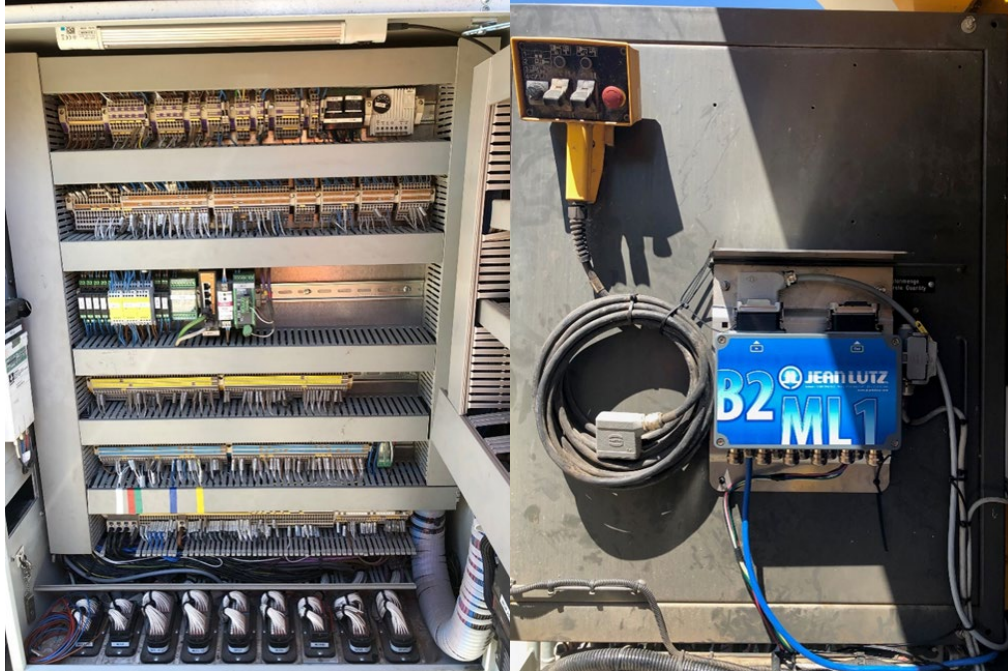
Figure 5-2. Jean Lutz equipment mounted in electrical unit tapping into sensors.

The DIALOG was placed in the cab in a position that did not interfere with the rig operator (Figure 5-3). The data was wirelessly transmitted to an external computer for monitoring at a safe distance (behind the shaft inspector, Figure 5-3).
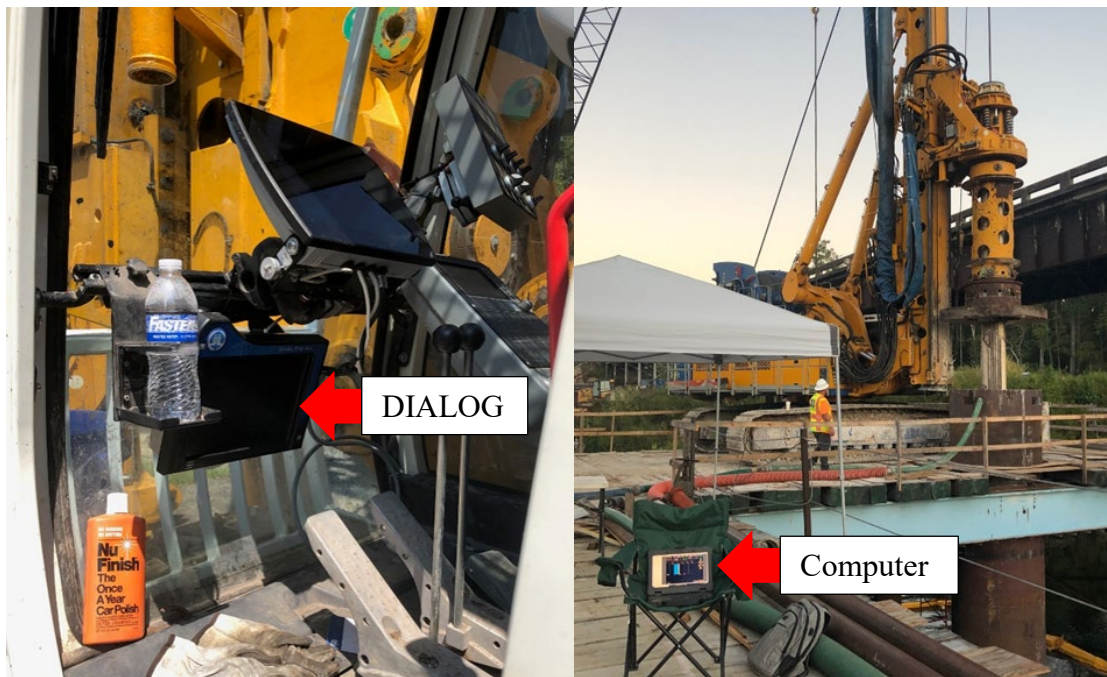
Figure 5-3. DIALOG mounted in cab and monitoring from a safe distance.

5.2 Converting Torque and Crowd for Specific Energy Assessment

Prior to the assessment of specific energy from MWD at CR-250, the hydraulic torque and crowd were converted to physical measures that are compatible with the specific energy equation (Equation 1-1). This required gathering drill rig specifications from the operator's manual. From the Bauer BG39 Premium Line manual, the following was identified:

- Maximum Torque (T_{max})= 287,250 ft-lbf = 3,447,005 in-lbf
- Maximum Crowd (F_{max}) = 89,924 lbf
- Maximum Operating Pressure (P_{max}) = 5,076 psi
- Hydraulic Flow Rate (Q) = 640 LPM = 39,055.2 in³/min

5.2.1 Converting Torque

From the specifications gathered, the maximum motor displacement (δ_{max}) was determined:

$$\delta_{max} = \frac{2 \times \pi \times T_{max}}{P_{max}} = \frac{2 \times \pi \times 3,447,005 \; in-lbf}{5076 \; psi} = 4{,}267 \; in^3/rev \qquad \text{(Eq. 5-1)}$$

Next, the minimum rotational speed (N_{min}) that coincides with T_{max} was determined:

$$N_{min} = \frac{Q}{\delta_{max}} = \frac{39,055.2 \; in^3/min}{4,267 \; in^3/rev} = 9.2 \; RPM \qquad \text{(Eq. 5-2)}$$

The value of N_{min} indicated that in a rotational speed range of 0 to 9.2 RPM, the maximum torque of 3,447,005 in-lbf can be achieved. At rotational speeds above 9.2 RPM, the maximum torque available begins to decrease and can be determined by Equation 5-3:

$$T = \frac{PQ}{2 \times \pi \times N} \qquad \text{(Eq. 5-3)}$$

From the information gathered, a torque versus rotational speed chart was developed (Figure 5-4).

Bauer BG39 Premium Line
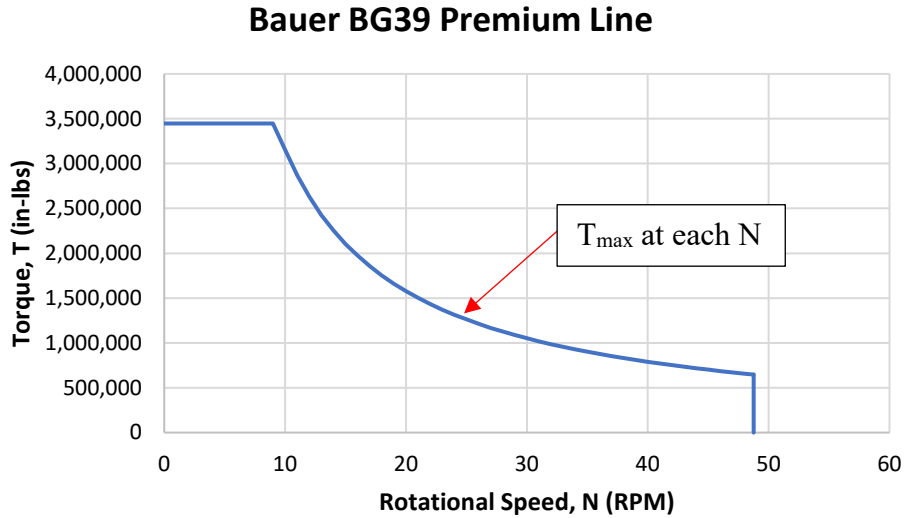
Figure 5-4. Bauer BG39 Premium Line T-N chart.

5.2.2 Converting Crowd

To convert crowd, a conversion coefficient (K_F - lbf/psi) was developed. The following specifications were gathered for crowd (Note: the crowd baseline pressure was determined from the drill rig after it was warmed up, Figure 5-5):

- Maximum Crowd (F_{max}) = 89,925 lbs
- Maximum Operating Pressure (P_{max}) = 5,076 psi
- Crowd Baseline Pressure (BP_{Crowd}) = 33 psi

Solve for K_F using the identified and measured input parameters:

$$K_F = \frac{F_{max}}{P_{max} - BP_{Crowd}} = \frac{89,925\ lbf}{5,076\ psi - 33\ psi} = 17.8\ \frac{lbf}{psi} \qquad \text{(Eq. 5-4)}$$

The developed conversion coefficient was used to transform the "real time" measured crowd hydraulic pressures to physical measures (lbf) as presented in Equation 5-5.

$$F\ (lbf) = K_F \left(\frac{lbf}{psi}\right) \times [F_{Pressure}(psi) - BP_{Crowd}(psi)] \qquad \text{(Eq. 5-5)}$$

After conversion takes place, measurements of torque and crowd become compatible with Teale's specific energy equation (Eq. 1-1).
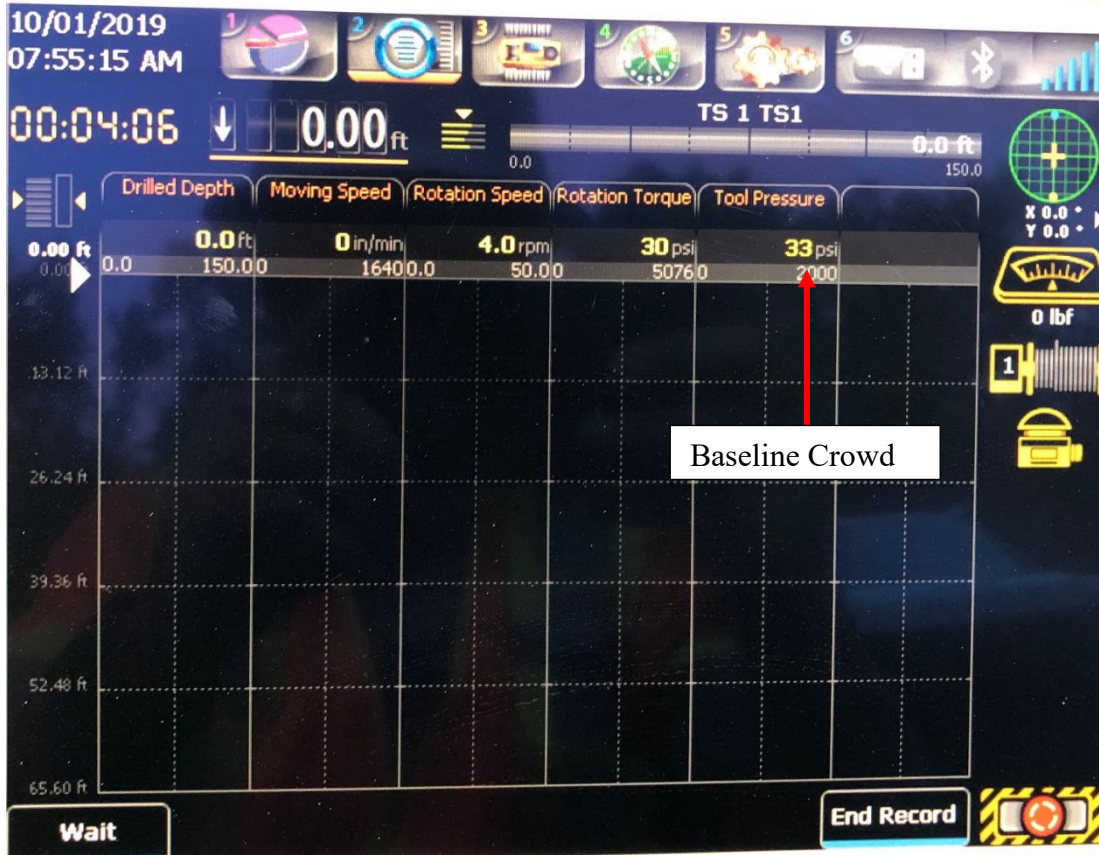
Figure 5-5. Identifying the baseline pressure for crowd after warming up the hydraulics.

5.3 *CR-250 Shaft Analysis via Core Data and MWD*

At CR-250, data from the B-tronic were combined with the Jean Lutz data for analysis. The rotational speeds recorded by the Lutz system were not accurate and therefore the B-tronic rotational speeds were used. This was due to a newer feature on the new drill rig that the Lutz system could not account for. This was an analog knob that allowed the rig operator to adjust the rotational speed range which directly affected the signal being copied by the Lutz system.

The B-tonic system provides the data in a time-referenced format whereas the Lutz system provides the data in a depth-referenced format. This required a rotational speed index to be developed using the B-tronic data (Figure 5-6). The RPM index produces an average rotational speed and torque value at each depth increment recorded by the B-tronic system. The index accounts for the time spent at each depth increment penetrating downward and creates an average value. The "# of Data" column in the index indicates the number of samples that were recorded at each depth increment that comprise the average.

Based on the recorded Lutz depth references, the developed spreadsheet searches the RPM index for the rotational speed and torque value above and below the referenced depth and interpolates an estimated value at the Lutz specified depth increment (Figures 5-7 through 5-9). Once the

estimated rotational speed and torque value are determined for the specified depth, specific energy is calculated.

Depth (ft)	N_{avg} (RPM)	T_{avg} (BAR)	# of Data	Data #
42.19	12.8	161	24	1
42.29	16.0	124	1	2
42.39	14.8	163	31	3
42.65	16.1	219	12	4
42.72	17.7	204	3	5
42.78	19.0	193	1	6
42.81	18.0	172	2	7
42.85	16.0	229	8	8
43.11	16.4	231	8	9
43.14	15.7	224	18	10
43.27	19.5	222	2	11
43.31	20.0	214	1	12
43.41	18.2	232	6	13
43.44	16.5	237	8	14
43.57	17.0	159	1	15
43.60	15.3	214	22	16
43.64	18.5	165	2	17
44.00	17.0	181	1	18
44.03	17.2	206	20	19
44.19	20.0	173	2	20

Figure 5-6. Rotational speed and torque index.

Depth (ft)	N (rpm)	T (Bar)	T (psi)	T (in-lbs)	u (in/min)	F (lbf)
42.26	=BZ7+(K7-BY7)*(CB7-BZ7)/(CA7-BY7)				778.1	681
42.33	15.5	237	3,435	1,376,219	1031.5	664
42.39	14.8	237	3,435	1,441,370	1031.5	664
42.46	15.2	231	3,354	1,375,665	1150.7	658

Figure 5-7. Interpolating rotational speed based on depth.

y_1 (ft)	N_1 (RPM)	y_2 (ft)	N_2 (RPM)
=INDEX($C$7:$C$405,MATCH(J7,$C$7:$C$405,1))			
INDEX(array, row_num, [column_num])			
INDEX(reference, row_num, [column_num], [area_num])			
42.39	14.8	42.65	16.1
42.39	14.8	42.65	16.1

Figure 5-8. Matching index values for depth based on depth recorded by Jean Lutz system.

y_1 (ft)	N_1 (RPM)	y_2 (ft)	N_2 (RPM)
42.19	=INDEX($D$7:$D$405,MATCH(J7,$C$7:$C$405,1))		
42.29	INDEX(array, row_num, [column_num])		
42.39	INDEX(reference, row_num, [column_num], [area_num])		
42.39	14.8	42.65	16.1
42.39	14.8	42.65	16.1

Figure 5-9. Matching index values for rotational speed based on depth recorded by Lutz system.

The Jean Lutz system was capable of recording the proper torque values in a depth-referenced format. Therefore, a comparison was made when using the B-tronic estimated torque from the index and the Jean Lutz depth referenced torque values comprised of continuous data collection averaged every 2 centimeters of penetration (Figure 5-10). In general, the strength assessments using either approach were comparable. There was less than a 5% difference between the two methods on average. The Jean Lutz torque values were selected for further analysis because they had more samples, and the resulting specific energy and strength assessments were slightly more conservative.

The unconfined compression strength (q_u) was estimated using the rock strength equation developed at Selmon Expressway (Eq. 3-12) for rock drilling buckets. Although there were slightly different tooth configurations between the rock drilling bucket used at Selmon and the rock drilling buckets used at CR-250, all drilling buckets were manufactured by Bauer. The Selmon developed equation worked quite well in the assessment of rock strength at CR-250, which is evident from the remainder of this chapter.
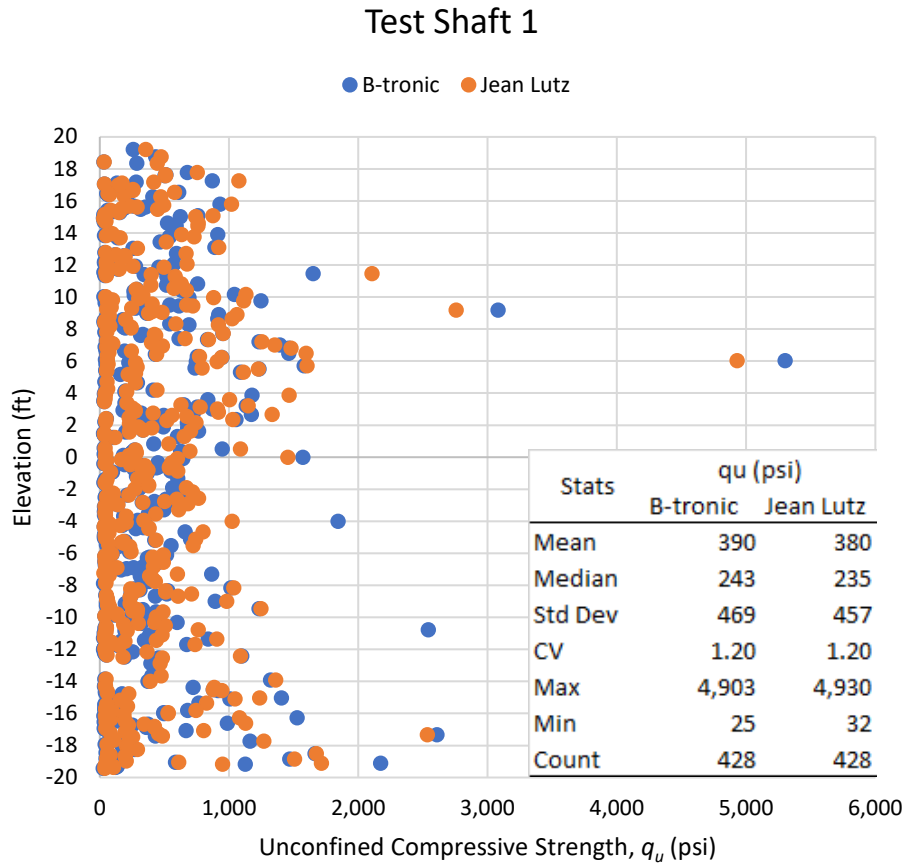
Test Shaft 1

Figure 5-10. Comparing q_u results based on B-tronic and Jean Lutz torque measurements.

Figure 5-11 provides the locations of each of the four shafts analyzed at CR-250. Test Shaft 1 was located on the west side of the river and was on land. Test Shaft 2 was located in the middle of the river. Shaft P5-1 was located on the east-side bank of the river, 11.5 feet left of the center line (all other shafts were on the center line). Shaft P6-3 was located on land, further east of the river compared to Shaft P5-1.
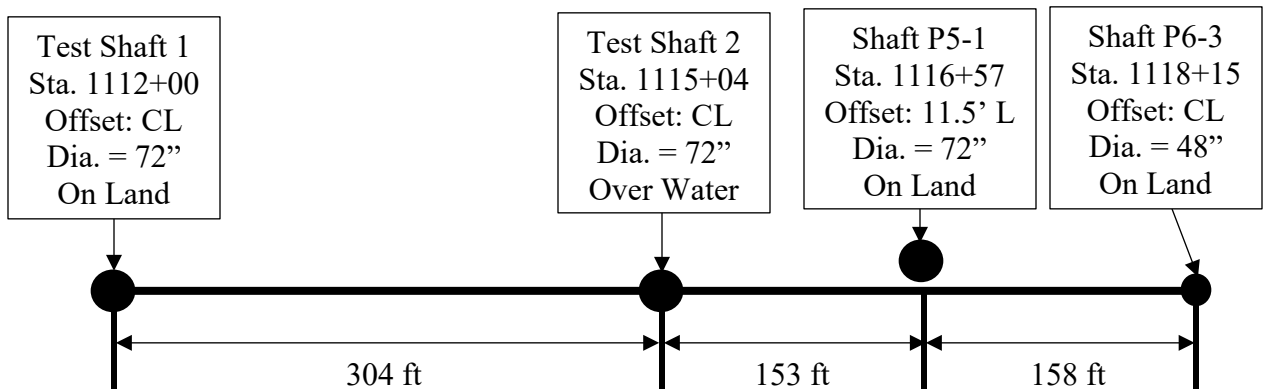
Figure 5-11. Shaft spacing at CR-250.

The MWD estimated rock strengths (q_u) were compared to the core strengths obtained within the vicinity of each shaft. The core strengths were typically located within 200 feet of the shafts (P6-3 required a distance of 400 feet). These lengths were used in order to generate enough core strength data for comparison with the MWD data collected in the footprint of each shaft, over the full elevation range where MWD took place in rock.

The core strengths and MWD strengths were comparable at all locations. Test Shaft 1 showed good agreement between MWD and the core data. The profiles (Figure 5-12) were fairly similar and the statistics were in excellent agreement (Figures 5-13 and 5-14).

Figure 5-12. TS-1 strength profiles from core data within 200' and MWD in shaft footprint.

Figure 5-13. Test Shaft 1 frequency distribution from core data and MWD.

Figure 5-14. Test Shaft 1 cumulative frequency distribution from core data and MWD.

Similar to Test Shaft 1, Test Shaft 2 also showed good agreement between MWD and the core samples. The shaft profiles (Figure 5-15) and the statistics (Figures 5-16 and 5-17) were similar.

Figure 5-15. Test Shaft 2 strength profiles from core data within 200' and MWD in shaft footprint.
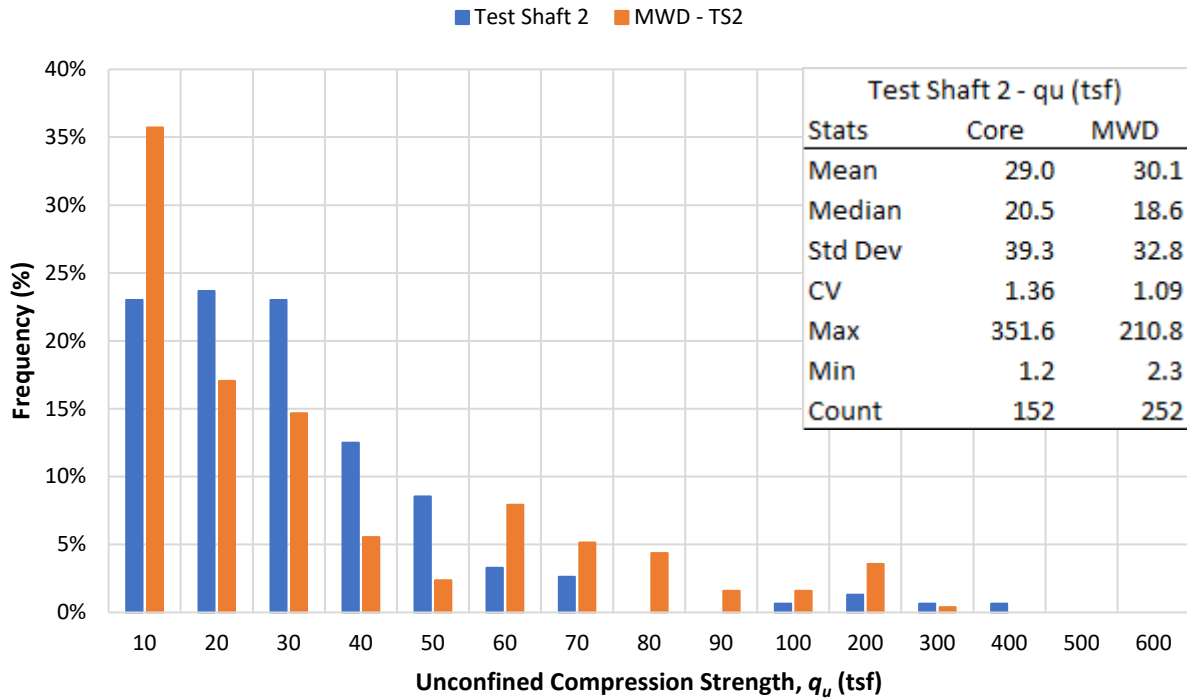
Figure 5-16. Test Shaft 2 frequency distribution from core data and MWD.

Figure 5-17. Test Shaft 2 cumulative frequency distribution from core data and MWD.

At Shaft P5-1, the shaft profiles (Figure 5-18) and the statistics (Figures 5-19 and 5-20) were fairly similar. However, the core data indicated higher strength material at an approximate elevation of +4 feet, whereas MWD did not. This was due to two core samples collected 156 feet away, which did not represent the true strength profile. It was necessary to include samples collected within 200 feet of the shaft in order to generate core strengths over the entire elevation range measured by MWD. MWD also indicated higher strength material at approximately -18 feet whereas the core samples showed the increase at approximately -20 feet (not depicted in plot but encountered in Test Shafts 1 and 2). The MWD assessment is correct because the material was so strong at this elevation that the rock drilling bucket was ineffective to excavate the rock and a core barrel and cross-cutter had to be used to complete the shaft.
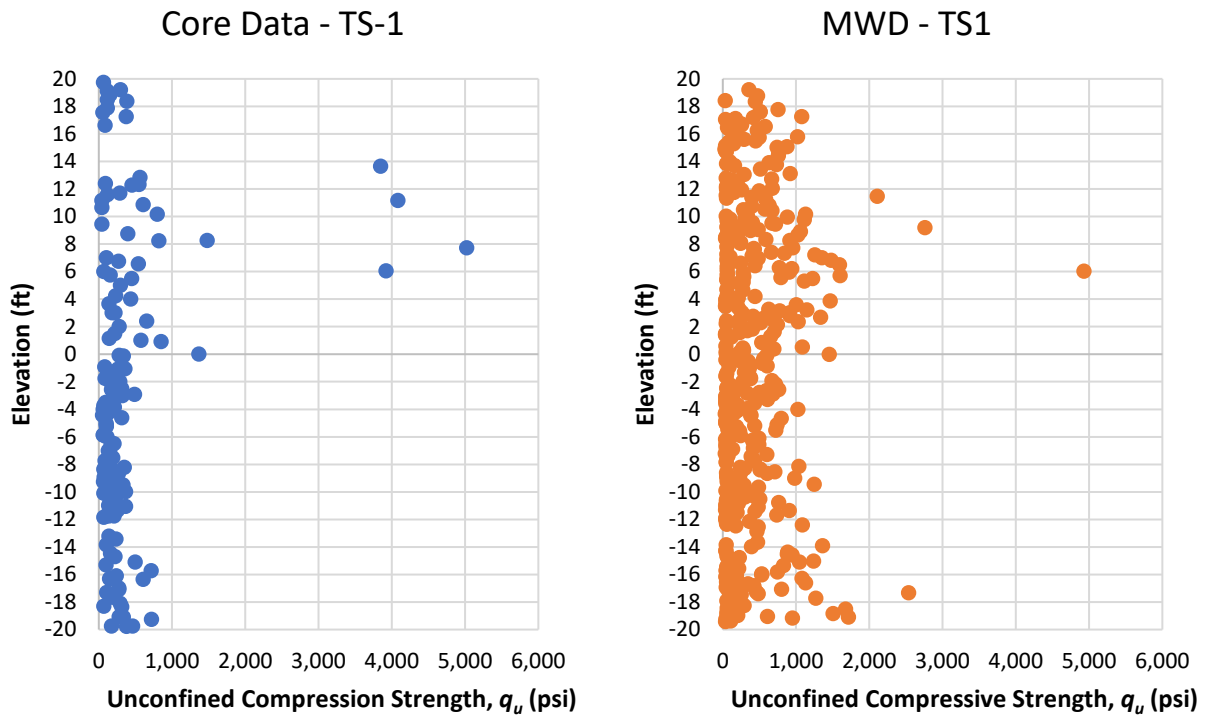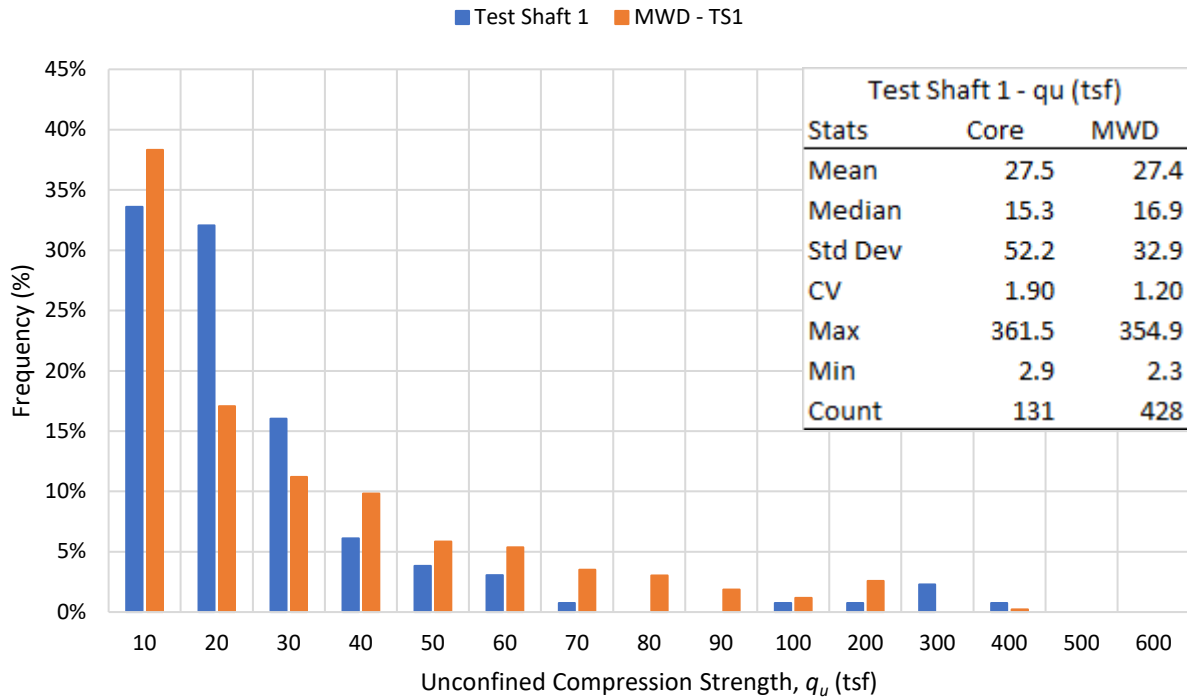

Figure 5-18. Shaft P5-1 strength profiles from core data within 200' and MWD in shaft footprint.

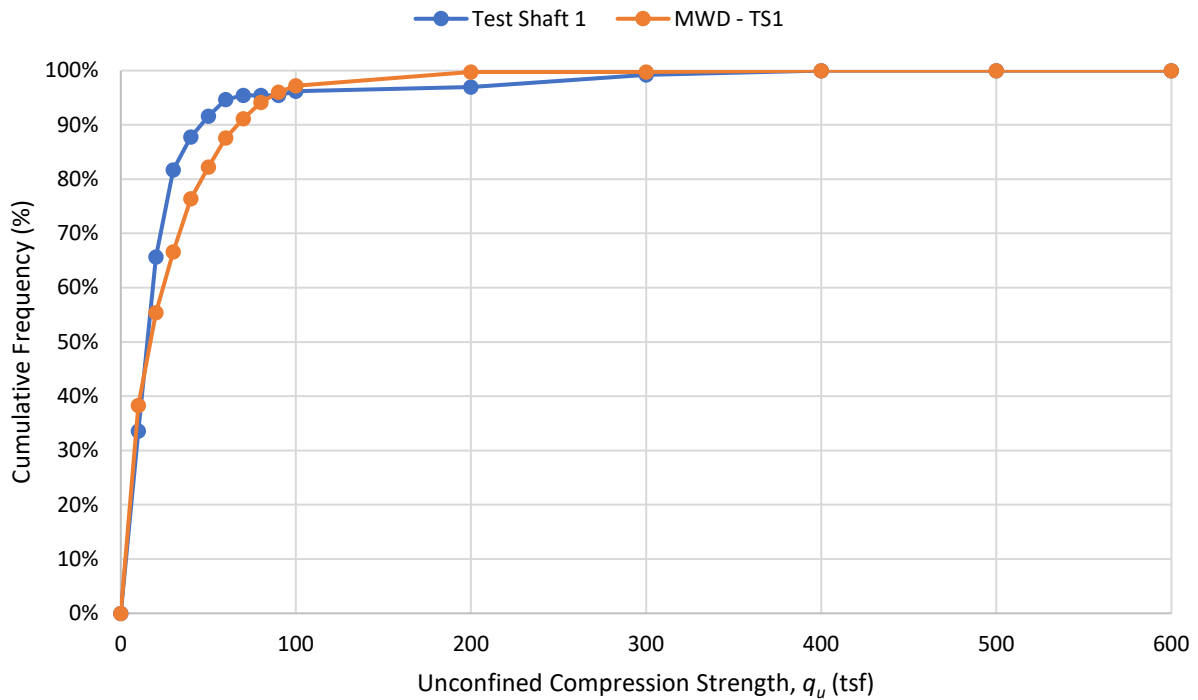Figure 5-19. Shaft P5-1 frequency distribution from core data and MWD.

Figure 5-20. Shaft P5-1 cumulative frequency distribution from core data and MWD.

75

At Shaft P6-3, the same two higher strength core samples considered in Shaft P5-1 were also considered for this shaft (Figure 5-21 through 5-23). Conversely, the higher strength samples were collected 2 feet away from Shaft P6-3 and MWD confirmed a similar strength increase at the same approximate elevation. Therefore, this higher strength layer was not present at Shaft P5-1 but was present at Shaft P6-3, indicating zonal anisotropy which will be discussed in the next section. Test Shaft 1 showed a similar increase at the same approximate depth as Shaft P6-3, which was not present in Test Shaft 2 or Shaft P5-1, further indicating zonal anisotropy was present at the site.
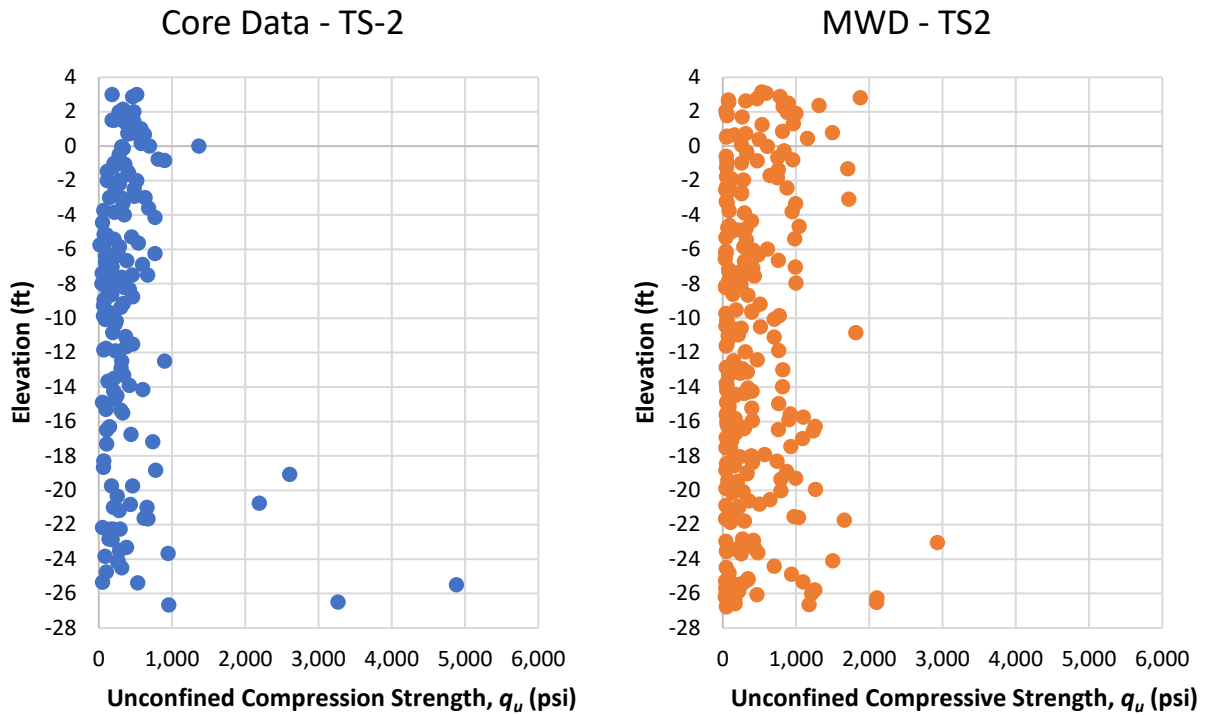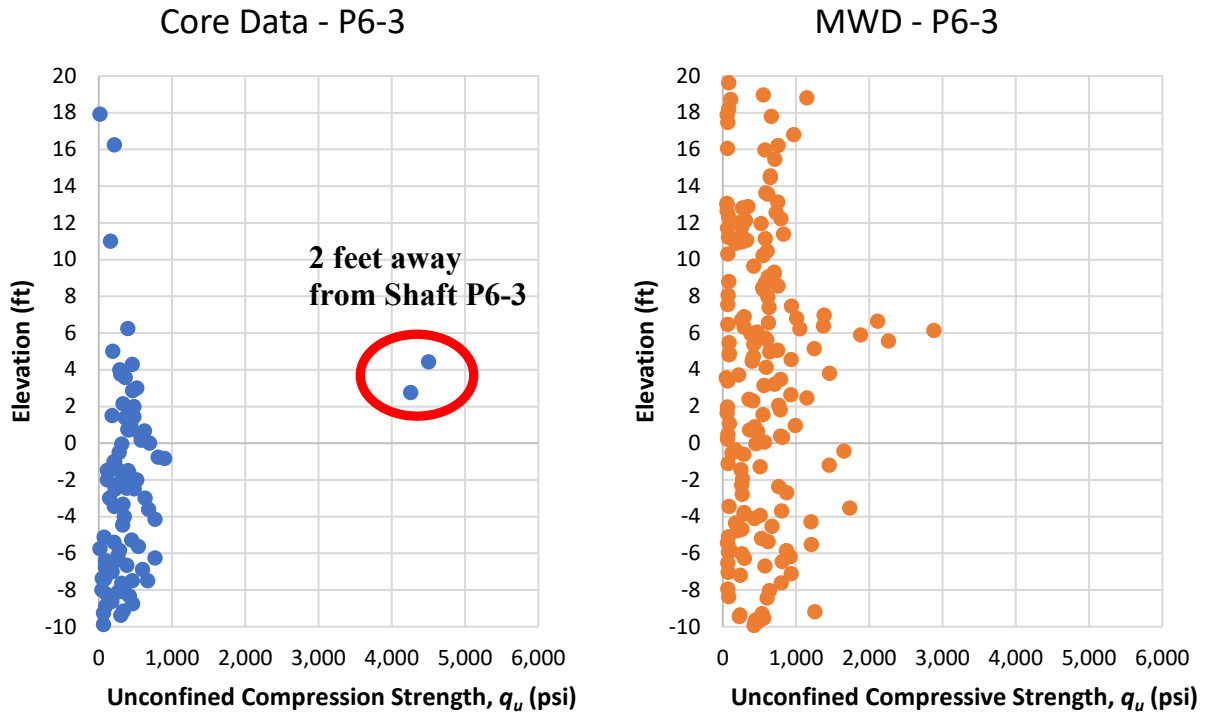

Figure 5-21. Shaft P6-3 strength profiles from core data within 400' and MWD in shaft footprint.

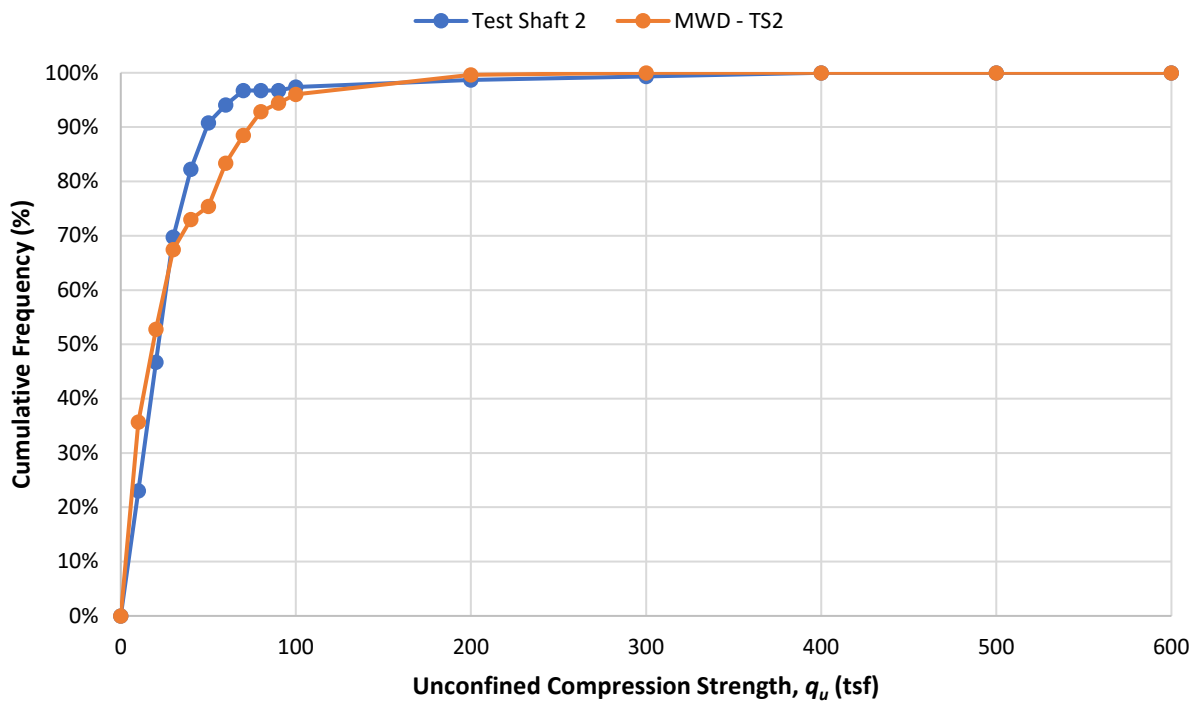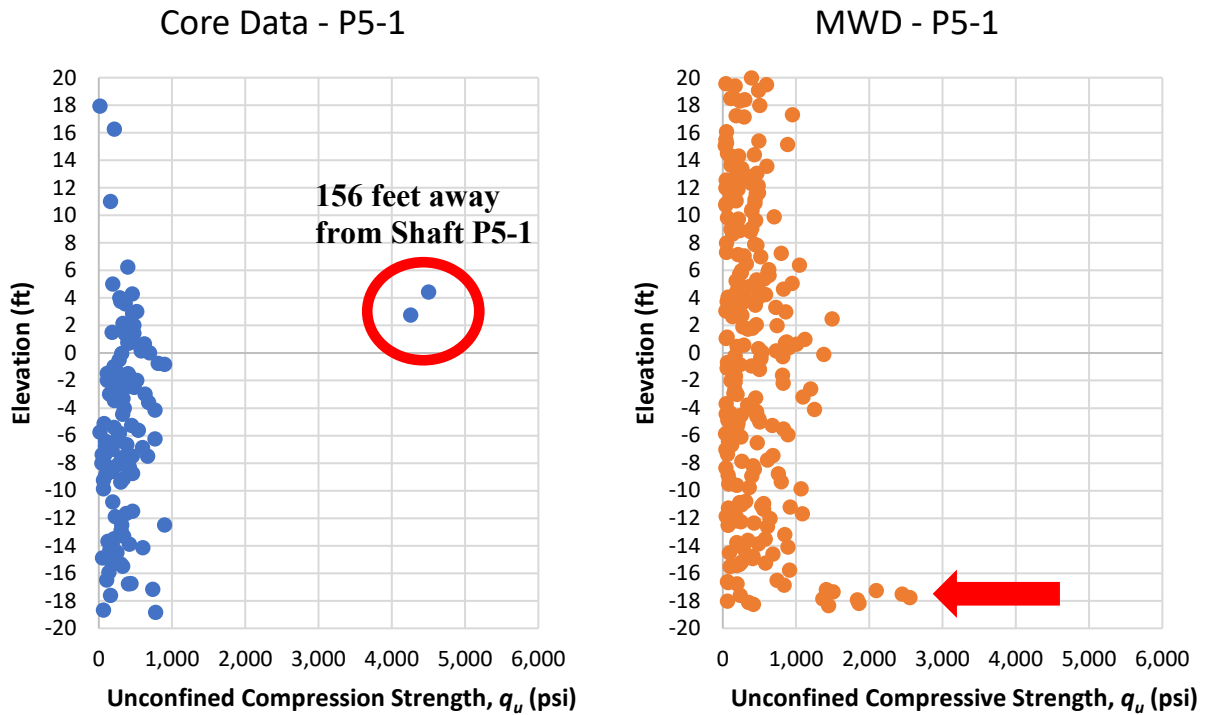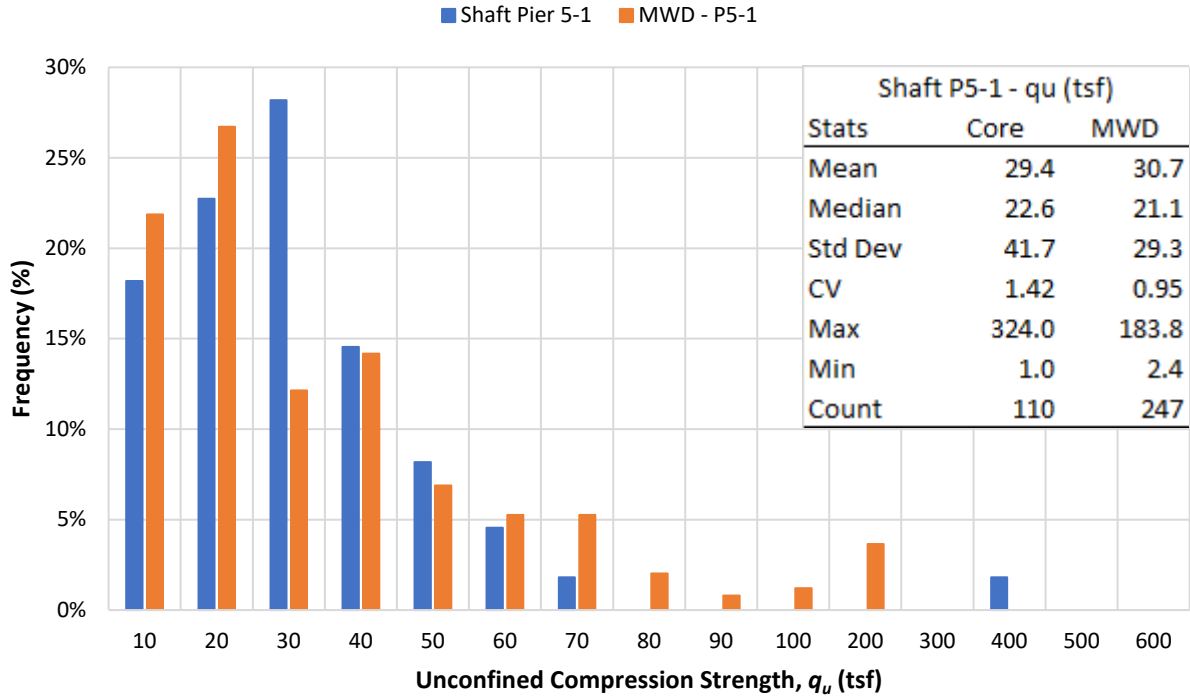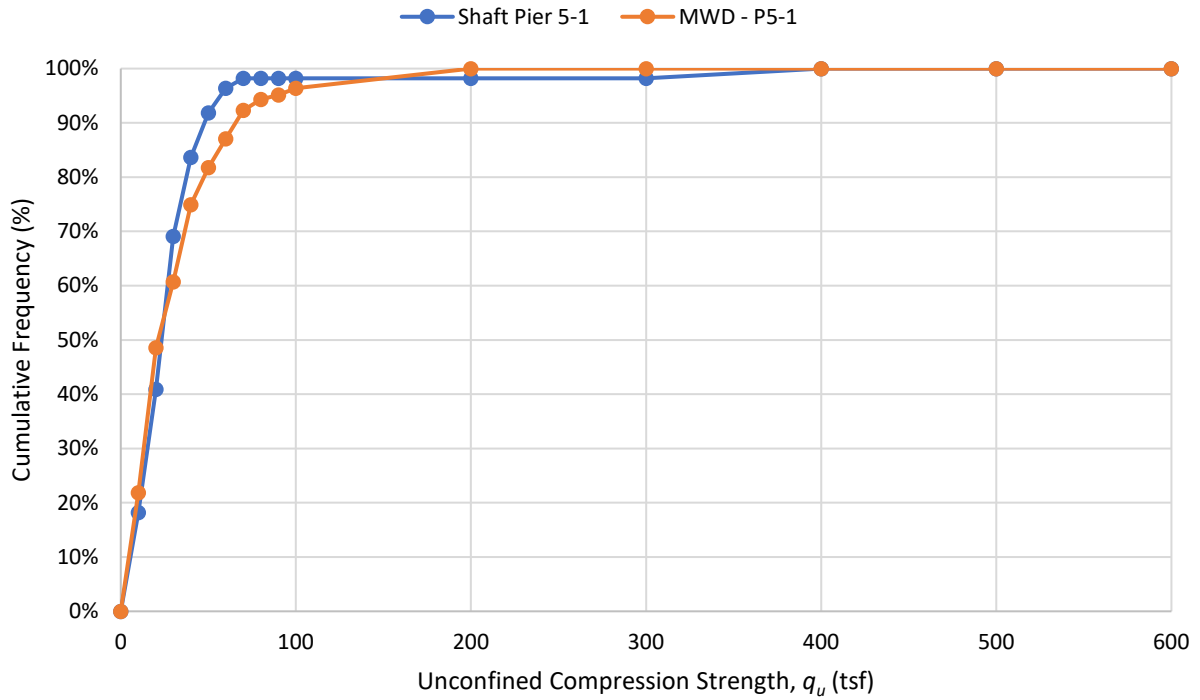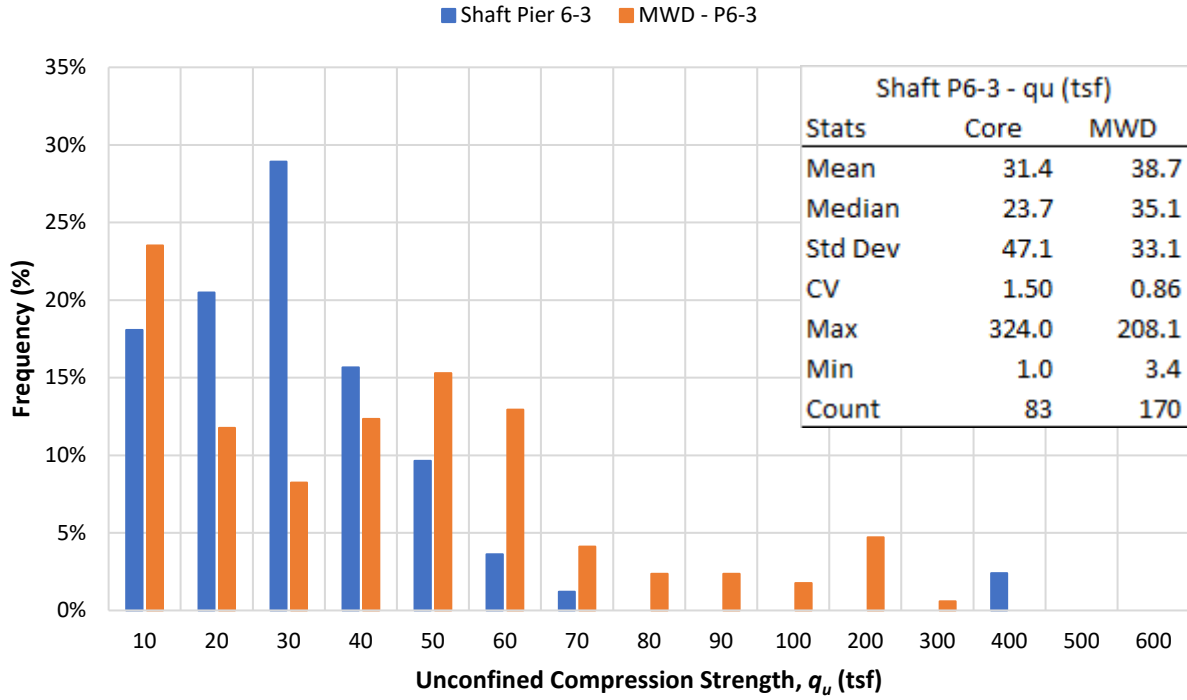Figure 5-22. Shaft P6-3 frequency distribution from core data and MWD.
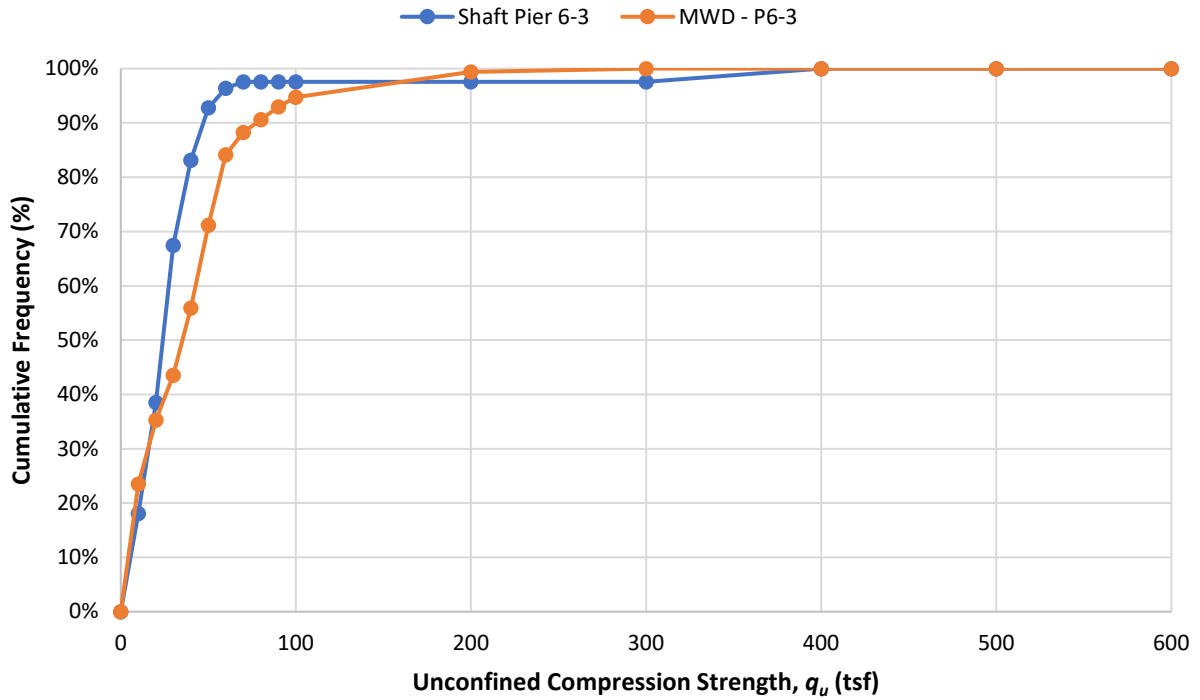
Figure 5-23. Shaft P6-3 cumulative frequency distribution from core data and MWD.

As presented, the core data and MWD strength assessments generally indicated similar layering and strengths at each location. However, MWD produced 1097 individual strength assessments in the investigated elevation range, at four sampled locations. This equates to 274 samples per location on average. Over the same investigated elevation range, 289 core samples were collected from 20 different borings. This equates to 14 samples per location. Therefore, MWD generated more than 10 times the amount of data than standard core sampling. Furthermore, MWD was collected in the footprint, at full scale, showing the benefits of MWD as a QA/QC tool.

5.4 *CR-250 Site Variability*

Presented in Table 5-1 and Figure 5-24 are the locations of all the borings (laboratory tested core samples) and MWD monitored drilled shafts at CR-250. Figure 5-25 provides the strength profile (q_u) obtained from all laboratory tested core samples and MWD q_u measurements from monitoring the shaft installations. Figure 5-26 provides the frequency distribution and summary of statistics for the core samples and MWD combined. Figures 5-27 and 5-28 provide the normalized horizontal and vertical variograms [γ (h) / σ] for the whole site. The current state of the practice is to characterize all rock with one set of strength parameters and mobilized side shear. Evident from the summary statistics (Figure 5-26), a CV (coefficient of variation) of 1.93 is quite high and will result in the need for a reduced LRFD *Φ* for design if a single layer and zone is selected for the site.

Table 5-1. CR250 core boring and drilled shaft MWD locations.

Boring	Station (ft)	Offset (ft)	GSE (ft)
	CR250 Boring and MWD Locations		
EB1-4	1110+61	-19.2	50.00
B-1	1110+71	-15.5	50.12
B-2	1112+24	-17.5	41.84
B-3A	1113+21	23.5	42.65
B-3	1113+65	77.0	42.57
B-3 S-1	1113+22	11.0	42.60
B-4	1115+28	31.0	29.80
B-4 S-1	1114+89	11.5	40.50
B-5	1116+93	25.0	44.40
B-6	1118+08	-34.0	41.98
P3 S-2	1113+22	-11.5	40.00
P4 LTS-2	1115+04	0.0	40.50
P5 S-2	1116+57	-11.5	44.50
EB6 S-3	1118+13	0.0	53.05
P2-1	1111+86	11.5	43.91
P2-2	1111+86	-11.5	44.45
P2-LTS1	1112+00	0.0	43.00
P4-TMH	1114+75	0.0	40.50
P5 S-1	1116+57	11.5	43.60
P4 S-2	1114+89	-11.5	40.50
MWD-TS1	1112+00	0	43.37
MWD-TS2	1115+04	0	45.93
MWD-P5-1	1116+57	11.5	41.31
MWD-P6-3	1118+15	0	55.64
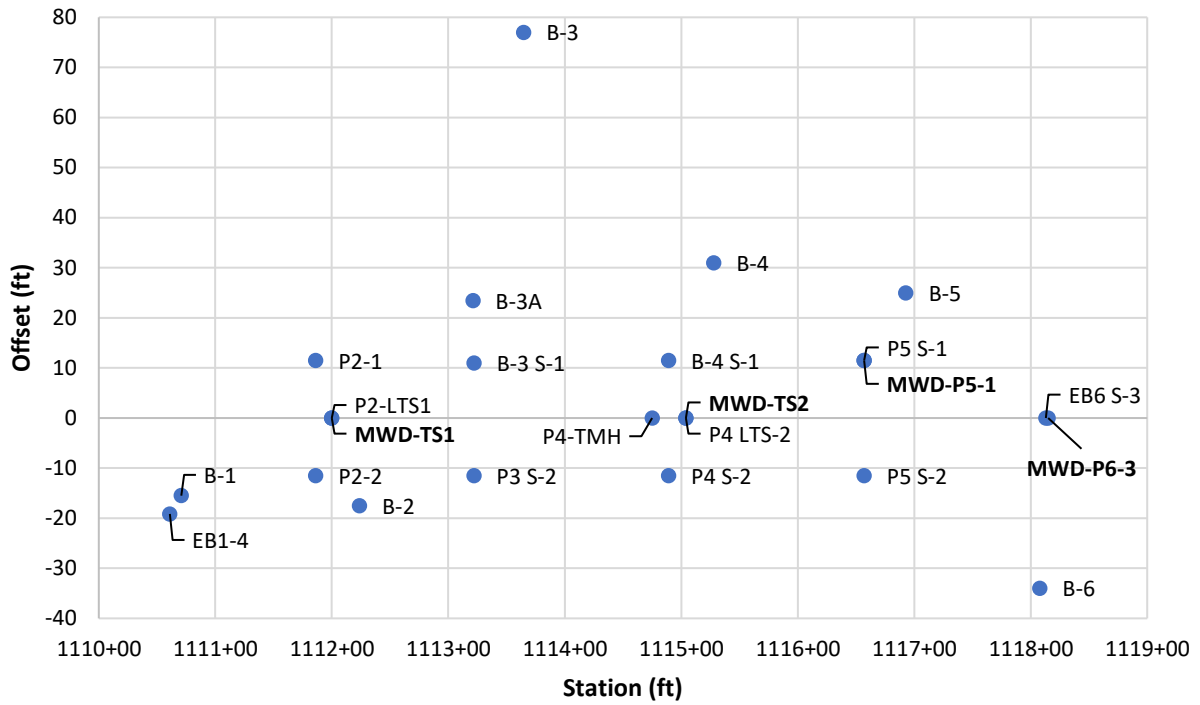
Figure 5-24. Plan view of all boring and MWD locations at CR-250.
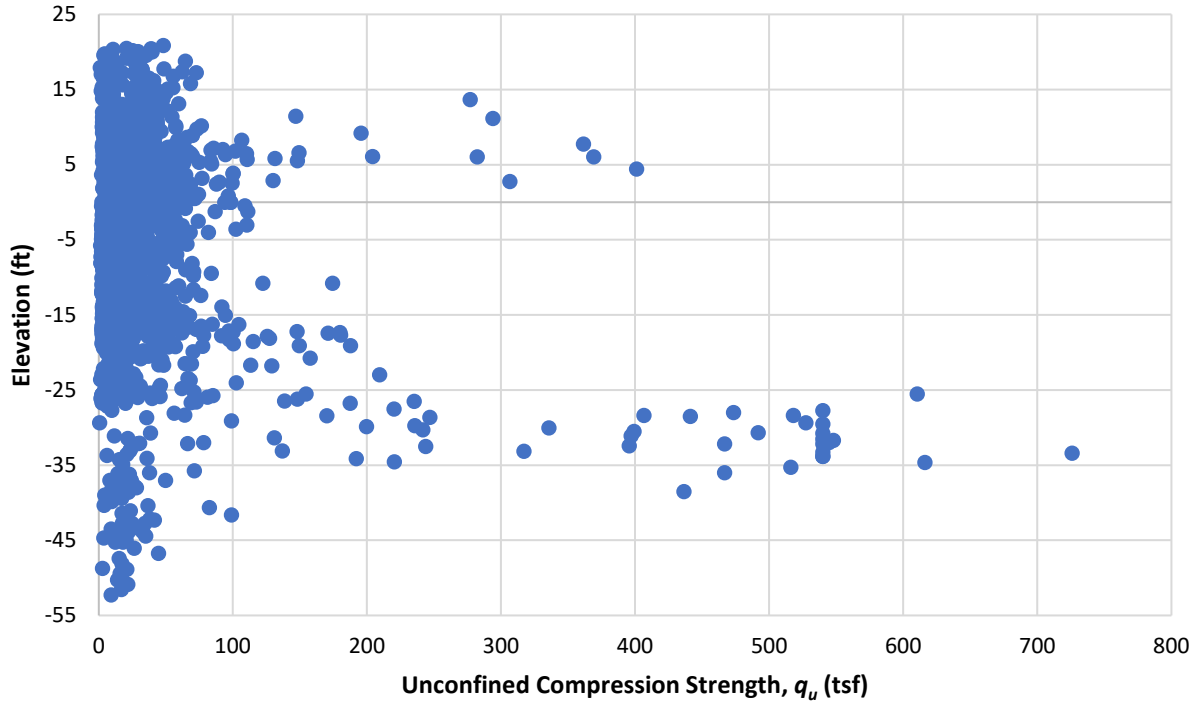
Figure 5-25. Rock strength profile at CR-250 from all core samples and MWD measurements.
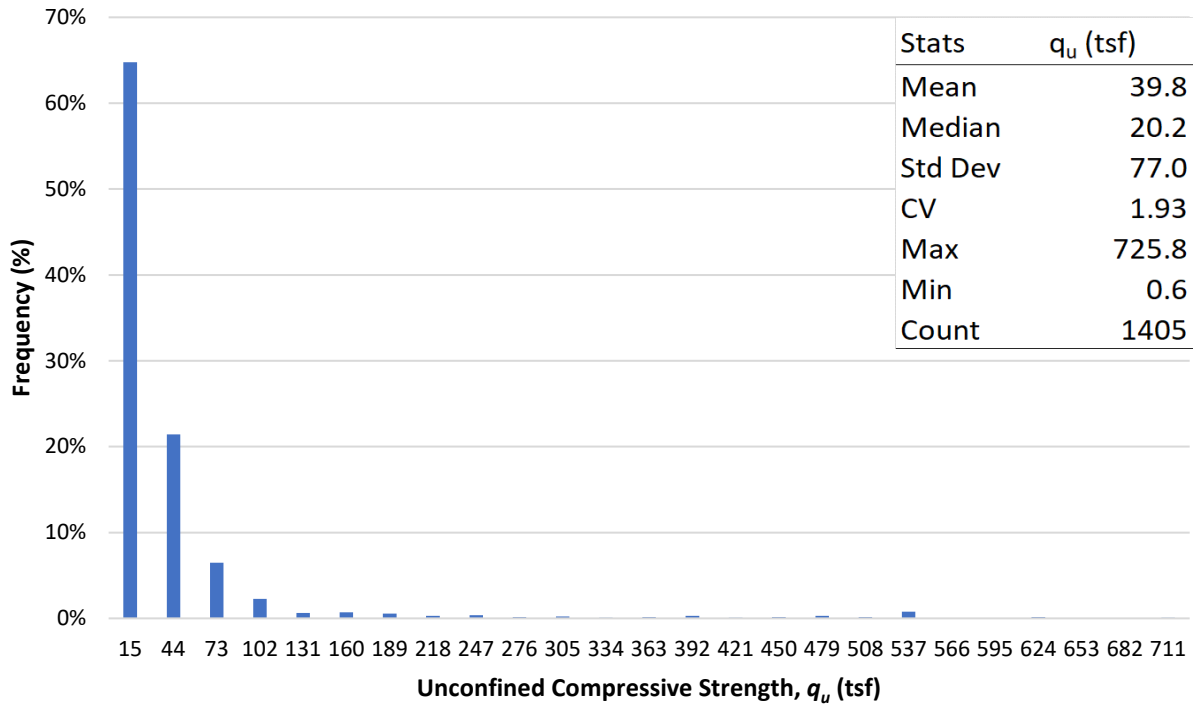
Figure 5-26. Frequency distribution from all core samples and MWD measurements at CR-250.

Horizontal Variogram
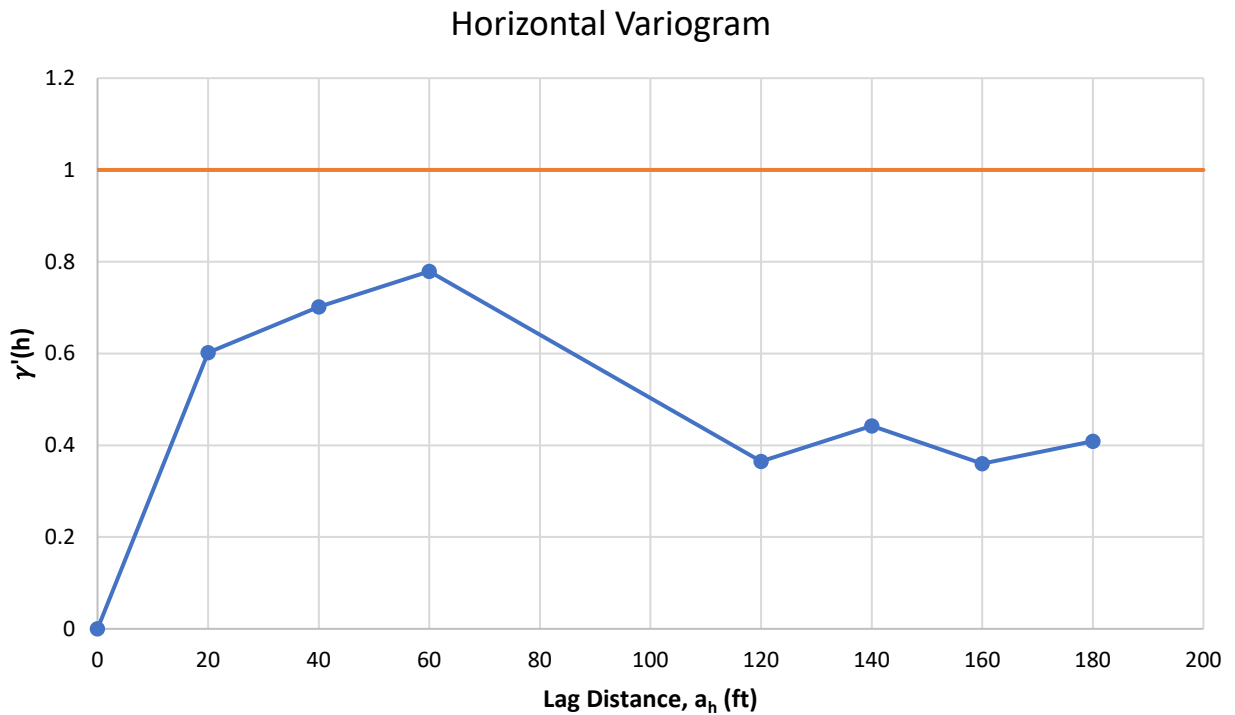
Figure 5-27. Horizontal Variogram from all core samples and MWD measurements at CR-250.
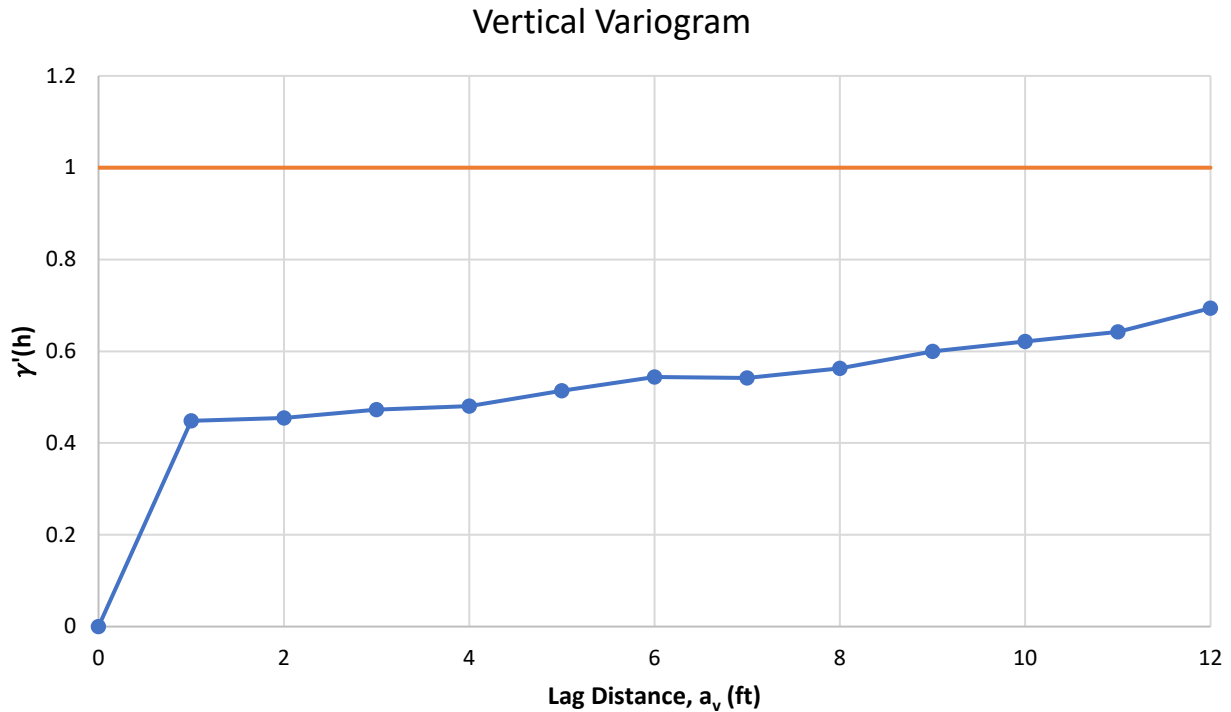
Figure 5-28. Vertical Variogram from all core samples and MWD measurements at CR-250.

Contributing to the high CV is horizontal layering which is identified in the vertical variogram Figure 5-28. Since the normalized variogram [γ (h) / σ] doesn't reach 1.0 (variability of site) over large vertical distances, large horizontal swaths of data have lower variability than others (i.e., layering). This is evident in Figure 5-25 from elevations -23 to -37-ft versus the other elevations. The normalized horizontal variogram [γ (h) / σ] shown in Figure 5-27, doesn't reach 1.0 as well, suggesting different zones exist on the site that have different strength characteristics (i.e., zonal anisotropy). For instance, if the borings in the vicinity of Test Shaft 1 and nearby borings (B-3 S-1, Pier 3 S-2, P2-1, P2-LTS1) as well MWD Pier 6 on far east of site (MWD- P6-3) with nearby boring EB 6 S-3 are characterized together (approx. 25% of site as shown in Figure 5-29), then the layering displayed in Figure 5-30 may be chosen. The subsequent layer statistics and normalized variograms for Layers 2 and 3 are given in Figures 5-31 through 5-37. Evidently, both layers have significantly different mean strengths with their vertical variograms approaching 1.0. Also note, the CV of each layer has been reduced over the single layer model with Layer 3 equal to 1.19 (versus 1.93 for a single layer model).
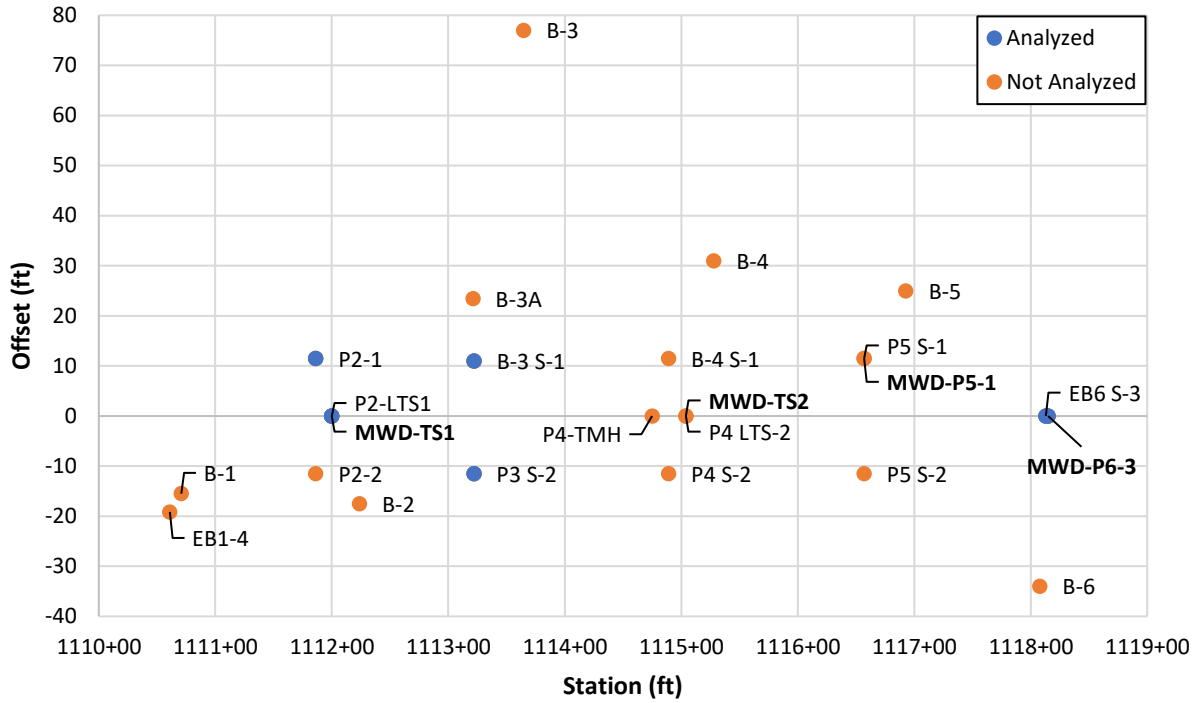
Figure 5-29. Separating site into higher strength upper zone (TS-1 and P6-3 @ Elev. 14 to -2 ft).
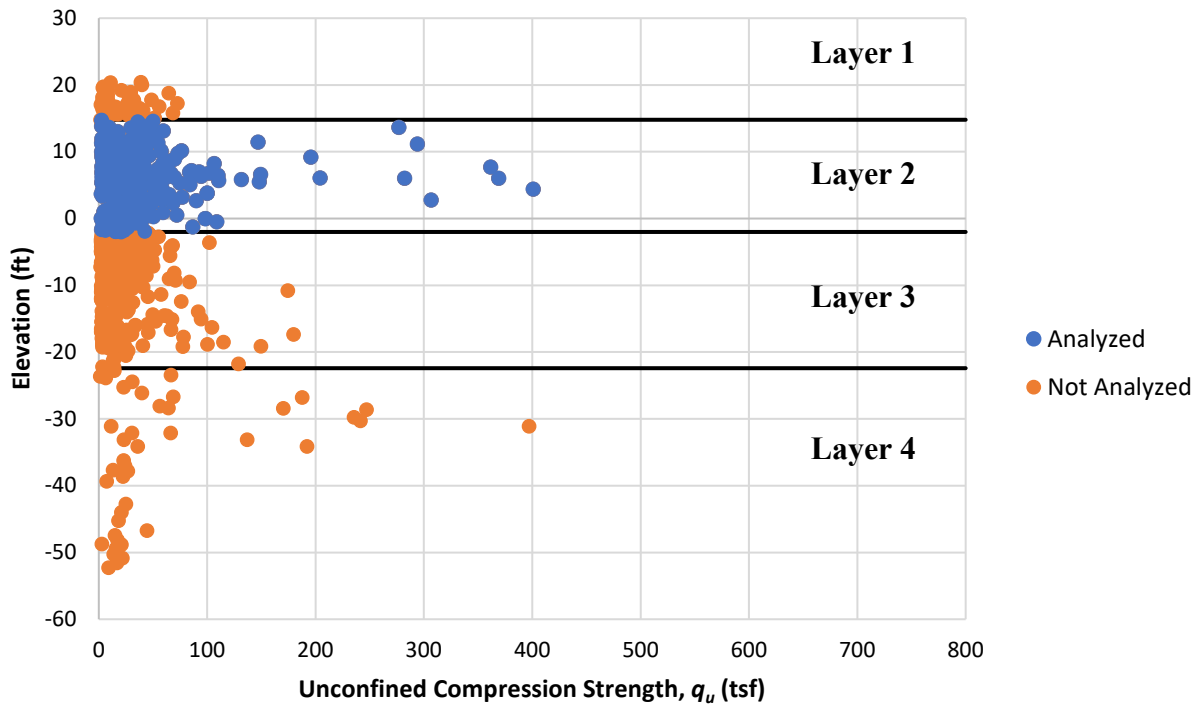
Figure 5-30. TS-1, shaft P6-3 and vicinity borings broken into layers (Layer 2 highlighted).
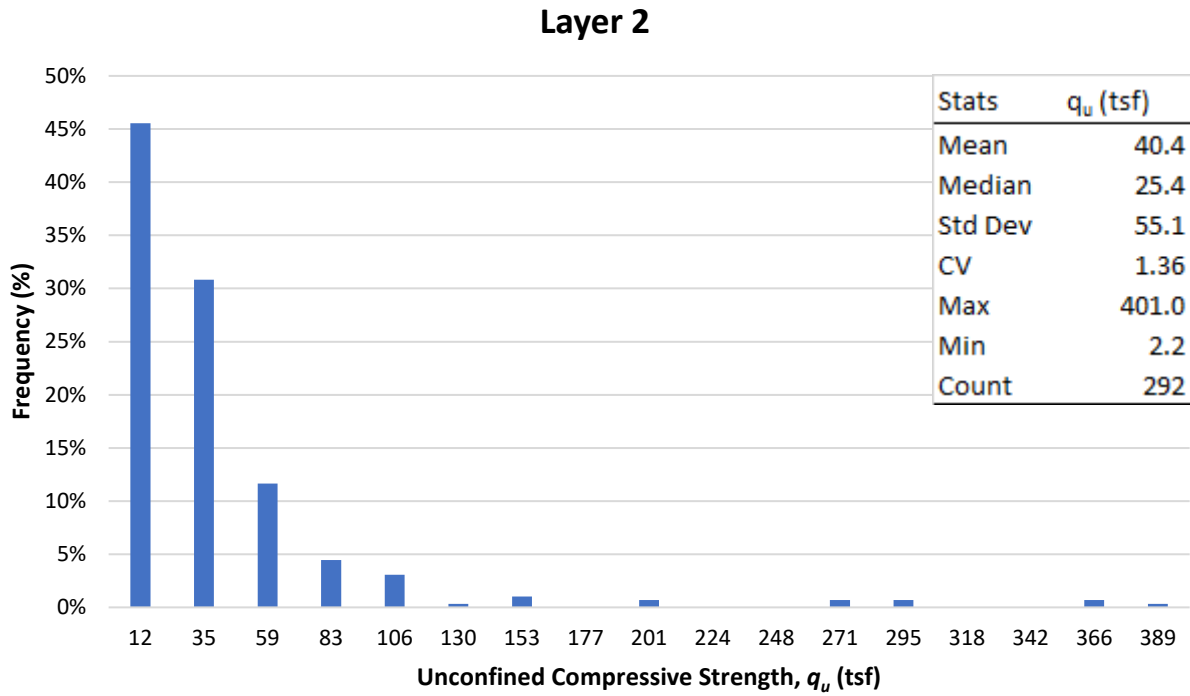
Layer 2

Figure 5-31. Frequency distribution for Layer 2—q_u from TS-1, shaft P6-3, and vicinity borings.

Horizontal Variogram
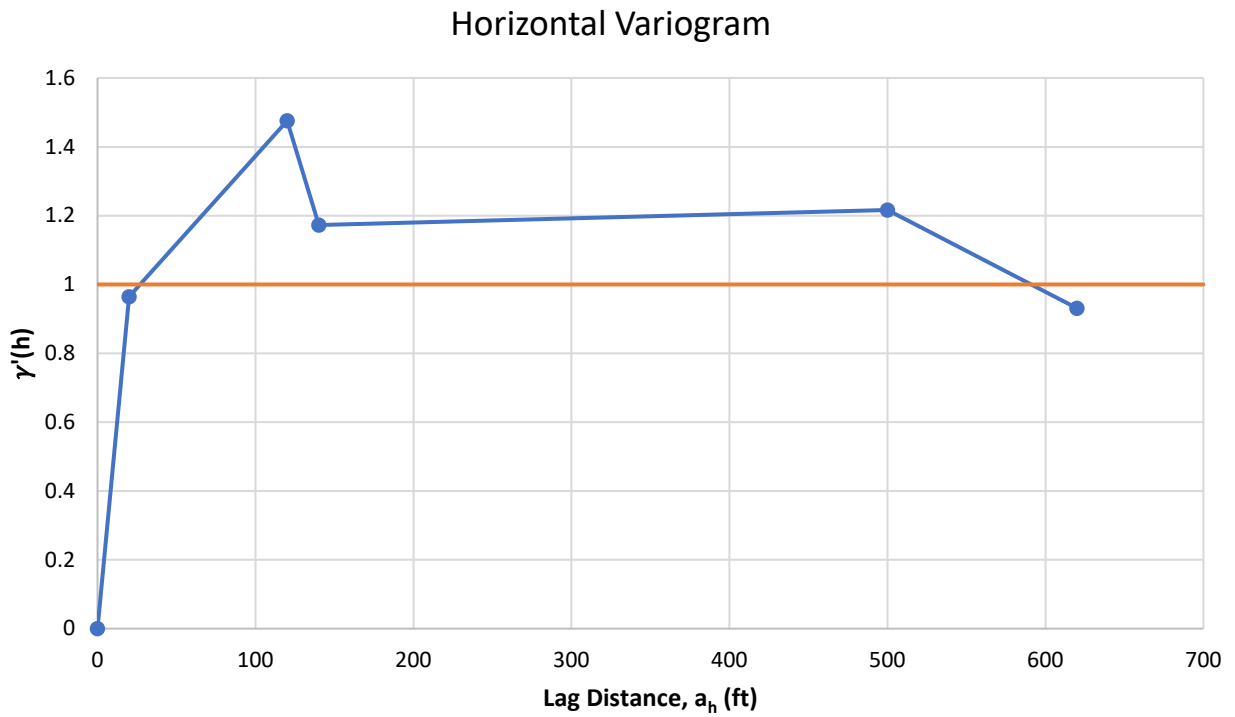
Figure 5-32. Horizontal variogram for Layer 2—q_u from TS-1, shaft P6-3, and vicinity borings.
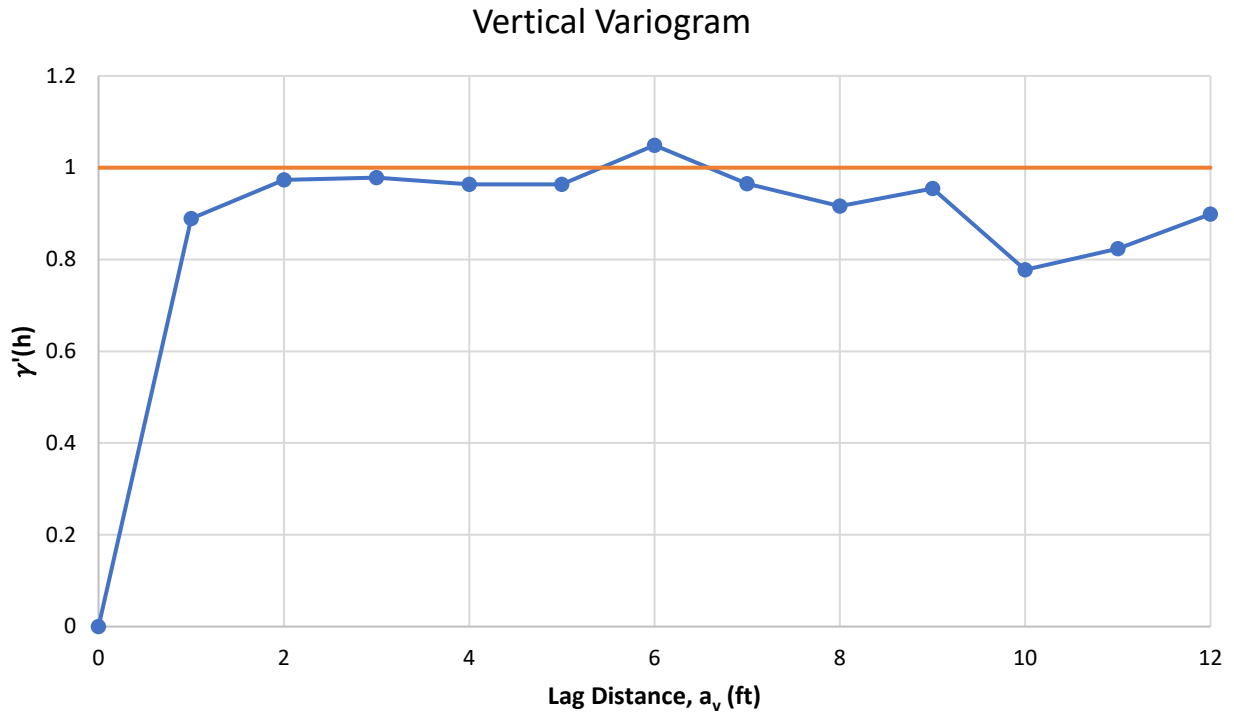
Figure 5-33. Vertical variogram for Layer 2—q_u from TS-1, shaft P6-3, and vicinity borings.
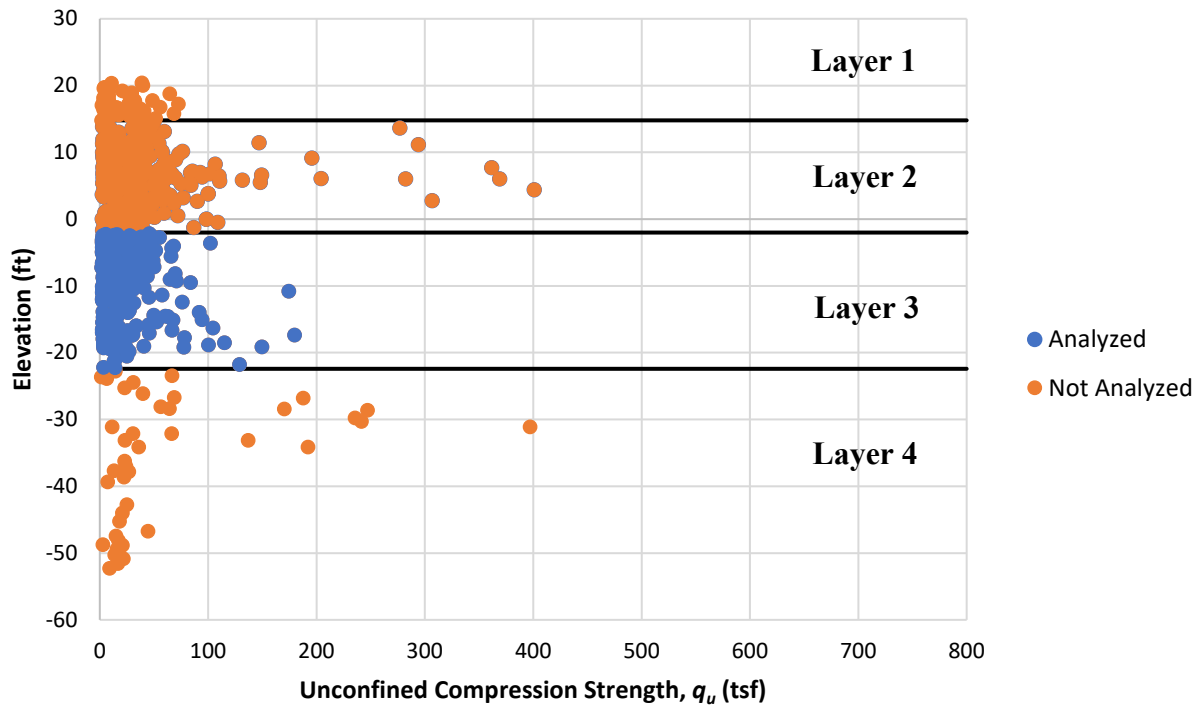
Figure 5-34. TS-1, shaft P6-3 and vicinity borings broken into layers (Layer 3 highlighted).

Layer 3

Stats	q_u (tsf)
Mean	22.2
Median	13.4
Std Dev	26.3
CV	1.19
Max	179.8
Min	1.7
Count	298
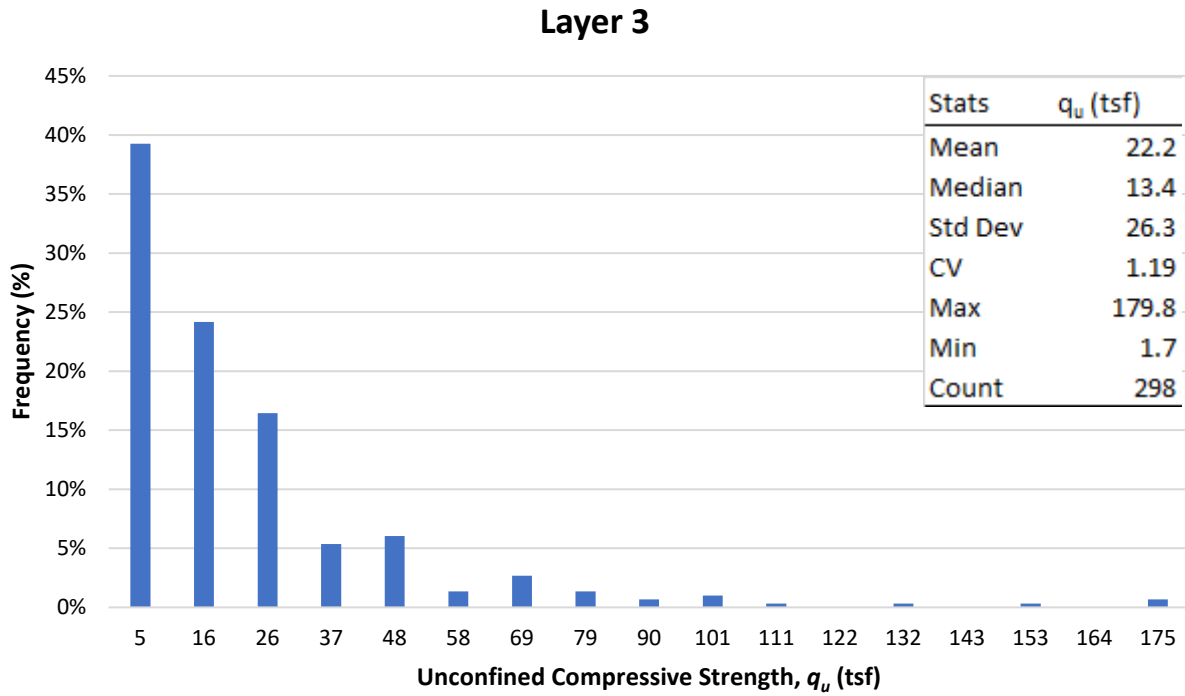
Figure 5-35. Frequency distribution for Layer 3—q_u from TS-1, shaft P6-3, and vicinity borings.

Horizontal Variogram
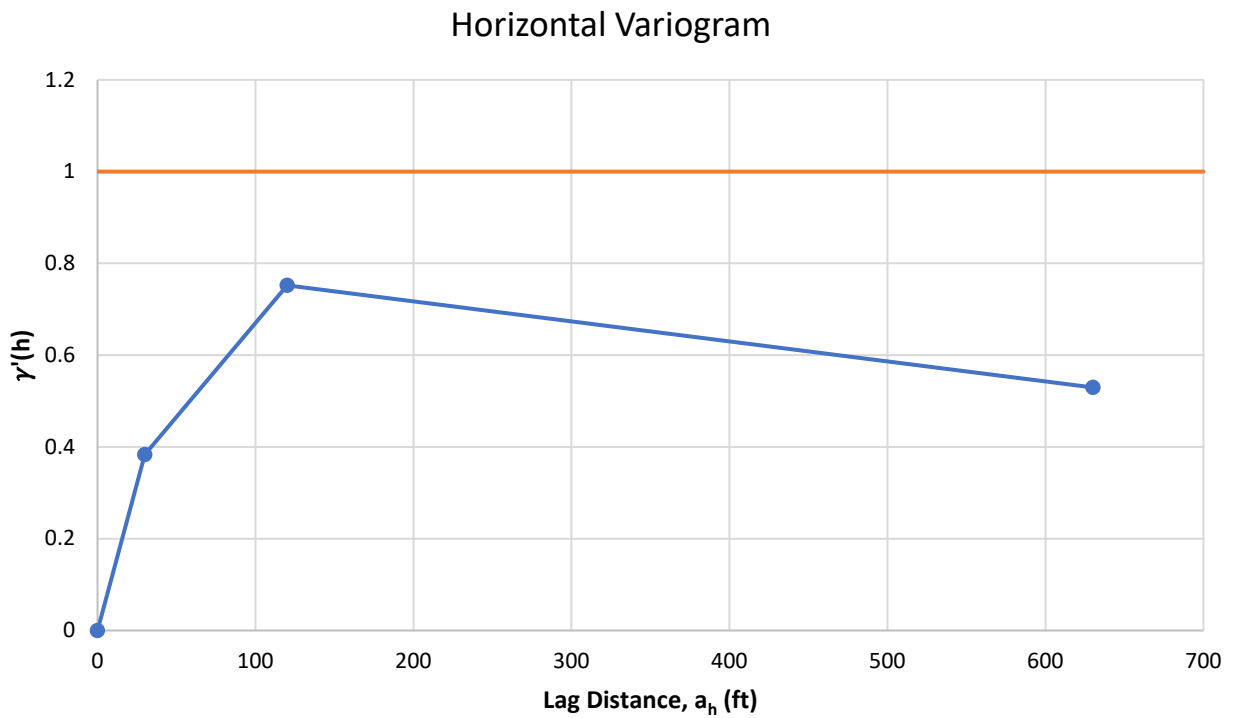
Figure 5-36. Horizontal variogram for Layer 3—q_u from TS-1, shaft P6-3, and vicinity borings.
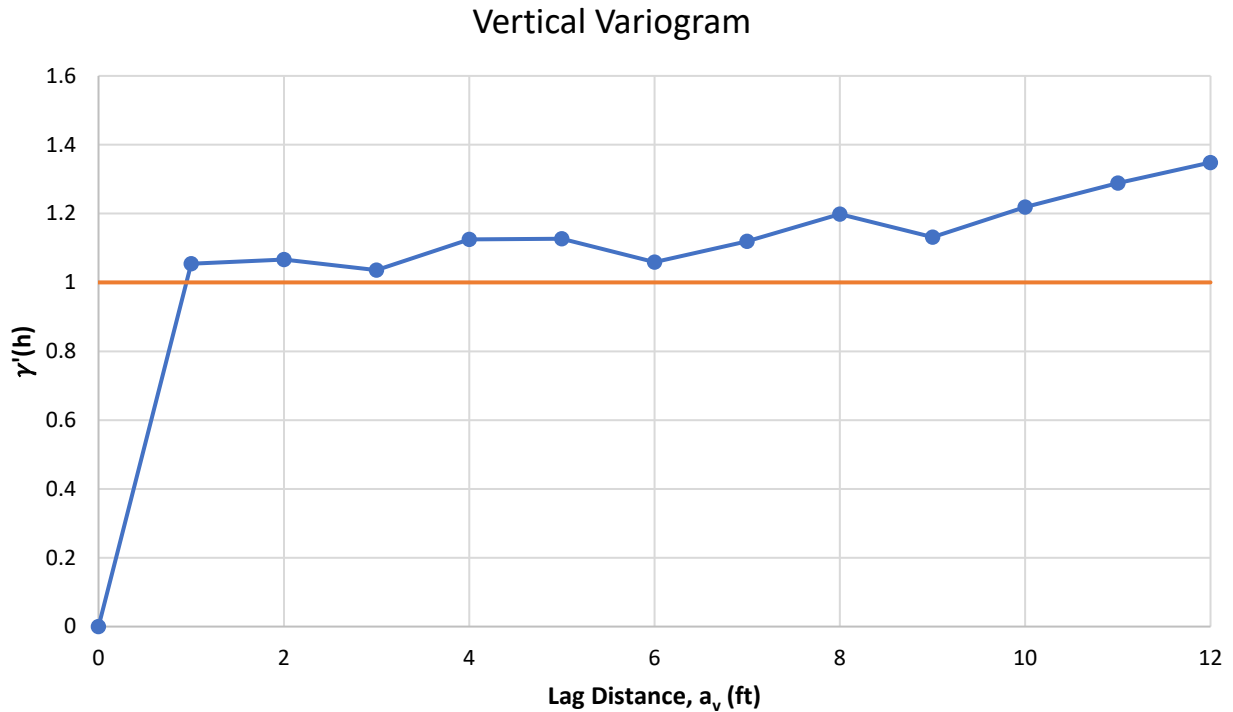
Figure 5-37. vertical variogram for Layer 3—q_u from TS-1, shaft P6-3, and vicinity borings.

If all the other piers and borings except those around shafts TS-1 and P6-3 were to be characterized together, Figure 5-38, then the CV of a single layer (Figure 5-39) would be reduced to 0.97 for the zone (Figure 5-40). From the vertical variogram, Figure 5-42, the vertical correlation length is now between 1 to 2 feet; with the normalized variogram [γ (h) / σ] reaching 1.0 with no cyclicity or asymptote less than 1.0. This indicates no horizontal layering is present within this larger zone.
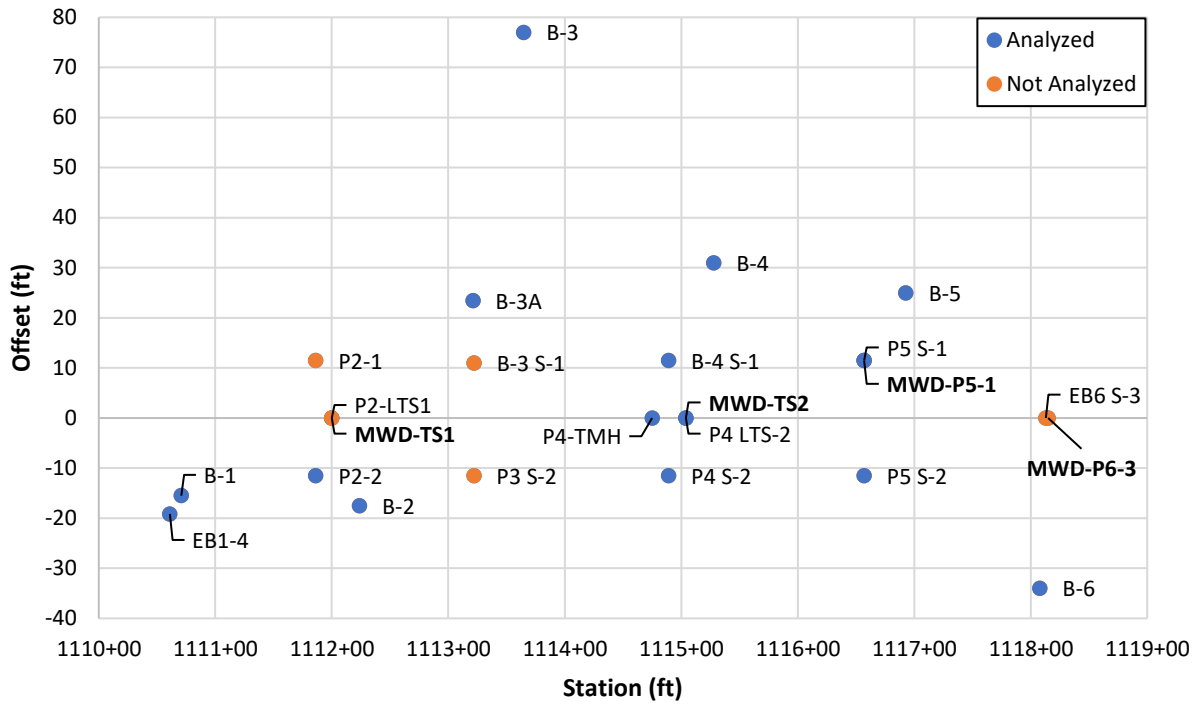
Figure 5-38. Borings and shaft locations at CR-250 minus TS-1, shaft P6-3, and vicinity borings.
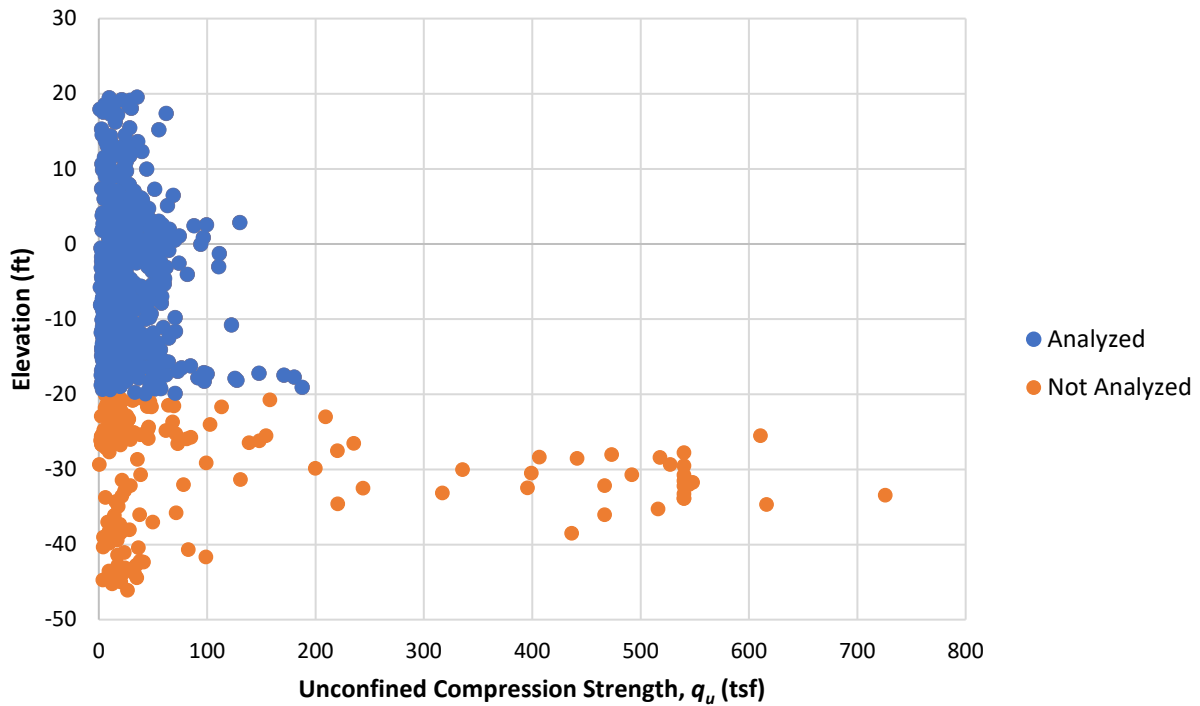
Figure 5-39. Strength profile for all shafts minus TS-1, shaft P6-3 and vicinity borings.
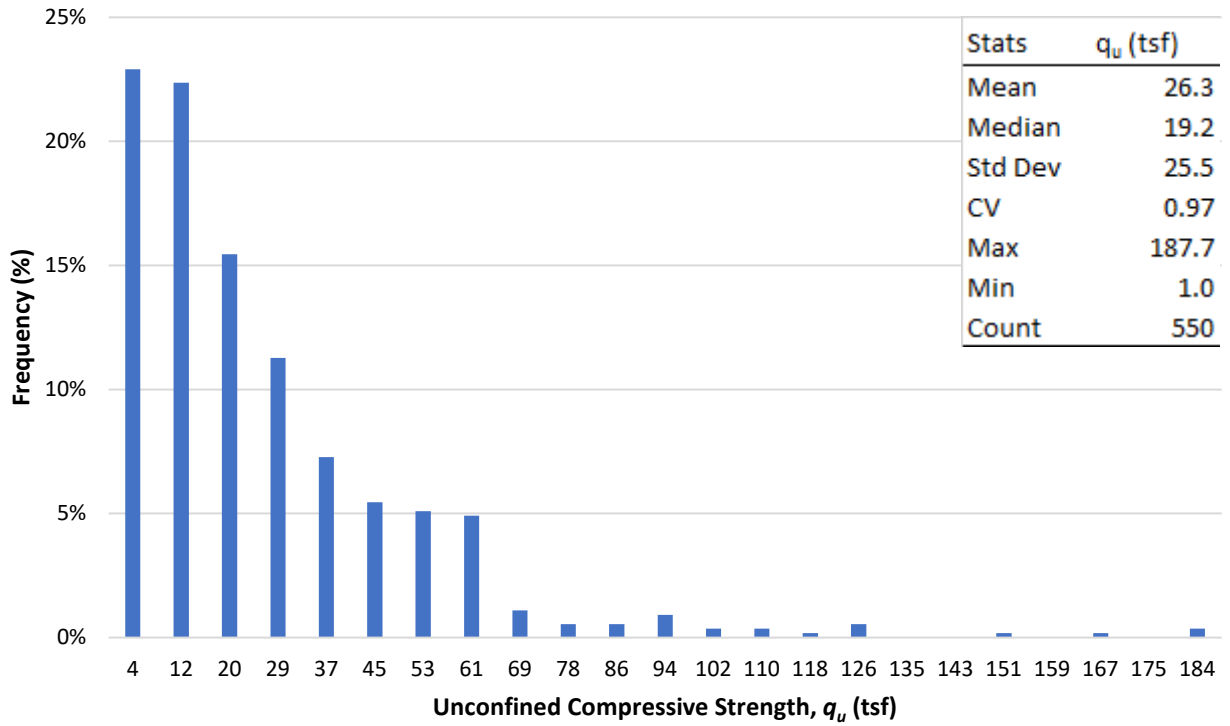
Figure 5-40. Frequency distribution for all shafts minus TS-1, shaft P6-3 and vicinity borings.
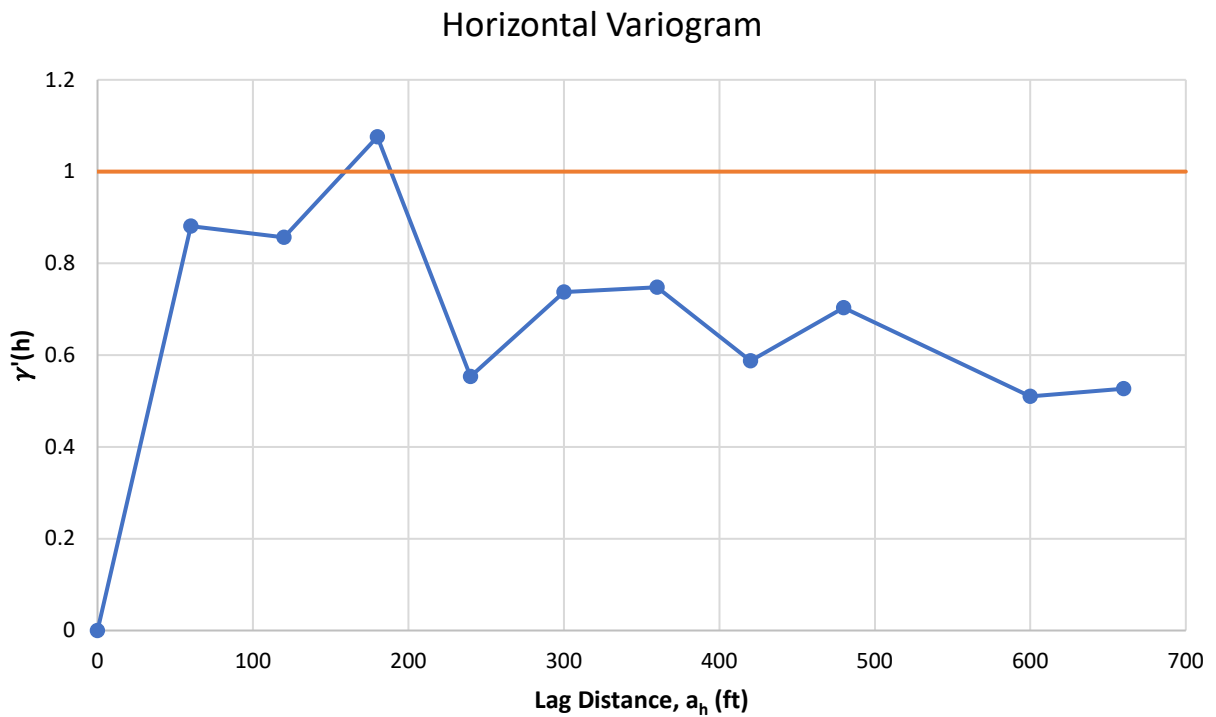
Figure 5-41. Horizontal variogram for all shafts minus TS-1, shaft P6-3 and vicinity borings.

89
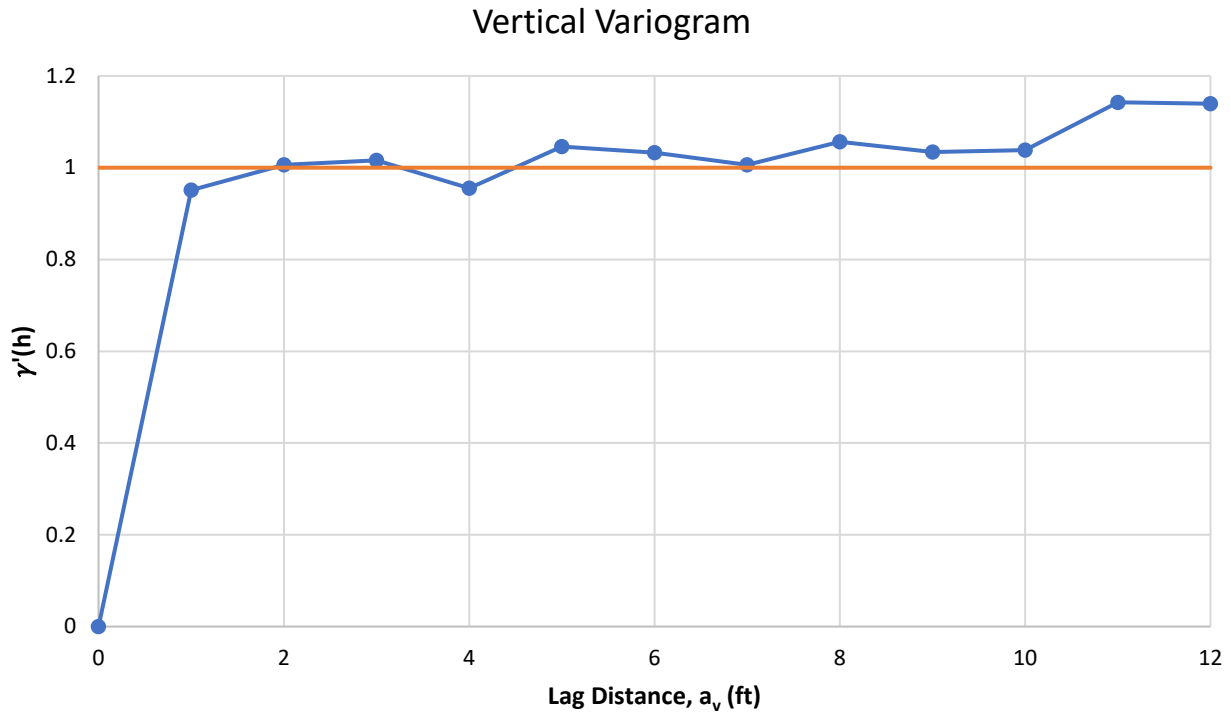
Figure 5-42. Vertical variogram for all shafts minus TS-1, shaft P6-3 and vicinity borings.

In the case of the horizontal variogram (Figure 5-41), a horizontal asymptote of 1.0 $[\gamma (h) / \sigma]$ is evident to a lag distance of 180 feet, and then the data drops to 0.55. This suggests that the presence of zones are reappearing over the whole site for the full length of the shafts and not just elevations +20 to -2.0 feet (Figure 5-30 through 5-33) for Test Shaft 1 (TS-1) and Pier 6-3 and vicinity borings. That is, the middle 1/3 of site (Piers 2 to 5) is different from outer 1/3 zones at each end. This can be confirmed if the site is broken down into 1/3 zones for the full length of shafts and not just elevations +20 to -2, as shown in Figure 5-43. The strength profile for the middle 1/3 is shown in Figure 5-44 and the geostatistics for the single layer (Elevation +20 to -20 ft) are given in Figure 5-45. Evident from Figures 5-46 and 5-47 is that both the vertical and horizontal variograms now go to 1.0. Also note that the CV of this layer has dropped to 0.97 versus 1.93 when all borings over the site (Figures 5-24 through 5-28) are considered.

90
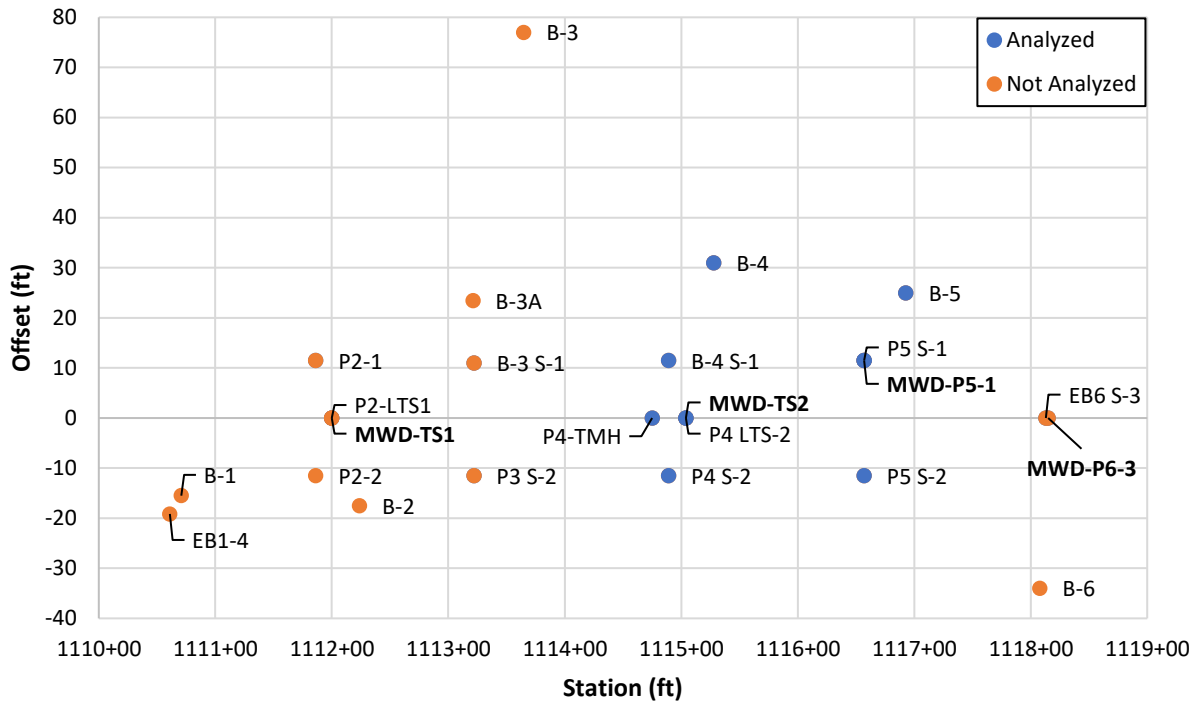
Figure 5-43. Borings and shafts for middle 1/3 of CR250—TS-2, P5-1 and vicinity borings.
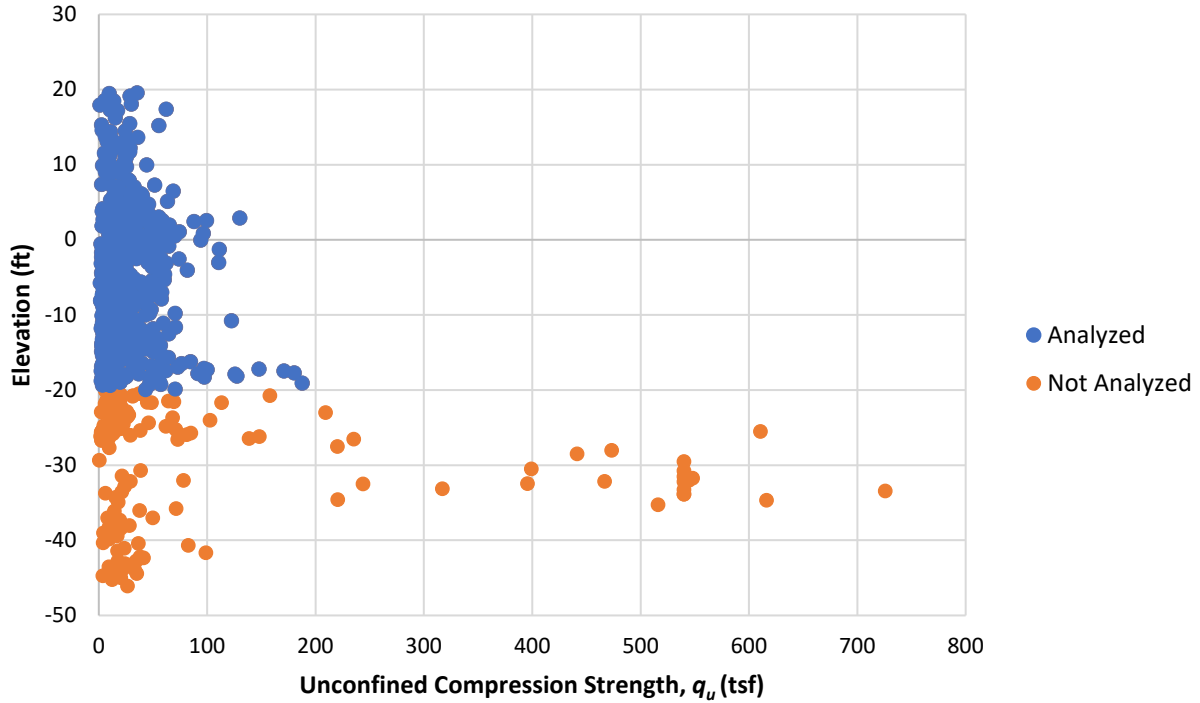
Figure 5-44. Strength profile for middle 1/3 of CR250—TS-2, P5-1 and vicinity borings.
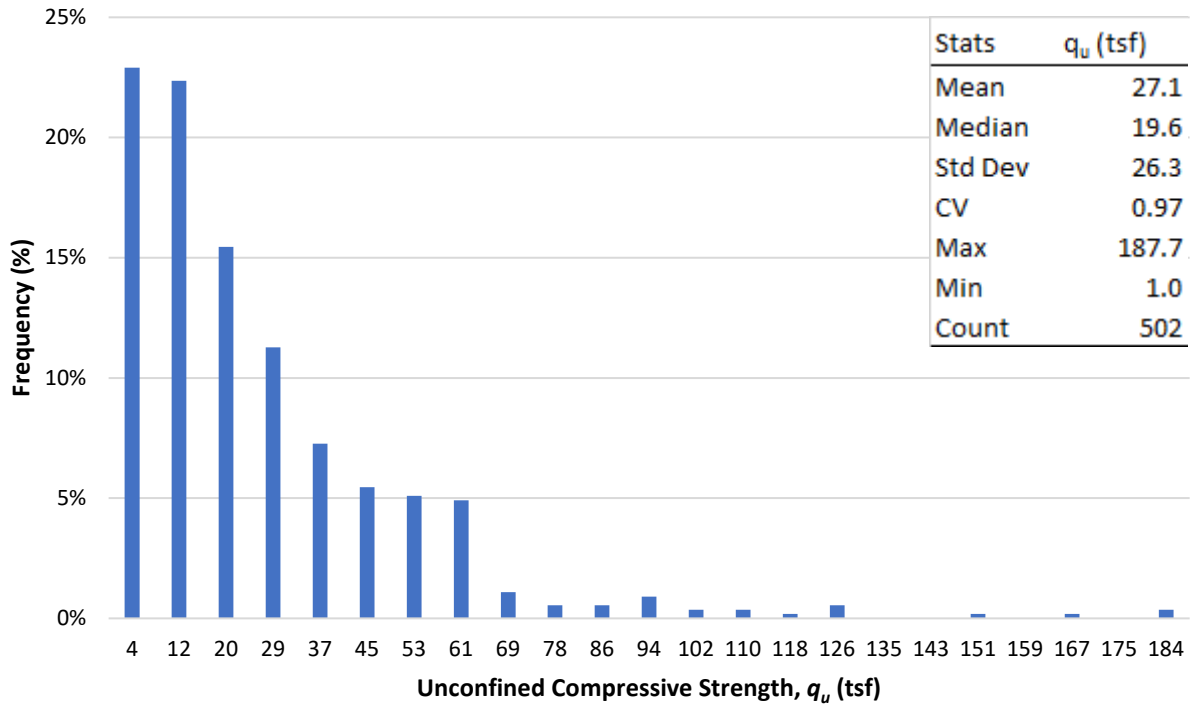
Figure 5-45. Frequency distribution for middle 1/3 of CR250—TS-2, P5-1 and vicinity borings.

Horizontal Variogram
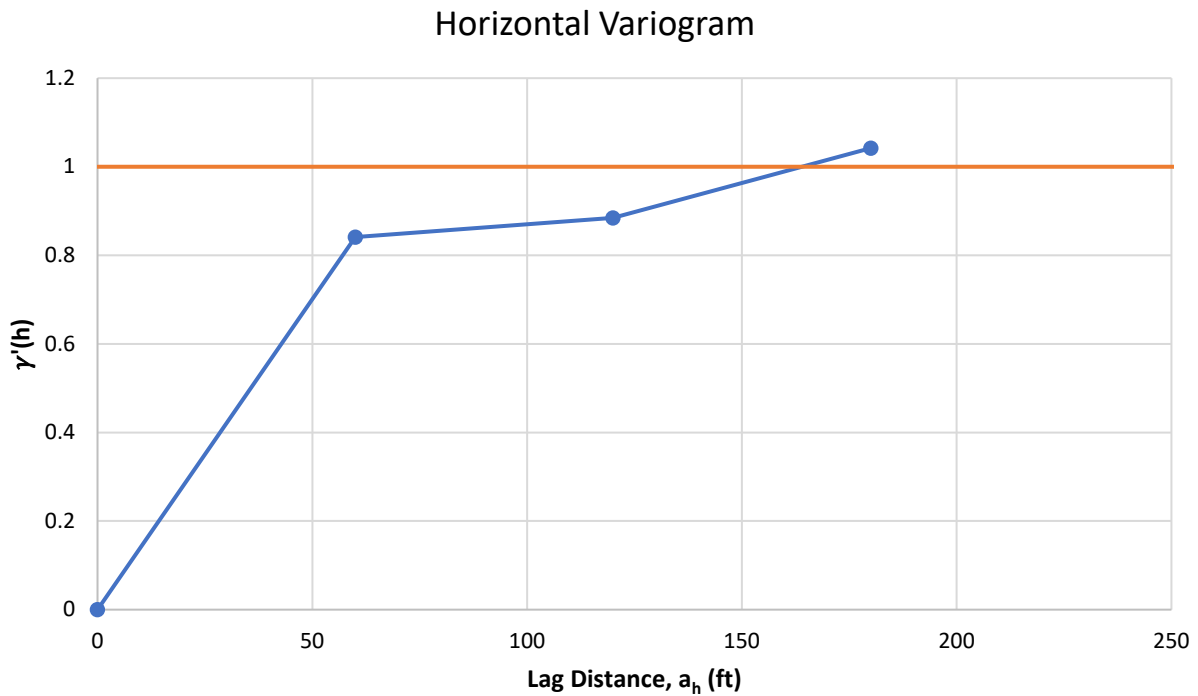
Figure 5-46. Horizontal variogram for middle 1/3 of CR250—TS-2, P5-1 and vicinity borings.
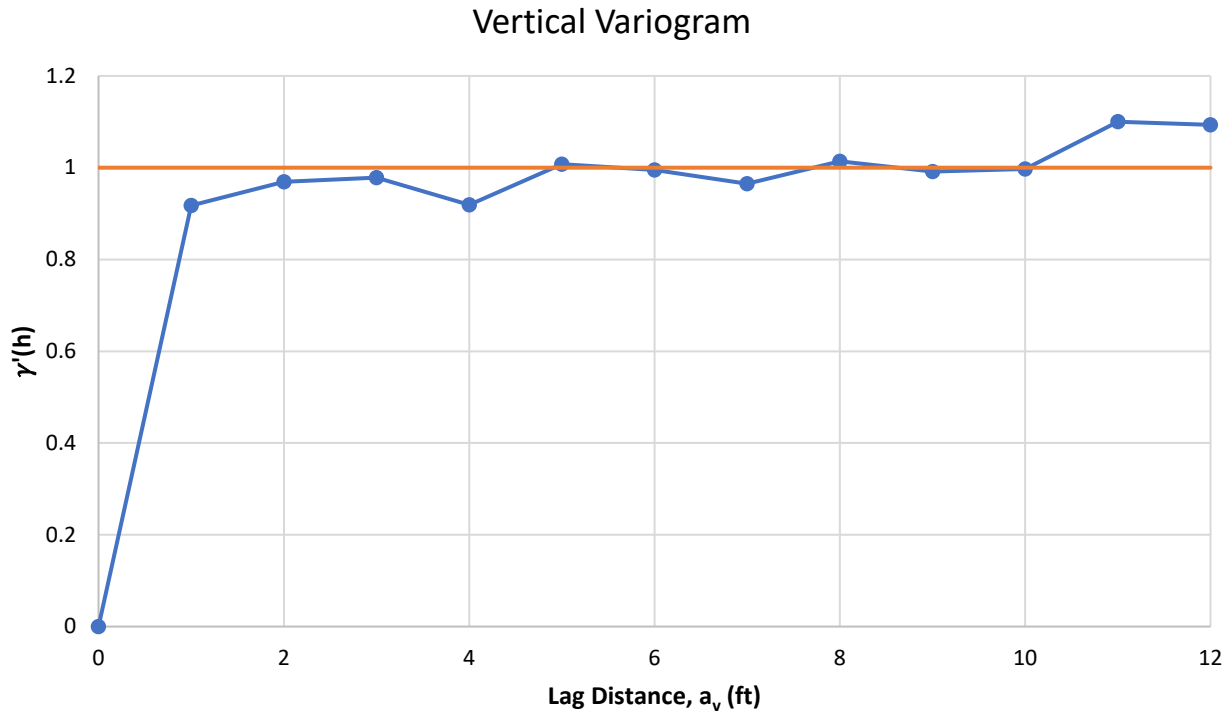
Figure 5-47. Vertical variogram for middle 1/3 of CR250—TS-2, P5-1 and vicinity borings.

5.5   *Load Test Analysis*

As discussed in the prior section, two load tests were conducted at the CR-250 site. The limestone formation present at the site was the Ocala limestone formation (Bryan et al. 2001). Based on the load test report, limited shaft displacement was achieved in both test shafts. The peak load measured in each segment, induced by the hydraulic jack, typically occurred at a displacement less than 0.07 inches. With such limited displacement within each segment, it is difficult to assess the load test results using individual load test layers. However, the total load carried in shear above and below the hydraulic jack can be compared to the estimated loads from the core data and MWD within each segment. This was the approach taken at CR-250 due to the limited displacements within each load tested segment. The MWD side shear loads were estimated using the unconfined compression strength equation (Eq. 3-12) developed at Selmon Parkway using a similar rock drilling bucket with side shear subsequently calculated using Equation 3-8. As discussed in Sections 5.3 and 5.4, Equation 3-12 showed good agreement with the laboratory tested core samples recovered at CR-250.

5.5.1   *Test Shaft 1*

According to the load test report for Test Shaft 1, the total side shear load carried above the jack in Segments 2, 3, 4, and 5 (Elevations +12.93 to -8.07 feet) was 4,444 kips. The total side shear load carried below the jack in Segments 6 and 7 (Elevations +12.93 to -8.07) was 3,733 kips. These loads are then compared to the core data and MWD estimates for each shaft segment. The core data load summary is provided in Table 5-2 and the MWD loads are summarized in Table 5-3.

Table 5-2. Test Shaft 1 core data load summary.

				Core Data Load Summary – Test Shaft 1			
Segment	Location	EL_{Top} (ft)	EL_{Bot} (ft)	ΔZ (ft)	q_u (psi)	fs (ksf)	P (kips)
2	Above	12.93	7.93	5.0	691	18.54	1,748
3	Above	7.93	2.93	5.0	859	22.62	2,131
4	Above	2.93	-2.07	5.0	399	11.23	1,059
5	Above	-2.07	-8.07	6.0	163	4.96	561
6	Below	-8.07	-13.07	5.0	185	5.57	525
7	Below	-13.07	-18.07	5.0	266	7.76	731
					Above	P (kips) =	5,499
					Below	P (kips) =	1,256
					Total	P (kips) =	**6,756**

Table 5-3. Test Shaft 1 MWD data load summary.

				MWD Data Load Summary – Test Shaft 1			
Segment	Location	EL_{Top} (ft)	EL_{Bot} (ft)	ΔZ (ft)	q_u (psi)	fs (ksf)	P (kips)
2	Above	12.93	7.93	5.0	499	13.76	1,297
3	Above	7.93	2.93	5.0	711	19.02	1,793
4	Above	2.93	-2.07	5.0	411	11.53	1,087
5	Above	-2.07	-8.07	6.0	285	8.27	936
6	Below	-8.07	-13.07	5.0	345	9.83	926
7	Below	-13.07	-18.07	5.0	473	13.12	1,236
					Above	P (kips) =	5,113
					Below	P (kips) =	2,163
					Total	P (kips) =	**7,275**

Based on the loads carried above the hydraulic jack, the side shear within these segments was approaching mobilization but was not fully mobilized. Based on the loads carried below the hydraulic jack, the side shear within these segments was likely mobilized. Below the jack, the estimated side shear from the load test was three times higher than the side shear estimate from the core data and nearly double the MWD estimated load. Therefore, it is likely that some of the reported load from side shear was actually end bearing (it is difficult to determine how much end bearing and side shear with limited shaft displacement). The strain gage load distribution from the load test report supports this assessment as a large jump in load is observed at the end of the load test which was likely due to end bearing.

5.5.2 Test Shaft 2

According to the load test report for Test Shaft 2, the total side shear load carried above the jack in Segments 2 and 3 (Elevations -16.0 to -32.1 feet) was 5,282 kips. The total side shear load carried below the jack in Segments 4 and 5 (Elevations +12.93 to -8.07) was 4,601 kips. These loads are then compared to the core data and MWD estimates for each shaft segment. The core data load summary is provided in Table 5-4 and the MWD loads are summarized in Table 5-5. Table 5-4. Test Shaft 2 core data load summary.

Core Data Load Summary – Test Shaft 2							
Segment	Location	EL_{Top} (ft)	EL_{Bot} (ft)	ΔZ (ft)	q_u (psi)	fs (ksf)	P (kips)
2	Above	0.00	-8.00	8.0	323	9.26	1,397
3	Above	-8.00	-16.00	8.0	258	7.55	1,138
4	Below	-16.00	-22.50	6.5	494	13.65	1,673
5*	Below	-22.50	-26.75	4.3	647	17.46	1,399
					Above	P (kips) =	2,535
					Below	P (kips) =	3,071
					Total	P (kips) =	**5,606**

*MWD elevation range did not span the full load test segment elevation range.

Table 5-5. Test Shaft 2 MWD data load summary.

MWD Data Load Summary – Test Shaft 2							
Segment	Location	EL_{Top} (ft)	EL_{Bot} (ft)	ΔZ (ft)	q_u (psi)	fs (ksf)	P (kips)
2	Above	0.00	-8.00	8.0	370	10.48	1,580
3	Above	-8.00	-16.00	8.0	289	8.38	1,263
4	Below	-16.00	-22.50	6.5	388	10.95	1,341
5*	Below	-22.50	-26.75	4.3	582	15.86	1,270
					Above	P (kips) =	2,843
					Below	P (kips) =	2,611
					Total	P (kips) =	**5,455**

*MWD elevation range did not span the full load test segment elevation range.

Above the jack, the test shaft loads were nearly double the core data and MWD estimates. However, the Sonic Caliper Report shows that the lower half of the shaft, which contained the hydraulic jack, was shifted and off center by three to four inches (crooked shaft). Consequently, this likely resulted in much higher loads being carried in the segments above the jack and an assessment of mobilization cannot be made.

Below the jack, the MWD data was limited. This was partially due to a strong a layer in the bottom 2.25 feet of the original shaft that had to be drilled out using a core barrel and cross-cutter. The core barrel and cross-cutter were used because the rock bucket was inefficient in the removal of the high strength layer of limestone that was present. In addition to the loss of data from changing tools, the casing seal on Test Shaft 2 was breached and this led to the shaft being drilled out an additional three feet. The UF researchers were not made aware the shaft was being extended to resolve the casing breach and therefore MWD was not conducted on the additional

three feet of shaft. Consequently, MWD data is only available to an elevation of -26.75 feet, whereas the shaft tip reached an elevation of -32.05 feet (five feet of MWD data is missing for the assessment).

Based on the loads applied by the jack, Segment 4 was likely mobilized and the portion of Segment 5 (Elevation -22.5 to -26.75 feet) in which MWD was completed was also likely mobilized. The additional load below the jack was likely carried by side shear as the strength of the rock continued to increase with depth. Table 5-6 provides the core data for the full length of Segment 5 and includes Segment 6 (Elevation -29.0 to -32.05 feet) in which MWD was not conducted. Based on Table 5-6, it is unlikely that the shaft was fully mobilized below the jack in Test Shaft 2. Also, the load estimate in Segment 6 (P = 5,213 kips) is likely too high as side shear in limestone generally peaks around f_s = 50 ksf. However, even at f_s = 50 ksf the load would have been approximately 2,900 kips and side shear mobilization would not have been achieved.

Table 5-6. Test Shaft 2 core data load summary including Segment 6.

			Core Data Load Summary Including Segment 6 – Test Shaft 2				
Segment	Location	EL_{Top} (ft)	EL_{Bot} (ft)	ΔZ (ft)	q_u (psi)	fs (ksf)	P (kips)
2	Above	0.00	-8.00	8.0	323	9.26	1,397
3	Above	-8.00	-16.00	8.0	258	7.55	1,138
4	Below	-16.00	-22.50	6.5	494	13.65	1,673
5	Below	-22.50	-29.00	6.5	1,438	36.19	4,434
6	Below	-29.00	-32.05	3.1	3,935	90.68	5,213
					Above	P (kips) =	2,535
					Below	P (kips) =	11,320
							13,855

5.6 *Drilled Shaft MWD QA/QC for Production Shafts*

Drilled shaft QA/QC could have been conducted on the production shafts at CR-250 via MWD using two methods. The first method would be to use the load test-MWD correlations developed at Selmon Parkway. This includes the conservative correlation provided in Figure 3-12 in which the soil layering was not removed prior to establishing correlation, or the developing a new side shear correlation using Equation 3-12 which removed the soil prior to establishing correlation and only included rock. The second method to provide production shaft QA/QC would be to use the total specific energy recorded in the production shafts compared to the total specific energy recorded from a load tested shaft. Both methods will be covered in the following sections.

5.6.1 *Load Test – MWD Correlation QA/QC*

From the data collected at Selmon Parkway, two load test vs MWD correlations were developed. The first correlation is provided in Figure 3-12. This correlation was developed by directly comparing the average specific energy recorded in mobilized segments of the test shafts to the respective mobilized side shear recorded during the load tests. This correlation includes the soil

layering that was present at the Selmon site. The second correlation that was developed is provided in Figure 3-19 with the regression equation provided in Equation 3-12. The second correlation removed the soil layering and only includes the relationship between specific energy and rock strength (q_u) for rock drilling buckets. This correlation was transformed into a side shear vs specific energy correlation using Equation 3-8. When both correlations are plotted together (Figure 5-48), it is obvious that the first correlation (Rock & Soil) that included the soil is more conservative than the correlation that only included rock (Rock).
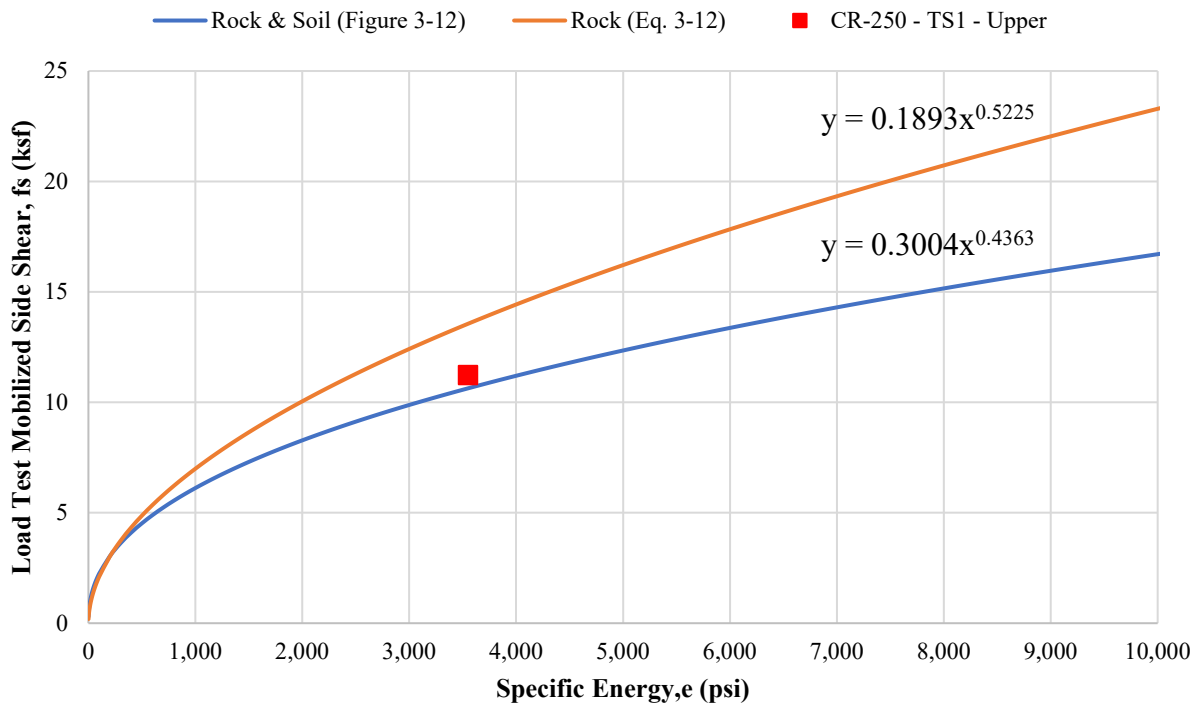
Figure 5-48. Side shear vs specific energy correlations developed at Selmon Parkway.

From the Test Shaft 1 load test data, the shaft segments above the hydraulic jack were in isolated side shear and approaching mobilization. If the average specific energy recorded (e = 3,549 psi) over this section of the shaft (Elevations +12.93 to -8.07 feet) is plotted versus the average side shear recorded from load testing within this section of the shaft (f_s = 11.23 ksf), it is observed that the data point falls between the two regression curves in Figure 5-48. If the shaft segment had been fully mobilized, it is expected that the data point would have fallen on or closer to the orange regression curve as the geo-material excavated within this section of the shaft was all identified as rock. However, it is recommended to use the blue regression curve and associated equation (Figure 3-12) to provide the drilled shaft MWD QA/QC as it is more conservative. This can be tested using the factored design loads and specific energy recorded for production shafts P5-1 and P6-3.

The factored design load for production shaft P5-1 was 2,218 kips. The average specific energy recorded in the rock socket of shaft P5-1 was 2,273 psi. The average specific energy equates to a side shear value of f_s = 8.8 ksf and an MWD side shear load of R_n = 5,121 kips using the more

conservative correlation (blue regression curve in Figure 5-48). If an LRFD Φ value of 0.5 was used for the QA/QC effort, the factored MWD side shear load would be $\Phi R_n = 0.5 * 5,121$ kips = 2,560 kips. This would provide a capacity to demand ratio of 1.15 which meets the design criteria and ensures the shaft is adequate to support the intended loading. If an LRFD Φ value of 0.7 was used for the QA/QC effort, the factored MWD side shear load would be $\Phi R_n = 0.7 * 5,121$ kips = 3,584 kips. This would provide a capacity to demand ratio of 1.62 which greatly exceeds the design criteria and suggests the shaft length could have been reduced.

The factored design load for production shaft P6-3 was 1,138 kips. The average specific energy recorded in the rock socket of shaft P6-3 was 2,788 psi. The average specific energy equates to a side shear value of $f_s = 9.6$ ksf and an MWD side shear load of $R_n = 2,927$ kips using the more conservative correlation (blue regression curve in Figure 5-48). If an LRFD Φ value of 0.5 was used for the QA/QC effort, the factored MWD side shear load would be $\Phi R_n = 0.5 * 2,927$ kips = 1,463 kips. This would provide a capacity to demand ratio of 1.29 which meets the design criteria and ensures the shaft is adequate to support the intended loading. If an LRFD Φ value of 0.7 was used for the QA/QC effort, the factored MWD side shear load would be $\Phi R_n = 0.7 * 2,927$ kips = 2,049 kips. This would provide a capacity to demand ratio of 1.80 which greatly exceeds the design criteria and suggests the shaft length could have been reduced.

At both production shaft locations, the MWD QA/QC efforts proved that both shafts meet demands of the engineering design. The spatial uncertainty was removed as the MWD effort was conducted within the footprint of each shaft at full scale. This provides superior QA/QC compared to any other conventional method.

5.6.2   Total Specific Energy MWD QA/QC

The second method of drilled shaft MWD QA/QC would be to set a minimum value for total specific energy that must be achieved within the rock socket of the production shafts. The total specific energy is defined by Equation 5-6:

$$e_{total}(kips) = e_{avg}(psf) \times \pi \times D(ft) \times L(ft) \times \frac{1\ kip}{1,000\ lbf} \qquad \text{(Eq. 5-6)}$$

where,

e_{avg} = average specific energy recorded over the rock socket segment (psf)
D = diameter of the drilling tool (ft)
L = length of the rock socket segment (ft)

This method of drilled shaft QA/QC was discussed in Rodgers et al. (2018c) in which the total specific energy was referred to as, "specific energy capacity". The method was developed for sites where limited information was gained from load testing (e.g., CR-250) or for sites where load testing did not occur.

At CR-250, the load test segments above the hydraulic jack in Test Shaft 1 (Elevations +12.93 to -8.07 feet) can be used to establish the minimum total specific energy requirement that must be

achieved during drilling within the rock sockets of the production shafts. It was observed that these segments in Test Shaft 1 were not fully mobilized but carried a total side shear load of P_{TS1} = 4,444 kips. Over this segment of Test Shaft 1, the total specific energy recorded was e_{total} = 202,294 kips. The factored design load for production shaft P5-1 was P_{5-1} = 2,218 kips and the factored design load for production shaft P6-3 was P_{6-3} = 1,138 kips. The factored design load for each of the production shafts is first divided by the side shear load measured above the hydraulic jack in Test Shaft 1 and then multiplied by the total specific energy measured above the hydraulic jack in Test Shaft 1 to calculate the minimum total specific energy that must be achieved in each production shaft:

$$e_{total\ P5-1} = \frac{P_{5-1}}{f_{s\ TS-1}} \times e_{total\ TS-1} = \frac{2,218\ kips}{4,444\ kips} \times 202,294\ kips = 100,965\ kips \qquad \text{(Eq. 5-7)}$$

and,

$$e_{total\ P6-3} = \frac{P_{6-3}}{f_{s\ TS-1}} \times e_{total\ TS-1} = \frac{1,138\ kips}{4,444\ kips} \times 202,294\ kips = 51,803\ kips. \qquad \text{(Eq. 5-8)}$$

Equation 5-7 indicates that only 50% of the total specific energy recorded in Test Shaft 1 is needed to achieve the required design load for production shaft P5-1. Equation 5-8 indicates that only 26% of the total specific energy recorded in Test Shaft 1 is needed to achieve the required design load for production shaft P6-3. The total specific energy recorded over the rock socket of shaft P5-1 was e_{total} = 191,520 kips which is nearly double the total specific energy required. The total specific energy recorded over the rock socket of shaft P6-3 was e_{total} = 122,810 kips which is more than double the total specific energy required. In both shaft locations the total specific energy recorded over the rock sockets greatly exceeded the minimum requirements and ensures that both shafts are adequate to support the intended loading.

This approach to drilled shaft QA/QC is conservative as a reduction in specific energy equates to a smaller reduction in shaft side shear. This is illustrated in Figure 5-49 where the average specific energy recorded in the segments above the hydraulic jack in Test Shaft 1 is plotted with the respective side shear value based on the conservative blue line regression equation developed at Selmon Parkway (Figure 5-48; Rock and Soil).
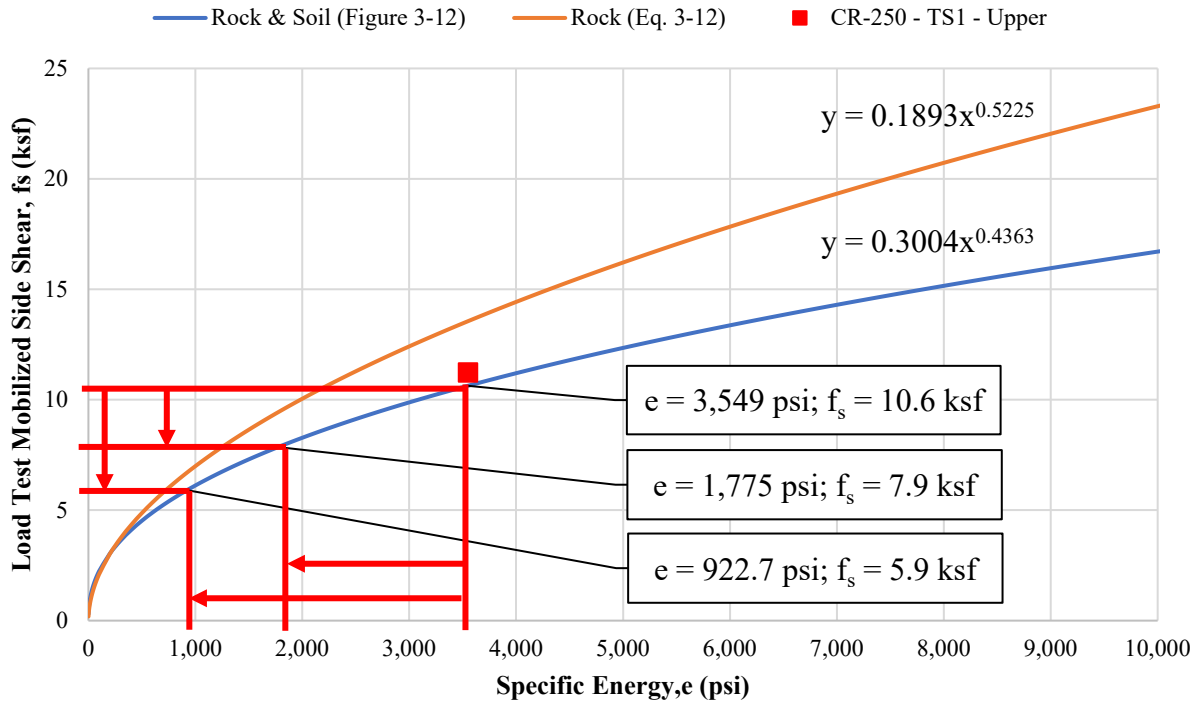
Figure 5-49. Side shear vs specific energy correlations indicating a reduction in specific energy equates to a smaller reduction in drilled shaft side shear.

When the average specific energy is reduced based on the factored design load of production shaft P5-1 divided by the side shear measured in Test Shaft 1:

$$e_{P5-1} = \left(\frac{2{,}218\ kips}{4{,}444\ kips}\right) \times 3{,}549\ psi = 1{,}775\ psi \tag{Eq. 5-9}$$

this results in an approximate 50% reduction in average specific energy. However, the resulting side shear is only reduced by 25%:

$$\%\ reduction\ in\ f_{s\ P5-1} = \left(1 - \frac{7.9\ ksf}{10.6\ ksf}\right) \times 100\% = 25\% \tag{Eq. 5-10}$$

When the average specific energy is reduced based on the factored design load of production shaft P6-3 divided by the side shear measured in Test Shaft 1:

$$e_{P5-1} = \left(\frac{1{,}138\ kips}{4{,}444\ kips}\right) \times 3{,}549\ psi = 922.7\ psi \tag{Eq. 5-11}$$

this results in an approximate 74% reduction in average specific energy. However, the resulting side shear is only reduced by 44%:

$$\%\ reduction\ in\ f_{s\ P5-1} = \left(1 - \frac{5.9\ ksf}{10.6\ ksf}\right) \times 100\% = 44\% \tag{Eq. 5-12}$$

Therefore, the proposed QA/QC method using total specific energy provides a conservative approach to ensure the production shafts meet the criteria of the engineering design. Setting the minimum total specific energy requirement for the production shafts could be established using less of a reduction or through a different approach. This work just shows one approach to setting the minimum requirement. Additionally, this QA/QC approach would need to be integrated into LRFD design methodology and further investigation is warranted to establish such criteria and methods.

6. Conclusions

This research is a continuation of the work completed in BDV31-977-20 in which measuring while drilling (MWD) was conducted on full-scale drilled shafts using rock augers. The focus of this research was MWD conducted on full-scale drilled shafts using rock drilling buckets. Through this research effort, the number of FDOT MWD data points collected during full-scale drilled shaft installations was doubled. Based on the results of this study the following conclusions can be drawn:

- A correlation was developed between specific energy and the rock strength of Florida limestone using rock drilling buckets. This was completed using the side shear measured in individual mobilized shaft segments and the specific energy measured within each respective shaft segment while drilling with a rock bucket.
- The mechanical efficiency of a rock drilling bucket differs from that of a rock auger. This is due to the differences in each drilling tool's geometry. Consequently, a unique relationship is shared between specific energy and rock strength for each unique drilling tool (e.g., rock auger vs. rock drilling bucket).
- MWD provides highly detailed records of the geological conditions encountered at a site versus traditional SPT borings. The significant increase in strength assessments collected via MWD within a single sampled location allows a correlation structure to be obtained from a single boring or shaft for an individual pier. This cannot be achieved using any other current conventional method.
- Performing variogram analyses with the high resolution MWD data allows areal trends such as zonal anisotropy and layering to be identified. This provides a means to quantify the true variability present at a site. Consequently, a site can now be properly broken up into zones and layers for each pier which reduces the coefficient of variability (CV) and increases the reliability of the as-built foundations.
- MWD provides a means to quantify the quality and length of rock sockets during the drilling process which ensures the as-built foundations meet/exceed the design parameters, providing QA/QC to the drilling contractor and foundation design engineer.
- MWD data collected from load tested shafts can be used to make an informed engineering decision as to which side shear values should be considered in design as MWD provides additional information in assessing and implementing load test results.
- Performing MWD during drilled shaft installations removes the spatial uncertainty at each shaft location and reduces the spatial error used in design.

7. Recommendations

The following recommendations are based on this study's findings:

- Further research should be conducted for drilled shaft MWD. From the first research effort, BDV31-977-20, ten data points were collected during full-scale drilled shaft installations to verify the laboratory developed relationship between specific energy and rock strength for rock augers. From this research effort, 12 data points were collected during full-scale shaft installations to establish a relationship between specific energy and rock strength for rock drilling buckets. Due to the differences in mechanical efficiency each tool provides, the collection of data points for each drilling tool must be treated separately. Therefore, it is recommended that more data be collected for both drilling tools at full-scale to further investigate the MWD approach.

- Per the scope of work, drilled shaft rigs that employ a mechanically driven torque system were to be monitored and investigated as a secondary objective. These types of drill rigs are typically crane mounted. Unfortunately, all drill rigs monitored during this round of research were hydraulically driven and an investigation could not be completed. Therefore, it is recommended to investigate the use mechanically driven drill rigs in future drilled shaft projects that utilize the rig type.

- Technical specifications for MWD should be added to future FDOT contracts in which drilled shafts are to be installed. This would ensure more data is collected to further investigate the MWD approach for use in drilled shaft design as well as assist with QA/QC during construction on the site. The technical specifications should be based on the established ISO (2016) standards and findings from each of the FDOT's MWD research efforts.

- Further research should be conducted for geotechnical site investigation MWD applications (e.g., BDV31-820-006). As discussed in this report, current methods of geotechnical site characterization do not specifically address the high degree of subsurface variability often encountered throughout the state of Florida. Demonstrated in this report, the MWD approach resolves the lack of geotechnical data collected, allows a reliable correlation structure to be developed from sampled locations, and provides a method to properly identify areal trends that can lead to shaft failure. BDV31-820-006 demonstrated that MWD is not only viable for geotechnical site investigation, it is highly advantageous compared to the current state of the practice. Furthermore, the FHWA recently identified MWD as the leading advanced method of geotechnical exploration (FHWA EDC-5, Advanced Geotechnical Methods in Exploration [A-GaME]) currently in development. Therefore, this branch of geotechnical MWD should be pursued heavily. By doing so, continuity could be developed between MWD site investigation and MWD construction monitoring. This would also provide insight to the upscaling effect from assessing small scale core samples for design compared to the measured capacity of full-scale bored piles (e.g., drilled shafts and auger cast piles) used to support large structures. The collaborative effort would lead to the use of truly reliability-based LRFD resistance factors in the state of Florida, increased reliability in shaft performance, and a direct reduction in cost per shaft.

References

ASTM. 2014. Standard Test Methods for Compressive Strength and Elastic Moduli of Intact Rock Core Specimens under Varying States of Stress and Temperatures. *American Society for Testing and Materials, ASTM International*. ASTM D7012-14. West Conshohocken; PA. doi.org/10.1520/D7012-14E01.

ASTM 2016. Standard Test Method for Splitting Tensile Strength of Intact Rock Core Specimens. *American Society for Testing and Materials, ASTM International*. ASTM D3967-16. West Conshohocken; PA. doi.org/10.1520/D3967-16.

Brown, D.A., Turner, J.P., and Castelli, R.J. 2010. Drilled Shafts: Construction Procedures and LRFD Design Methods. Publication No. FHWA-NHI-10-016, Federal Highway Administration. Washington, D.C.

Bryan, J.R., Scott, T.M., and Means, G.H. 2001. Roadside Geology of Florida. *Mountain Press Publishing Company*. Missoula, MT.

Chen, X., Gao, D., Guo, B., and Feng, Y. 2016. Real-time optimization of drilling parameters based on mechanical specific energy for rotating drilling with positive displacement motor in the hard formation. *Journal of Natural Gas Science and Engineering*, 35(A): 686-694.

Detournay, E. and Defourny, P. 1992. A phenomenological model for the drilling action of drag bits. *International Journal of Rock Mechanics and Mining Sciences*, 29(1): 13–23.

Detournay, E., Richard, T., and Shepherd, M. 2008. Drilling response of drag bits: Theory and experiment. *International Journal of Rock Mechanics and Mining Sciences*, 45(8): 1347–1360.

Florida Department of Transportation (FDOT). 2015. Soils and Foundation Handbook. Florida Department of Transportation, State Materials Office. Gainesville, FL.

Graham, D., Dapp, S., Brown, D., and McGillivray, R. 2013. Selmon Expressway, Tampa: Case History of Drilled Shaft Design for Extreme Variability. *In* proceedings of the 38th Annual Conference on Deep Foundations. Deep Foundations Institute (DFI).

Gringarten, E., Deutsch, C.V. 2001. Teacher's Aide Variogram Interpretation and Modeling. *Mathematical Geology*, 33, 507–534. doi.org/10.1023/A:1011093014141.

Hoberock, L.L., and Bratcher, G.J. 1996. A new approach for determining in-situ rock strength while drilling. *ASME Journal of Energy Resources Technology*, 118(4): 249–255.

ISO/IEC. 2016. Geotechnical Investigation and Testing – Field Testing – Part 15: Measuring While Drilling. ISO 22476-15:2016, International Standards Organization. Geneva, Switzerland.

Karasawa, H., Ohno, T., Kosugi, M., and Rowley, J.C. 2002a. Methods to estimate the rock strength and tooth wear while drilling with roller-bits—Part 1: Milled-tooth bits. *ASME Journal of Energy Resources Technology*, 124(3): 125.

Karasawa, H., Ohno, T., Kosugi, M., and Rowley, J.C. 2002b. Methods to estimate the rock strength and tooth wear while drilling with roller-bits—Part 2: Insert bits. *ASME Journal of Energy Resources Technology*, 124(3): 133–140.

Lambe, T.W., and Whitman, R.V. 1969. Soil Mechanics. John Wiley & Sons, New York.

Li, Z., and Itakura, K. I. 2012. An analytical drilling model of drag bits for evaluation of rock strength. *Soils and Foundations*, 52(2): 216–227.

McVay, M., Townsend, F., and Williams, R. 1992. Design of socketed drilled shafts in limestone. *Journal of Geotechnical Engineering*, 118(10): 1626–1637. doi:10.1061/(ASCE)0733-9410(1992)118:10(1626)

McVay, M. and Rodgers, M., Drilled Shaft Resistance Based on Diameter, Torque and Crowd (Drilling Resistance vs. Rock Strength) Phase II, Final Report, FDOT BDV31-977-20, Florida Department of Transportation, Tallahassee, Florida, June 2016, 258 pages.

Ohno, T., Karasawa, H., Kosugi, M., and Rowley, J.C. 2004. Proposed practical methods to estimate rock strength and tooth wear while drilling with roller-cone bits. *ASME Journal of Energy Resources Technology*, 126(4): 302–310.

O'Neill, M., Townsend, F., Hassan, K., Buller, A., and Chang, P. 1996. Load Transfer for Drilled Shafts in Intermediate Geomaterials. *Publication FHWA-RD-95-172, Federal Highway Administration*. Washington, DC.

Rodgers, M., McVay, M., Ferraro, C., Horhota, D., Tibbetts, C., and Crawford, S. 2018a. Measuring Rock Strength While Drilling Shafts Socketed into Florida Limestone. *ASCE Journal of Geotechnical and Geoenvironmental Engineering*, 144(3), pp. 04017121-1—04017121-8. doi:10.1061/(ASCE)GT.1943-5606.0001847.

Rodgers, M., McVay, M., Horhota, D., and Hernando, J. 2018b. Assessment of Rock Strength from Measuring While Drilling Shafts in Florida Limestone. *Canadian Geotechnical Journal*, 55(8): 1154-1167. doi:10.1139/cgj-2017-0321.

Rodgers, M., McVay, M., and Horhota, D. 2018c. Monitoring While Drilling Shafts in Florida Limestone. *In* proceedings of the IFCEE 2018: Installation, Testing, and Analysis of Deep Foundations (GSP 294), 5-10 March 2018. American Society of Civil Engineers, pp. 613-621. doi:10.1061/9780784481578.058.

Rodgers, M., McVay, M., Horhota, D., Sinnreich, J., and Hernando, J. 2018d. Assessment of Shear Strength from Measuring While Drilling Shafts in Florida Limestone. *Canadian Geotechnical Journal*. doi:10.1139/cgj-2017-0629.

Rodgers, M., McVay, M., Horhota, D., Hernando, J., and Paris, J. 2020. Measuring While Drilling in Florida Limestone for Geotechnical Site Investigation. *Canadian Geotechnical Journal*. doi.org/10.1139/cgj-2019-0094.

Teale, R. 1965. The concept of specific energy in rock drilling. *International Journal of Rock Mechanics and Mining Science*, 2(1), 57–73.

Viana Da Fonseca, A., and Coelho, S. 2006. Characterization of highly variable rock weathering by using DPR. *In* Proceedings of the GeoShanghai International Conference (GSP 150), May 2006. doi:10.1061/40862(194)16

Wolcott, D.S., and Bordelon, D.R. 1993. Lithology determination using downhole bit mechanics data. *In* proceedings of the 68th Annual Technical Conference and Exhibition of the Society of Petroleum Engineers (SPE 26492), October 1993. Society of Petroleum Engineers, pp. 769–778. doi:10.2118/26492-MS.